Friezes and Geometry

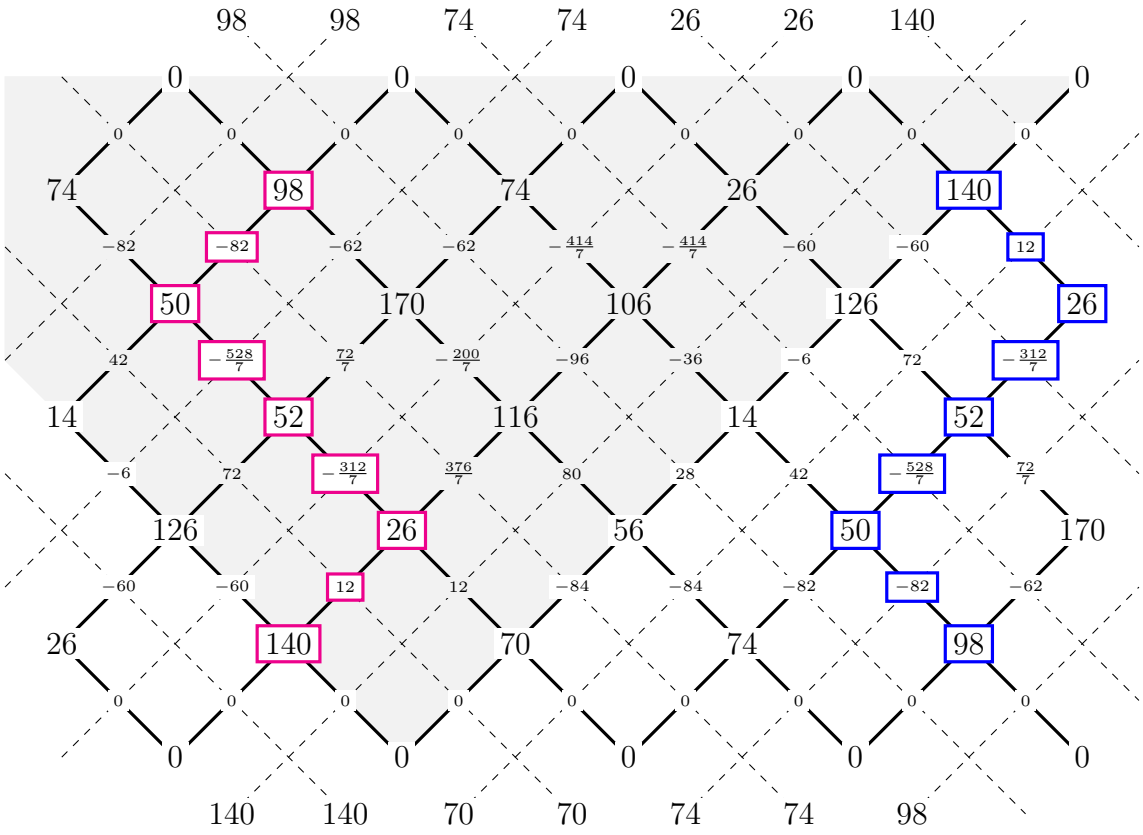
by

Katie Waddle

A dissertation submitted in partial fulfillment
of the requirements for the degree of
Doctor of Philosophy
(Mathematics)
in The University of Michigan
2026

Doctoral Committee:

Professor Sergey Fomin, Chair
Professor Anna Felikson
Professor Mark Guzdial
Professor Thomas Lam
Professor George Seelinger


98 98 74 74 26 26 140
0 0 0 0 0
0 0 0 0 0 0 0 0 0 0
74 98 74 26 140
−82 −82 −62 −62 −414/7 −414/7 −60 −60 12
50 170 106 126 26
42 −528/7 72/7 −200/7 −96 −36 −6 72 −312/7
14 52 116 14 52
−6 72 −312/7 376/7 80 28 42 −528/7 72/7
126 26 56 50 170
−60 −60 12 12 −84 −84 −82 −82 −62
26 140 70 74 98
0 0 0 0 0 0 0 0 0 0
0 0 0 0 0
140 140 70 70 74 74 98

Caitlin Waddle
waddle@umich.edu
ORCID iD: 0000-0003-3274-7523

© Caitlin Waddle 2026

DEDICATION

to the students of San Francisco International High School

la vida es larga

ACKNOWLEDGEMENTS

I am deeply grateful for my advisor Sergey Fomin's gracious welcome to research in algebraic combinatorics. Over the last 5 years we have spent countless hours discussing ideas, editorial suggestions, and professional activities. I was also fortunate to take several meticulously prepared courses from him. Throughout our time together he has taken care to teach me both math and the practice of math: good writing, math pedagogy, formulating interesting research questions, chasing down sources. From the beginning he has treated me as a colleague, and this has profoundly influenced my identity as a mathematician.

Portions of this research were funded by NSF grants DMS-1840234, DMS-2054231 and DMS-2348501. I performed all computations in `Sage`, and explored examples using `Geogebra`. I thank Sergei Tabachnikov, Anna Felikson, and Linus Setiabrata for interesting discussions and feedback. I'm grateful to Sergey Fomin for sharing his observation that the diamond rule in a frieze pattern can be geometrically interpreted as Casey's formula. I also thank Michael Shapiro, who asked whether Theorems 2.2 and 2.3 could be obtained from each other, which began the exploration that led to Chapter 2.

I had the privilege to attend several conferences during my time in Michigan. I am grateful to the organizers of the conference Frieze patterns in algebra, combinatorics and geometry at the Centre International de Recontres Mathématiques in May of 2025 for allowing me to share the work in this thesis. The American Institute of Mathematics workshop Gender Equity in the Mathematical Sciences (GEMS) of Combinatorics in March of 2023 and the Roots of Unity workshop in June of 2022 also provided collegial environments where I met several mentors and friends, including Dorian, Selvi, Esther, Mariel, Mitsuki, and John.

Michigan has a wonderful combinatorial community, and I am grateful to all those who shared their math with me over the years, and all those who generously listened as I learned to share mine well. Among many others, I received a great deal of both mentorship and camaraderie from George, Lei, Melissa, Scott, João, Shelby, Drew, Mia, Ram, Oliver, Oscar, Jose, Janet, Tim, Nate, Nir, and Yushan.

I was able to participate in a number of different impactful groups at Michigan. Thank you especially to my fellow Association for Women in Math student chapter executive board members for the warm and welcoming spaces we created over the years, I'm proud of what we built together. Thanks to the Learning Community for Inclusive Teaching for keeping

our work grounded in supporting students. And thanks to the many various members of my Conor O'Neill's trivia team over the years.

My journey to research mathematics began at San Francisco State University. I owe a debt of gratitude there to Dusty and Emily, as well as Kim, Chun-Kit, Serkan, Matt, Angel, Vanessa, Brittney, Anastasia, Rose, Dante, Jodi, June, Hal, Aditi, and many others.

I moved to Ann Arbor without knowing a soul, and am leaving with many friends who feel like family. I would especially like to recognize Han, Havi, and Amanda, I'm so grateful for your friendship. Cheers to Caitie and James, Margaret, Beth, Tracy, and the Femme Trans Women biking group at Common Cycle. Thanks to my many housemates, especially Abha, Mar, Allie, Ryan, and Rachel, and thank you to Teresa and Alex for helping me through the pandemic. Emily, you are the single best Craigslist find of all time.

My mom, Carey, my dad, John, and my sisters, Sarah and Ellie, have been with me every step of this process. Thank you from the bottom of my heart. I am also grateful to my friends around the country who cheered me on during my doctoral studies: Els and Victoria in Boston, Anna, Becky, Chris, and Frances in Washington, D.C., Jordan, Hannah, Nick, and Shira in the Bay, Puja and Elizabeth in Eugene, and all of the crew in Minnesota. Finally, thank you, Evie, for making me a teacher.

TABLE OF CONTENTS

DEDICATION ii

ACKNOWLEDGEMENTS iii

LIST OF FIGURES vi

ABSTRACT viii

CHAPTER

1 Introduction **1**

1.1 Coxeter-Conway frieze patterns 2
1.2 Geometric interpretations of Coxeter-Conway friezes 5
1.3 New frieze patterns from geometric configurations 9

2 Geometric Incarnations of 3-term Relations **18**

2.1 Four incarnations of the 3-term relation 18
2.2 Each equation implies the others 20
2.3 The torus action 22
2.4 The cross-ratio 23
2.5 Models of the hyperbolic plane 24
2.5.1 The upper half plane 24
2.5.2 The Poincaré disk 25
2.5.3 The hyperboloid 25
2.6 Horocycles and lambda lengths 26
2.7 Proof of Proposition 2.6 28
2.8 Generalizations and historical notes 29

3 Spherical Friezes **31**

3.1 Measurements associated to spherical triangles 31
3.2 Spherical quadrilaterals 37
3.3 Spherical Heronian friezes 43
3.4 Rational expressions for spherical Heronian friezes 60
3.5 Spherical Cayley-Menger friezes 66
3.6 Spherical Cayley-Menger friezes vs. spherical Heronian friezes 80

BIBLIOGRAPHY 85

LIST OF FIGURES

FIGURE

1.1 Friezes on the facade of a building at the University of Toronto, where H. S. M. Coxeter served as a professor for 60 years [Wad25]. 1
1.2 A Coxeter-Conway frieze pattern of width 4. 3
1.3 Generic Coxeter-Conway frieze pattern of width 2 and order 5. The entries outlined in magenta lie on a traversing path. To see the glide symmetry, flip the gray shaded region upside down and paste it to the right of its original location. 3
1.4 A portion of the index set for a Coxeter-Conway frieze of order 4. 4
1.5 Distances between four points on a circle 5
1.6 A Coxeter-Conway frieze and heptagon that correspond combinatorially. 7
1.7 Left: Measurements in a spherical quadrilateral $A_1A_2A_3A_4$ include: (i) six squared distances: $a = x_{14}, b = x_{12}, c = x_{23}, d = x_{34}, e = x_{13}, f = x_{24}$; (ii) four measurements $S^K(A_i, A_j, A_k)$ associated with the triangles $A_iA_jA_k$: $p = S^K(A_1, A_2, A_3), q = S^K(A_1, A_3, A_4), r = S^K(A_1, A_2, A_4), s = S^K(A_2, A_3, A_4)$. Right: the same measurement data, arranged in a spherical Heronian diamond. 12
1.8 An example of a spherical Heronian frieze. To see the glide symmetry, flip the gray shaded region upside down and paste it to the right of its original location. The magenta and blue entries form two traversing paths. 14
1.9 A spherical Cayley-Menger frieze of order 6. 16

2.1 Distances between four points on a circle 18
2.2 Bitangent distances between four circles tangent to a fifth circle 19
2.3 Hyperbolic distances between horocycles 20
2.4 The measurements d_{ij}, t_{ij}, and δ_{ij} 22
2.5 The ideal points W_1' and W_2' used to compute the hyperbolic distance between W_1 and W_2 25
2.6 The signed hyperbolic distance between two horocycles 27
2.7 Measurements used to calculate d_{ij} 29

3.1 Measurements associated to triangulations of a spherical quadrilateral. 38
3.2 Left: A spherical quadrilateral $A_1A_2A_3A_4$ as discussed in Example 3.15. Right: A spherical Heronian diamond. 45
3.3 Spherical distances (in km) between four American cities [Swa]. 48
3.4 Squared Euclidean distances between the four cities (in km^2). 48
3.5 Left: In a spherical polygon, any four vertices A_i, A_j, A_k, A_l form a spherical quadrilateral. Right: The corresponding spherical Heronian diamond. 52

3.6 A portion of the index set I_6^{SH}, it extends infinitely to the right and left. For the points of the form $\left(i+\frac{1}{2}, j\right)$ and $\left(i, j+\frac{1}{2}\right)$ (indicated with black filled-in circles), the labels are not shown. Interior nodes lie in the gray shaded region. The dashed lines have labels of the form $(i+\frac{1}{2}, \diagup)$ or $(\diagdown, j+\frac{1}{2})$. 53
3.7 A spherical Heronian frieze of order 6. This frieze corresponds to a hexagon on a sphere with radius 7. 54
3.8 The vertices of the spherical hexagon $A_1A_2A_3A_4A_5A_6$ lie on the sphere of radius 7 centered at the origin in $\mathbb{R}^3$. 56
3.9 The same spherical Heronian frieze as in Figure 3.7, this time illustrating the glide symmetry. To see it, flip the gray shaded region upside down and paste it to the right of its original location. The blue and magenta highlighted entries form two separate traversing paths. Thanks to the glide symmetry, their entries form identical sets. Both paths correspond to the triangulation shown in Figure 3.10. 57
3.10 Frieze entries for the hexagon $A_1A_2A_3A_4A_5A_6$ from Figure 3.8. These frieze entries lie on the traversing path shown in Figure 3.9. 58
3.11 The trimmings of triangulation G with respect to diagonal $\{2, 6\}$ and triangle $\{1, 3, 7\}$ respectively. 61
3.12 The procedure described in Lemma 3.67. 63
3.13 Using flips to derive an identity for S_{246}^K. 64
3.14 A visualization of a portion of the index set I_6^{SCM}. The set extends to the right and left. All nodes in the grey shaded region are interior. 70
3.15 A portion of a spherical Cayley-Menger frieze $\mathbf{z}$ of order 6. This frieze corresponds to the hexagon on a sphere with radius 7 in Figure 3.8, the same polygon that gives rise to the spherical Heronian frieze in Figure 3.7. To visualize the glide symmetry, flip the gray shaded region upside down and paste it to the right of its original location. The blue and magenta entries form two separate traversing paths, their entries form identical sets. 71
3.16 Notation for partial derivatives of $M_4^K(a, b, c, d, e, f)$. 73
3.17 Four interlocking Cayley-Menger diamonds. 75
3.18 The same Cayley-Menger frieze as Figure 3.15. The entries highlighted in magenta are the thickening of the traversing path on the left indicated by magenta lines. 79
3.19 Four interlocking spherical Heronian diamonds as in Proposition 3.99. The starred entries appear in the coherence condition on the corresponding spherical Cayley-Menger diamonds. 82

ABSTRACT

A fundamental problem in distance geometry aims to recover a finite tuple of points, viewed up to oriented isometry, from a small collection of input measurements. This thesis explores approaches to this problem based on the use of frieze patterns, numerical arrays whose entries satisfy certain local algebraic relations.

The thesis consists of two main parts. The first part focuses on quadratic 3-term relations that underlie Coxeter-Conway frieze patterns. It surveys and extends existing work interpreting the values appearing in these relations as geometric measurement data, and establishes direct connections between several geometric contexts in which these relations arise.

The aim of the second part of the thesis is to exhibit the broader applicability of frieze patterns as a tool in distance geometry. We identify measurement data that determines a finite configuration of points on a two-dimensional sphere in three-dimensional Euclidean space. Extending the work of Fomin and Setiabrata, we introduce spherical Heronian and Cayley-Menger frieze patterns that organize this measurement data. Like classical Coxeter-Conway frieze patterns, these new frieze patterns exhibit glide symmetry and a form of the Laurent phenomenon.

CHAPTER 1

Introduction



Figure 1.1: Friezes on the facade of a building at the University of Toronto, where H. S. M. Coxeter served as a professor for 60 years [Wad25].

Distance geometry studies point configurations via measurements of pairwise distances between the points. More generally, one can consider any intrinsic measurements that do not depend on a choice of coordinate system. In a Euclidean space, such measurements can include distances, angles, (oriented) volumes, etc. A typical problem asks for a small set of inputs, or initial data, that uniquely determine a configuration up to orientation-preserving isometry. One can further ask for explicit formulas that express, in terms of the initial data, arbitrary measurements of a particular kind—say, all pairwise distances in a configuration.

This thesis explores the use of frieze patterns to organize the data in distance geometry problems. A (generalized) frieze pattern is a numerical array with finitely many infinite rows in which each local grouping of numbers satisfies a set of relations. Starting with the entries along a path that traverses the frieze from top to bottom, one can use the local relations to propagate outwards and recover the rest of the entries. In particular, when the entries

represent geometric data, then the subset of data along any traversing path in the frieze can serve as an initial data set from which the rest of the data can be recovered.

Frieze patterns have been applied to distance geometry problems since their introduction by H. S. M. Coxeter in 1971. Coxeter previously studied friezes in art and architecture, there the term is used for periodic visual patterns on a strip or ribbon that exhibit various symmetries [Cox69] (cf., Figure 1.1). The mathematics of such symmetries has been studied for millennia, see, e.g., [FT64]. While investigating rational recurrences among the lengths of great-circle arcs on a sphere (a problem of Napier and Gauss known as Pentagramma Mirificum), Coxeter organized the geometric measurement data in a numerical array that he called a frieze pattern [Cox71]. Coxeter and J. H. Conway went on to develop a combinatorial interpretation of frieze patterns with positive integer entries via triangulations of polygons and Ptolemy's theorem [CC73].

In the 1970s, Coxeter and others continued to explore frieze patterns combinatorially [CR72, BCI74, Lan75, She76], as well as geometrically through orthoschemes [Böh71, Cox74]. In subsequent decades, the study of frieze patterns was mostly abandoned, and they were mostly viewed as a kind of recreational curiosity [CR94, Sta99]. This changed around 2002, when Fomin and Zelevinsky observed [FZ02b] that frieze patterns provide an instance of the Laurent phenomenon (cf. Theorem 1.5) in the context of the recently introduced cluster algebras [FZ02a]. The connection between frieze patterns and cluster algebras was fleshed out in several papers, including [Pro20, CC06, CCS06, ARS10]. Frieze patterns subsequently found numerous applications in the study of quiver representations, discrete integrable systems, moduli spaces, and other mathematical fields. Relevant historical details, applications, and generalizations can be found in the excellent surveys [MG15, Pre23, Fab25] and in the compendium [Fel25].

1.1 Coxeter-Conway frieze patterns

Definition 1.1. A Coxeter-Conway frieze pattern (or simply a frieze) is a multi-line array of numbers (organized as shown in Figure 1.2) that satisfies the following conditions:

1. The first and last rows are filled with 0's.
2. The second and penultimate rows are filled with 1's.
3. Adjacent entries a, b, c, d in the frieze that form a 2×2 diamond $\begin{smallmatrix} & b & \\ a & & c \\ & d & \end{smallmatrix}$ satisfy the relation $ac - bd = 1$, known as the unimodular rule.

The width of the frieze is the number of rows strictly between the two rows of 1's. A frieze of width d has order $n = d + 3$.

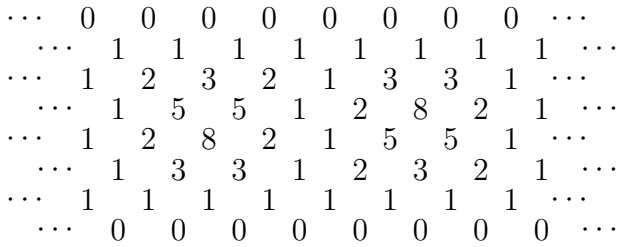


Figure 1.2: A Coxeter-Conway frieze pattern of width 4.

Remark 1.2. The unimodular rule's name comes from viewing a diamond of entries $\begin{smallmatrix} & b & \\ a & & c \\ & d & \end{smallmatrix}$ as a 2×2 matrix rotated counterclockwise by $\pi/4$. Using this perspective, Coxeter-Conway frieze patterns are sometimes called SL_2-friezes. Cordes and Roselle [CR72] and later Assem, Reutenauer, and Smith [ARS10] generalized SL_2-friezes to get SL_2-tilings of the plane, an assignment of numbers to points in $\mathbb{Z}^2$ such that each local diamond satisfies the unimodular rule. SL_2-tilings are a particular case of objects in theoretical physics called T-systems. SL_2-friezes and tilings were further generalized to SL_k-friezes and tilings, see, e.g., [BR10, MGOST14].

Remark 1.3. Coxeter required the entries of frieze patterns to be positive [Cox71], and Coxeter and Conway [CC73] mostly focused on enumeration of positive integral frieze patterns. Modern scholars of SL_k-friezes and tilings (see Remark 1.2) generally require tameness, the more general condition that $(k+1) \times (k+1)$ diamonds of entries (viewed as matrices) are singular. Coxeter-Conway SL_2 frieze patterns with positive entries are tame. For further discussion, see [MG15, Cun17].

Figure 1.3 shows a generic width 2 Coxeter-Conway frieze pattern with variable entries.

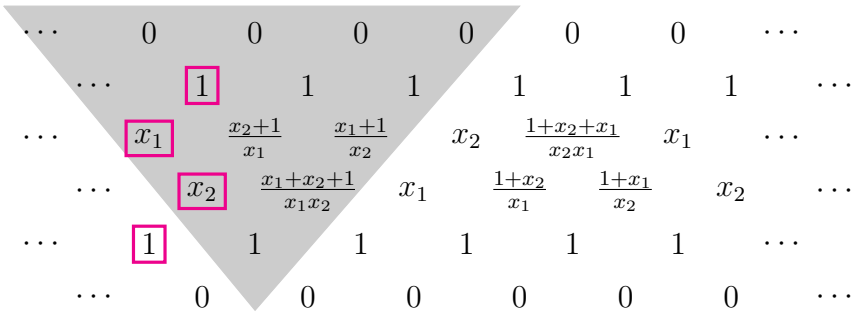


Figure 1.3: Generic Coxeter-Conway frieze pattern of width 2 and order 5. The entries outlined in magenta lie on a traversing path. To see the glide symmetry, flip the gray shaded region upside down and paste it to the right of its original location.

Definition 1.4. A traversing path is a set of entries in the frieze along a path from top to bottom (see, e.g., the entries $1, x_1, x_2, 1$ outlined in magenta in Figure 1.3).

Starting with the entries along a traversing path in a frieze, one can recursively apply the unimodular rule to compute all the remaining entries in the frieze. A priori, one might expect the entries to take the form of increasingly complex rational expressions. As Figure 1.3 exemplifies, this is not the case.

Theorem 1.5 ([FZ02a, FZ02b])**.** *Let* $\mathbf{z}$ *be a Coxeter-Conway frieze. Let* π *be a traversing path in* $\mathbf{z}$*, and let* $\mathbf{z}_\pi$ *be the collection of the entries along* π*. Then every entry of the frieze can be written as a Laurent polynomial in the entries in* $\mathbf{z}_\pi$*.*

The property described in Theorem 1.5 is known as Laurentness.

Remark 1.6. As a consequence of Proposition 1.5, if we place 1's along any traversing path in a frieze and propagate outwards using the local relations, all the entries in the frieze will be integers. Note that there exist Coxeter-Conway friezes with integer entries and no traversing path of 1's [Cox71].

We index the entries in a Coxeter-Conway frieze of order n by the set

$$I_n = \{(i, j) \in (\mathbb{Z} \times \mathbb{Z}) \mid i \leq j \leq i + n\} \subseteq \mathbb{Z}^2$$

which is rotated clockwise by $\pi/4$ so that the points (i, i) lie along the bottom of the strip and the points $(i, i + n)$ run along the top, see, e.g., Figure 1.4.

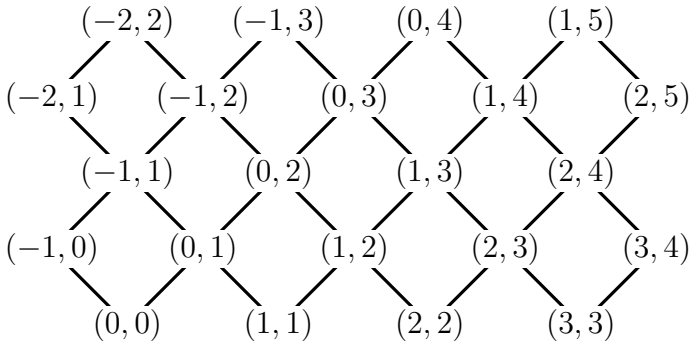


Figure 1.4: A portion of the index set for a Coxeter-Conway frieze of order 4.

Starting from the entries along a traversing path in a frieze and propagating outwards, one might expect to observe infinitely many unique entries. Indeed, for some choices of initial entries this happens (see [Cun17, Zab25]). However, the following is true.

Theorem 1.7 ([Cox71])**.** *Let* $\mathbf{z}$ *be a Coxeter-Conway frieze with positive entries (or more generally, a frieze that is tame, see Remark 1.3). Then* $\mathbf{z}$ *is* n*-periodic: the entries at locations* (k, ℓ) *and* $(k+n, \ell+n)$ *are equal. In fact,* $\mathbf{z}$ *possesses glide symmetry, cf. Figure 1.3.*

1.2 Geometric interpretations of Coxeter-Conway friezes

Theorem 1.7 (the periodicity of Coxeter-Conway frieze patterns) is a surprising algebraic statement. It is reasonable to ask whether we can connect frieze patterns to more obviously periodic objects. One approach is to interpret the entries of frieze patterns as geometric measurements. As a first attempt, we will consider point configurations in the real Euclidean plane $\mathbb{E}^2$.

Let $\mathrm{Aut}(\mathbb{E}^2)$ denote the group of isometries of $\mathbb{E}^2$. Let P_n denote a regular convex n-gon in $\mathbb{E}^2$ with side lengths 1. Note P_n is unique up to the action of $\mathrm{Aut}(\mathbb{E}^2)$, we can assume it is inscribed in the circle $\mathbf{S}_n$ with radius $\frac{1}{2\sin(\pi/n)}$ centered at the origin. Label its vertices $A_1, \ldots, A_n$ in consecutive counterclockwise order. Denote by d_{ij} the (positive) distance between A_i and A_j in P_n.

Proposition 1.8. *Let* $\mathbf{z} = \mathbf{z}(P_n)$ *be a numerical array with index set* I_n*. Set entry* $z_{(i,j)} = d_{\langle i \rangle \langle j \rangle}$ *where* $\langle m \rangle$ *denotes the unique integer* k *in* $\{1, \ldots, n\}$ *satisfying* $m \equiv k \,(mod\ n)$*. Then* $\mathbf{z}(P_n)$ *is a Coxeter-Conway frieze.*

The proof of Proposition 1.8 relies on the following theorem of Ptolemy.

Theorem 1.9 ([Pto14, Book 1, Sec. 10, Lem. 1.1], cf. Theorem 2.1)**.** *Let* A_1, A_2, A_3, A_4 *be four points arranged counterclockwise on a circle* $\mathbf{S}$ *on the Euclidean plane. For* $1 \leq i < j \leq 4$*, let* d_{ij} *denote the distance from* A_i *to* A_j*, see Figure 1.5. Then*

$$d_{12}d_{34} + d_{14}d_{23} = d_{13}d_{24}.$$

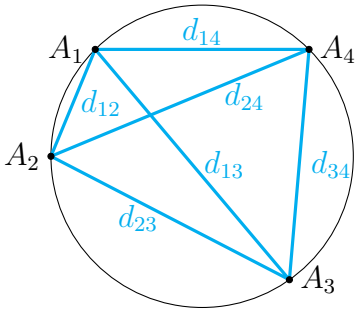


Figure 1.5: Distances between four points on a circle

Proof of Proposition 1.8. Conditions 1 and 2 hold, since

$$z_{i,i}, z_{i,i+n} = d_{\langle i\rangle,\langle i\rangle} = 0\,,$$
$$z_{i,i+1}, z_{i,i+n-1} = d_{\langle i\rangle,\langle i+1\rangle} = 1\,.$$

It remains to verify the unimodular rule in $\mathbf{z}(P_n)$ (condition 3). Consider entries

$$z_{i,j}, z_{i,j+1}, z_{i+1,j}, z_{i+1,j+1} \in \mathbf{z}(P)\,,$$

that form a diamond $\begin{smallmatrix} & (i,j+1) & \\ (i,j) & & (i+1,j+1) \\ & (i+1,j) & \end{smallmatrix}$. The points $A_i, A_{i+1}, A_j, A_{j+1}$ form an inscribed quadrilateral, thus by Ptolemy's Theorem 1.9:

$$z_{i,i+1}z_{j,j+1} + z_{i,j+1}z_{i+1,j} = z_{ij}z_{i+1,j+1}\,.$$

Since $z_{i,i+1} = z_{j,j+1} = 1$, the unimodular rule holds: $z_{ij}z_{i+1,j+1} - z_{i,j+1}z_{i+1,j} = 1$. □

A key feature of the correspondence between P_n and $\mathbf{z}(P_n)$ is the following.

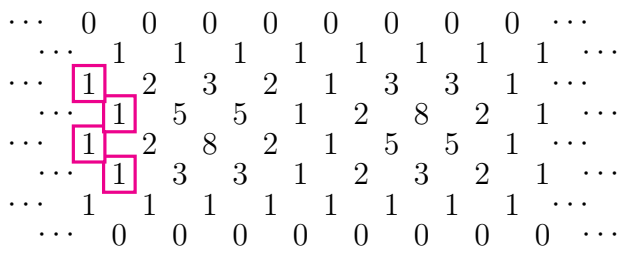
Proposition 1.10 (cf. Definition 3.30, Remark 3.53)**.** *Let $\mathbf{z}_-$ be the entries along a traversing path π in $\mathbf{z}(P_n)$. The entries $z_{ij} \in \mathbf{z}_-$ are the distances d_{ij} corresponding to diagonals in a triangulation T of P_n.*

In the setting of Proposition 1.10, if a diagonal A_iA_j in T is removed, there exists a unique diagonal A_kA_l that can replace it to form a new triangulation T', a move called a flip (cf. Definition 3.65). The new corresponding distance d_{kl}, and hence the entry z_{kl}, can be computed using Ptolemy's theorem, á la the unimodular rule. Swapping A_iA_j for A_kA_l results in a new triangulation T', whose associated distances are the entries along a new traversing path π' in $\mathbf{z}(P_n)$. As we continue flipping diagonals, we cycle through finitely many possible triangulations, and ultimately return to T, illuminating the periodicity of $\mathbf{z}(P_n)$ we asserted in Theorem 1.7.

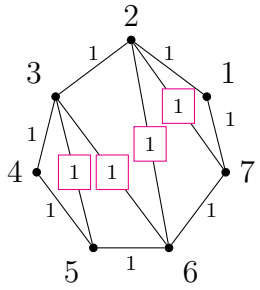
However, the above arguments cannot be used to establish Theorem 1.7. Far from it, there exists exactly one Coxeter-Conway frieze $\mathbf{z}(P_n)$ for each n. Its entries are mostly non-integral. For example, in $\mathbf{z}(P_4)$ we have $\mathbf{z}_{i,i+2} = \sqrt{2}$ for all i. To elucidate the periodicity phenomenon in Theorem 1.7 and extend it to other contexts, there are several natural directions for exploration, including the following three:

1. Chapter 2 surveys and extends existing work interpreting the entries of Coxeter-Conway frieze patterns as geometric measurement data. See a summary of main results below.

2. Coxeter and Conway [CC73] gave a combinatorial interpretation of frieze patterns via triangulations of polygons considered as combinatorial objects. For an example of a Coxeter-Conway frieze and its combinatorially associated polygon, see Figure 1.6.



(a) A Coxeter-Conway frieze pattern of order 7. The magenta entries lie along a traversing path.



(b) A triangulated heptagon. The magenta labels correspond to the traversing path in (a).

Figure 1.6: A Coxeter-Conway frieze and heptagon that correspond combinatorially.

Later, it was found that tame Coxeter-Conway frieze patterns correspond combinatorially to the type A cluster algebras, such as Grassmannians of planes (for an explanation see [Fel23]). The correspondence involves a quiver that can be defined on a triangulation of a polygon. See, for example, a survey [Wil14], a textbook [FWZ24], the collection of resources [Fom25], as well as interesting visualizations in [dSG25]. The unimodular rule in a frieze corresponds to the mutation rule in a cluster algebra of type A.

3. In geometric settings, it is natural to consider polygons with varying side lengths. For example, Ptolemy's Theorem 1.9 applies more generally. Relatedly, the connection to cluster algebras described above motivates the introduction of frieze patterns corresponding to cluster algebras with coefficients. Hence, frieze patterns with coefficients were introduced in [Pro20, CHJ20]. There, condition 2 of Definition 1.1 is relaxed and condition 3 is appropriately modified. These objects have been studied and generalized further. See, e.g., [CH21, Mal23, Cun23, dSGHL23].

Main results of Chapter 2

For each n, there exists exactly one order n Coxeter-Conway frieze pattern $\mathbf{z}(P_n)$ whose entries represent distances in a polygon P_n in $\mathbb{E}^2$ (see Proposition 1.8). On the other hand, there are different geometric configurations that can realize all Coxeter-Conway frieze patterns.

The key observation in the construction of $\mathbf{z}(P_n)$ was the interpretation of the unimodular rule as Ptolemy's Theorem relating the distances d_{ij} in a cyclic quadrilateral (Theorem 1.9). Ptolemy's Theorem can be viewed as an instance of an abstract 3-term relation of the form $a_{12}a_{34} + a_{14}a_{23} = a_{13}a_{24}$. Other instances include:

- Casey's theorem relating bitangent distances t_{ij} among four circles $H_1, \ldots, H_4$ with radii $r_1, \ldots, r_4$ adjacent to a common circle (cf. Theorem 2.2):

$$t_{12}t_{34} + t_{14}t_{23} = t_{13}t_{24}\,,$$

- Penner's theorem relating lambda lengths λ_{ij} between ideal points $A_1, \ldots, A_4$ decorated by horocycles $H_1, \ldots, H_4$ on the boundary of the hyperbolic plane (cf. Theorem 2.3):

$$\lambda_{12}\lambda_{34} + \lambda_{14}\lambda_{23} = \lambda_{13}\lambda_{24}\,,$$

- and Plücker's identity for the maximal minors P_{ij} of a 2×4 matrix (cf. Theorem 2.4):

$$P_{12}P_{34} + P_{14}P_{23} = P_{13}P_{24}\,.$$

For precise definitions and statements see Chapter 2.

It is natural to wonder whether the above relations can be directly deduced from each other. We make the following algebraic observation (cf. Observation 2.5):

Observation 1.11. Let $(a_{12}, a_{13}, a_{14}, a_{23}, a_{24}, a_{34})$ and $(b_{12}, b_{13}, b_{14}, b_{23}, b_{24}, b_{34})$ be two 6-tuples of numbers. Suppose that there exist nonzero numbers q_1, q_2, q_3, q_4 such that $b_{ij} = q_i q_j a_{ij}$ for $1 \leq i < j \leq 4$. The numbers a_{ij} satisfy the 3-term relation

$$a_{12}a_{34} + a_{14}a_{23} = a_{13}a_{24}$$

if and only if the numbers b_{ij} satisfy the 3-term relation

$$b_{12}b_{34} + b_{14}b_{23} = b_{13}b_{24}.$$

We apply Observation 1.11 to the measurements $d_{ij}, t_{ij}, \lambda_{ij}, P_{ij}$ (which play the roles of a_{ij}, b_{ij}), thereby directly connecting the contexts in which these measurements arise. Specifically, we show that these measurements are related to each other by rescaling, as follows.

Proposition 1.12 (cf. Proposition 2.6)**.** *In the settings described above,*

$$\begin{aligned} t_{ij} &= \sqrt{1-r_i}\sqrt{1-r_j}d_{ij}\,, \\ t_{ij} &= \lambda_{ij}\sqrt{2r_i}\sqrt{2r_j}\,, \\ d_{ij} &= 2P_{ij}\,. \end{aligned}$$

Structure of Chapter 2

Section 2.1 introduces four geometric incarnations of the three-term relation

$$a_{12}a_{34} + a_{14}a_{23} = a_{13}a_{24}\,.$$

Our main observation about scaling in relations of this type is given in Section 2.2, along with our application of the observation, Proposition 2.6. We recast the rescaling as a torus action in Section 2.3, and rephrase it using cross-ratios in Section 2.4. We provide the necessary background on models of the hyperbolic plane, horocycles, and lambda lengths in Section 2.5-2.6. Proposition 2.6 is proved in Section 2.7. In Section 2.8 we conclude with generalizations and historical context.

1.3 New frieze patterns from geometric configurations

In Chapter 3, we study point configurations and associated measurement data in the setting of spherical geometry.

Let $\mathbf{S}$ be a sphere of radius R in 3-dimensional Euclidean space. Viewed up to oriented isometry, the space of n-point configurations on $\mathbf{S}$ has dimension $2n-3$. We seek to identify a size $O(n)$ subset of initial measurements from which all pairwise distances between n given points can be recovered. We require the corresponding formulas to be rational, in particular to avoid the use of trigonometric functions or their inverses. In service of this goal, we measure pairwise distances between points on $\mathbf{S}$ in the ambient Euclidean space, rather than via geodesics on the sphere. (The two types of distances can be readily converted into each other.)

We present two solutions to the problem above. In the first solution, the initial input consists of $2n-3$ squared Euclidean distances between certain pairs of points in an n-point configuration on the sphere, together with $n-2$ additional binary bits of information specifying the orientations of certain spherical triangles. The second solution utilizes $3n-4$ squared distances. In each case, the initial data determine the n-point configuration uniquely up to an isometry of the sphere.

To capture the measurement data involved in our algorithms and the algebraic relations among them, we introduce two different but closely related record-keeping devices that we call spherical friezes. These friezes extend from Euclidean to spherical settings the Heronian friezes of Fomin and Setiabrata [FS21], which were in turn inspired by the classical Coxeter-Conway friezes [Cox71, CC73]. The spherical friezes display how the initial measurements propagate to determine the others. They can also be viewed as purely algebraic instruments: numerical arrays whose neighboring entries satisfy certain relations. We prove that, like other types of friezes, spherical friezes exhibit glide symmetry and a form of the Laurent phenomenon.

Main results of Chapter 3

Fix a sphere $\mathbf{S}$ of radius R in 3-dimensional Euclidean space. A spherical polygon $A_1 \cdots A_n$ is an ordered n-tuple of points $A_1, \ldots, A_n \in \mathbf{S}$. The group $\mathrm{Aut}(\mathbf{S})$ of orientation-preserving isometries of $\mathbf{S}$ acts on the space $\mathbf{S}^n$ of such n-tuples. Spherical distance geometry does not distinguish between spherical polygons that lie in the same $\mathrm{Aut}(\mathbf{S})$-orbit. Accordingly, we will only be interested in numerical quantities (measurements) associated with a spherical polygon that are intrinsic, i.e. $\mathrm{Aut}(\mathbf{S})$-invariant. Such a measurement is a function $\mathbf{S}^n/\operatorname{Aut}(\mathbf{S}) \to \mathbb{R}$. The basic example is a squared Euclidean distance

$$x_{ij} = x(A_i, A_j) \tag{1.3.1}$$

between two points A_i, A_j lying on the sphere $\mathbf{S}$.

It is natural to seek a coordinatization of the configuration space $\mathbf{S}^n/\operatorname{Aut}(\mathbf{S})$ that enables calculations performed entirely in terms of intrinsic measurements. Since $\dim \mathbf{S}^n/\operatorname{Aut}(\mathbf{S}) = 2n-3$, we would like this coordinatization to involve at most $O(n)$ measurements whose values uniquely determine a spherical polygon, up to the $\mathrm{Aut}(\mathbf{S})$ action. We additionally ask that the formulas that express all basic measurements in terms of the chosen coordinates be rational, i.e., involve only the four arithmetic operations. This rules out the standard formulas found in the spherical geometry literature, as they involve square roots, trigonometric functions, and/or their inverses, see for example [Tod86, Chapter 8],[FF20],[BM12].

We begin by interpreting a spherical polygon as a purely combinatorial object, mapping its vertices $A_1, \ldots, A_n$ to the vertices of a convex n-gon on a real plane. Consider a triangulation of this planar n-gon obtained by drawing $n-3$ diagonals. The $2n-3$ sides and diagonals of this triangulation correspond to $2n-3$ measurements x_{ij} in the spherical polygon. However, these $2n-3$ measurements are not sufficient to determine the spherical

polygon up to the Aut($\mathbf{S}$) action, because each of the $n-2$ spherical triangles $A_iA_jA_k$ is only determined by the measurements x_{ij}, x_{ik}, x_{jk} up to a (potentially orientation-altering) isometry. Since each of these triangles can be placed on the sphere in two different ways, we get, up to the Aut($\mathbf{S}$) action, 2^{n-2} distinct spherical n-gons (or 2^{n-3} distinct n-gons, up to isometry). This ambiguity can be resolved by supplementing the initial data with additional measurements that "rigidify" the geometry of the configuration.

We implement two versions of this strategy. In the first version we make use of the following quantity that is invariant under the action of Aut($\mathbf{S}$).

Definition 1.13 (cf. Definition 3.2)**.** Let $A_1, A_2, A_3 \in \mathbf{S}$ be three points on a sphere $\mathbf{S}$ with center O, radius R, and Gaussian curvature $K = \frac{1}{R^2}$. We denote

$$S^K(A_1, A_2, A_3) = \frac{12V(OA_1A_2A_3)}{R}\,, \tag{1.3.2}$$

where $V(OA_1A_2A_3)$ is the signed Euclidean volume of the tetrahedron $OA_1A_2A_3$.

Remark 1.14. Informally, $S^K(A_1, A_2, A_3)$ is a stand-in for the (normalized) oriented Euclidean area of the triangle $A_1A_2A_3$. Rigid motions that change the orientation of the triangle also change the sign of this measurement, so it can be used to distinguish between the two triangles with given side lengths.

The following proposition illustrates the relationship between the measurements (1.3.1) and (1.3.2).

Proposition 1.15 (cf. Proposition 3.11)**.** *For $A_1, A_2, A_3 \in \mathbf{S}$, we have*

$$\Big(S^K(A_1, A_2, A_3)\Big)^2 = \det \begin{bmatrix} \frac{K}{2} & 1 & 1 & 1 \\ 1 & 0 & x_{12} & x_{13} \\ 1 & x_{21} & 0 & x_{23} \\ 1 & x_{31} & x_{32} & 0 \end{bmatrix} = H^K(x_{12}, x_{13}, x_{23})\,, \tag{1.3.3}$$

where we use the notation

$$H^K(x_{12}, x_{13}, x_{23}) = -x_{12}^2 - x_{13}^2 - x_{23}^2 + 2x_{12}x_{13} + 2x_{12}x_{23} + 2x_{13}x_{23} - Kx_{12}x_{13}x_{23}. \tag{1.3.4}$$

In the flat limit $R \to \infty$ (i.e., for $K = 0$), Proposition 1.15 recovers a well-known formula for the squared area of a triangle $A_1A_2A_3$ on the Euclidean plane in terms of the squared lengths x_{ij} of its sides A_iA_j, an application of the Cayley-Menger determinant. The case $K = 0$ of Proposition 1.15 can also be seen as a restatement of the classical Heron's

formula for the area of a Euclidean triangle. We therefore call equation (1.3.3) the (spherical) Heron equation. The determinant in (1.3.3) is known as the spherical Cayley-Menger determinant, which we learned about in T. Tao's blog post [Tao19], cf. [Aud11, BG43].

The squared side distances x_{ij}, x_{ik}, x_{jk}, together with one of the two possible values of $S^K(A_i, A_j, A_k)$ allowed by (1.3.3), determine a spherical triangle $A_iA_jA_k$ up to oriented isometry. This leads to our first coordinatization of $\mathbf{S}^n/\operatorname{Aut}(\mathbf{S})$ that involves the $2n-3$ squared distances x_{ij} associated to the sides and diagonals in a triangulation T of an n-gon, plus the $n-2$ measurements $S^K(A_i, A_j, A_k)$ associated to the triangles of T.

We next write formulas expressing all basic measurements for a spherical polygon in terms of this initial data. We begin with the case of a spherical quadrilateral $A_1A_2A_3A_4$, see Figure 1.7.

The ten measurements associated with the quadrilateral $A_1A_2A_3A_4$ (the $\binom{4}{2} = 6$ squared distances x_{ij} and the $\binom{4}{3} = 4$ measurements $S^K(A_i, A_j, A_k)$) satisfy four instances of the Heron equation (1.3.3):

$$\begin{aligned} p^2 &= H^K(b, c, e)\,, \\ q^2 &= H^K(a, d, e)\,, \\ r^2 &= H^K(a, b, f)\,, \\ s^2 &= H^K(c, d, f)\,. \end{aligned} \tag{1.3.5}$$

They also satisfy three additional relations stated in Proposition 1.16 below.

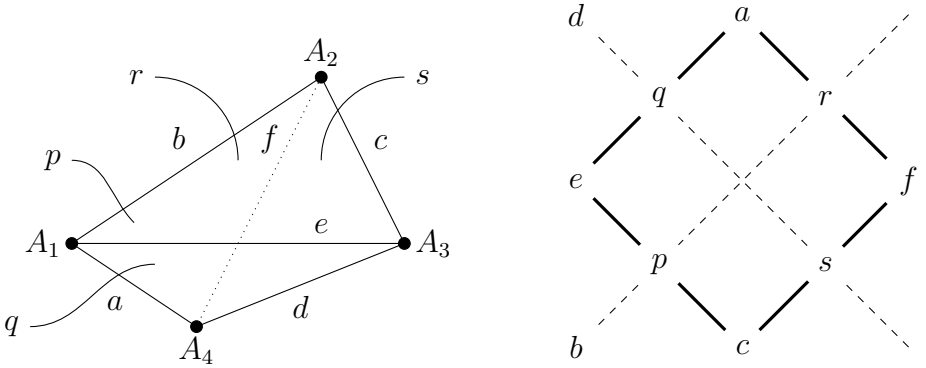


Figure 1.7: Left: Measurements in a spherical quadrilateral $A_1A_2A_3A_4$ include:
(i) six squared distances: $a = x_{14}, b = x_{12}, c = x_{23}, d = x_{34}, e = x_{13}, f = x_{24}$;
(ii) four measurements $S^K(A_i, A_j, A_k)$ associated with the triangles $A_iA_jA_k$:
$p = S^K(A_1, A_2, A_3), q = S^K(A_1, A_3, A_4), r = S^K(A_1, A_2, A_4), s = S^K(A_2, A_3, A_4)$.
Right: the same measurement data, arranged in a spherical Heronian diamond.

Proposition 1.16 (cf. Proposition 3.35)**.** *Let (a, b, c, d, e, p, q) be a 7-tuple of numbers arising from a spherical quadrilateral $A_1A_2A_3A_4$ as shown in Figure 1.7. Assuming points A_1, A_3 are not coincident or antipodal (i.e. $e \notin \left\{0, \frac{4}{K}\right\}$), we can compute f, r, s using the following formulas:*

$$\begin{aligned} f &= \frac{(p+q)^2 + (a-b+c-d)^2 - Ke(a-b)(c-d)}{4e\left(1-\frac{Ke}{4}\right)}, \\ r &= \frac{p\left(e+a-d-\frac{Kae}{2}\right) + q\left(e-c+b-\frac{Kbe}{2}\right)}{2e\left(1-\frac{Ke}{4}\right)}, \\ s &= \frac{p\left(e-a+d-\frac{Kde}{2}\right) + q\left(e+c-b-\frac{Kce}{2}\right)}{2e\left(1-\frac{Ke}{4}\right)}. \end{aligned} \tag{1.3.6}$$

Proposition 1.16 shows that all ten basic measurements for a spherical quadrilateral can be explicitly written as rational expressions in terms of a subset of seven measurements (five x_{ij}'s and two S^K's) associated with a particular triangulation of the quadrilateral.

Remark 1.17. In the special case $K = 0$, we recover the analogous result obtained in [FS21] for tuples arising from quadrilaterals in the Euclidean plane.

Definition 1.18 (cf. [FS21] and Remark 3.36)**.** Fix $K \in \mathbb{R}$. A spherical Heronian diamond is an ordered 10-tuple of numbers $(a, b, c, d, e, f, p, q, r, s)$ arranged in the diamond pattern shown in Figure 1.7 and satisfying equations (1.3.5)–(1.3.6). Explicitly,

- a, c, e, f are placed at the corners of the diamond;
- p, q, r, s are placed at the midpoints of the sides of the diamond;
- the dashed line heading Southeast (resp. Southwest) is labeled d (resp. b).

(The entries are arranged so that the four "measurements" associated with each side of the diamond (e.g., a, d, e, q) satisfy the spherical Heron equation (1.3.3).)

We finally set our sights on spherical polygons. Let $P = A_1A_2 \cdots A_n$ be a spherical polygon. Each subset of four vertices A_i, A_j, A_k, A_l forms a spherical quadrilateral, which in turn gives rise to a spherical Heronian diamond consisting of ten measurements. We assemble some of these diamonds into a numerical array that we call a spherical Heronian frieze, by analogy with [FS21]. To get a sense of what a spherical Heronian frieze looks like, see Figure 1.8.

We index the entries in a spherical Heronian frieze of order n by the set

$$\left\{(i,j) \in (\mathbb{Z}\times\mathbb{Z}) \cup \left(\tfrac{1}{2}\mathbb{Z}\times\mathbb{Z}\right) \cup \left(\mathbb{Z}\times\tfrac{1}{2}\mathbb{Z}\right) \mid i \le j \le i+n\right\} \subseteq \left(\tfrac{1}{2}\mathbb{Z}\right)^2,$$

which is rotated by $\pi/4$ so that the points (i, i) lie along the bottom of the strip and the points $(i, i+n)$ run along the top, cf. Figure 3.6. We also associate an additional entry of a spherical Heronian frieze with each half-integer line

$$\left\{\left(i+\tfrac{1}{2}, y\right) \mid y \in \mathbb{R}\right\} \text{ or } \left\{\left(x, j+\tfrac{1}{2}\right) \mid x \in \mathbb{R}\right\} \tag{1.3.7}$$

(see the dashed lines in Figure 1.8). We denote these lines $(i, \diagup)$ and $(\diagdown, j)$, respectively.

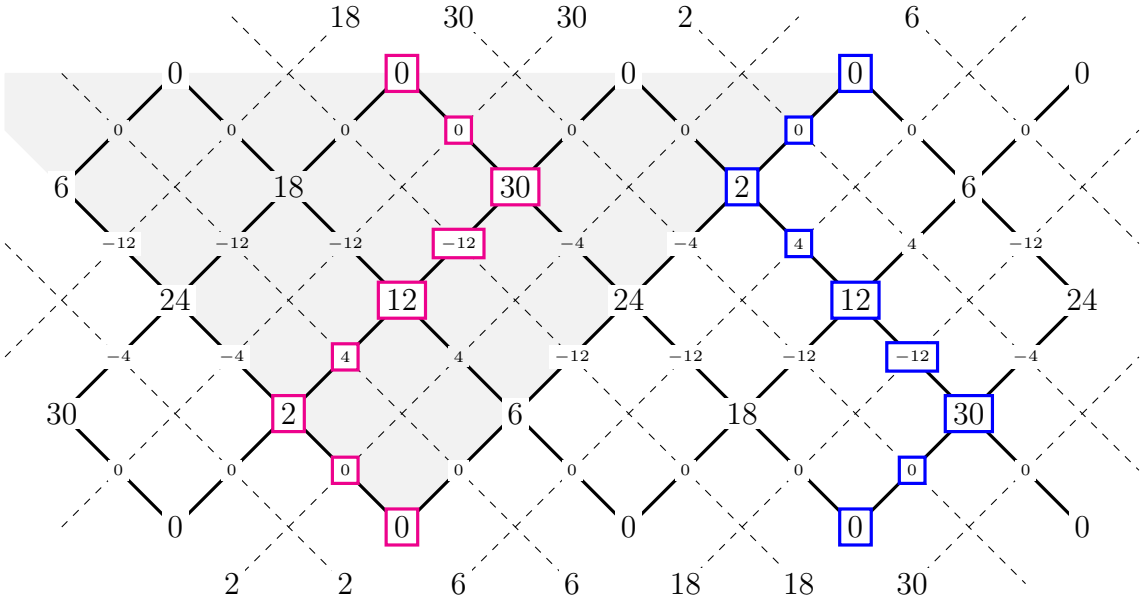


Figure 1.8: An example of a spherical Heronian frieze. To see the glide symmetry, flip the gray shaded region upside down and paste it to the right of its original location. The magenta and blue entries form two traversing paths.

A spherical polygon $P = A_1A_2\cdots A_n$ gives rise to a spherical Heronian frieze as follows. Working modulo n, we place each squared distance x_{ij} at the integer point (i, j) in the frieze. We place triangle measurements $S^K(A_i, A_{i+1}, A_j)$ and $S^K(A_i, A_j, A_{j+1})$ at $(i+\frac{1}{2}, j)$ and $(i, j+\frac{1}{2})$, respectively. Note that we only capture the S^K measurement for triangles that share a side with P. We associate the squared distances $x_{i,i+1}$ and $x_{j,j+1}$ with the lines $(i, \diagup)$ and $(\diagdown, j)$ (see (1.3.7)). This arrangement of data mirrors Coxeter-Conway frieze patterns [Cox71].

Spherical Heronian friezes provide our first solution to the original problem. We start with a triangulation T where each triangle shares a side with the polygon. The corresponding initial data consists of $2n-3$ squared distances x_{ij} associated with the sides and diagonals in T and $n-2$ measurements S^K associated with the triangles in T. Beginning the construction of a spherical Heronian frieze, we place this data at the appropriate locations as described above. (These locations form a traversing path in the frieze going from top to bottom, see Figure 1.8.)

We then recursively apply Proposition 1.16 to propagate outwards and recover the rest of the entries in the frieze, hence the remaining measurements of the spherical polygon. The outwards propagation from a traversing path follows the pattern of the Coxeter-Conway correspondence between triangulations of polygons and integral frieze patterns [CC73].

The rational formulas resulting from the propagation process are structurally simpler than one might expect. Like in the case of the classical Coxeter-Conway friezes, the entries in a spherical Heronian frieze satisfy a version of the Laurent phenomenon:

Proposition 1.19 (cf. Proposition 3.59)**.** *Let $\mathbf{z}_\pi$ be the initial data associated with a traversing path π in a spherical Heronian frieze $\mathbf{z}$. Then each entry of $\mathbf{z}$ can be written as a rational function of $\mathbf{z}_\pi$ whose denominator is a product of (powers of) factors of the form x_{ij} and $\overline{x}_{ij} = 1 - \frac{K}{4}x_{ij}$, for $x_{ij} \in \mathbf{z}_\pi$.*

Remark 1.20. The formulas expressing the entries in a spherical Heronian frieze in terms of the initial data associated to a traversing path (cf. Proposition 1.19) have nonzero denominators as long as each pair of points (A_i, A_j), $(i, j) \in \pi$ is neither coincident nor antipodal.

Like classical frieze patterns, spherical Heronian friezes possess glide symmetry.

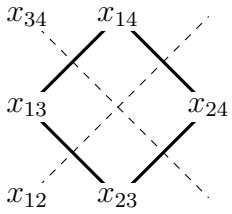
Theorem 1.21 (cf. Theorem 3.58)**.** *Let $\mathbf{z}_\pi$ be a collection of numbers $z_{i,j}$ associated to a traversing path π, with $z_{i,j} \notin \{0, \frac{4}{K}\}$ for (i, j) with $2 \leq j - i \leq n - 2$. Assume that these numbers satisfy the appropriate spherical Heron equations. Propagate outwards using equations* (1.3.6) *to obtain a spherical Heronian frieze $\mathbf{z}$ of order n. Then $\mathbf{z}$ is n-periodic: the entries at locations (k, ℓ) and $(k+n, \ell+n)$ are equal. In fact, $\mathbf{z}$ possesses glide symmetry, cf. Figure 1.8.*

We now pivot to a wholly different approach to the original spherical distance geometry question. We supplement the initial $2n - 3$ measurements coming from a triangulation with $n - 1$ additional diagonal measurements, which can be thought of as "bracing" edges, cf. [JT19]. Unlike the original $2n - 3$ squared distances, the expanded collection is not algebraically independent: they satisfy algebraic relations which we will state next.

Lemma 1.22 (5×5 spherical Cayley-Menger determinant, [Tao19], cf. Theorem 3.71)**.** *Let A_1, A_2, A_3, A_4 be four points on the sphere $\mathbf{S}$. Then*

$$\begin{bmatrix} \frac{K}{2} & 1 & 1 & 1 & 1 \\ 1 & 0 & x_{12} & x_{13} & x_{14} \\ 1 & x_{12} & 0 & x_{23} & x_{24} \\ 1 & x_{13} & x_{23} & 0 & x_{34} \\ 1 & x_{14} & x_{24} & x_{34} & 0 \end{bmatrix} = 0\,. \tag{1.3.8}$$

We define a spherical Cayley-Menger diamond (cf. [FS21]) to be a 6-tuple of numbers $x_{12}, \ldots, x_{34}$ satisfying equation (1.3.8) and arranged as shown below:



We tile these diamonds to form a spherical Cayley-Menger frieze, see Figure 1.9.

The spherical Cayley-Menger determinant is quadratic in the squared distances, so it cannot be used to propagate unambiguously from an initial data set associated with a traversing path. We solve this problem by deriving an additional coherence relation satisfied by the entries of four interlocking Cayley-Menger diamonds in a Cayley-Menger frieze arising from a polygon; we call a Cayley-Menger frieze coherent if this relation is satisfied throughout. Crucially, the coherence equation is linear with respect to the rightmost entry in a configuration of four interlocking diamonds. This allows outwards propagation.

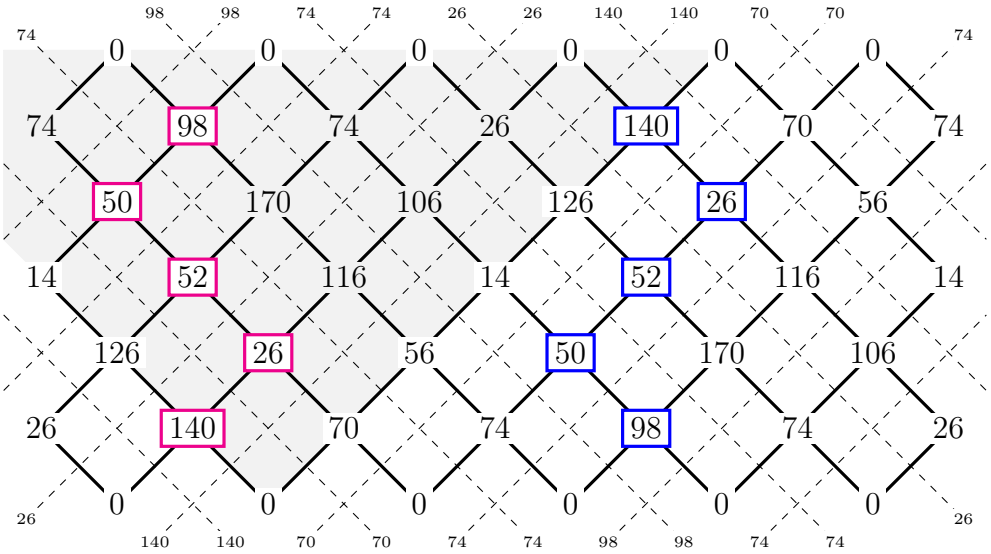


Figure 1.9: A spherical Cayley-Menger frieze of order 6.

Our second solution then proceeds similarly to the first. As propagation via the coherence equation involves four Cayley-Menger diamonds, we have to begin with initial data along a thickening of a traversing path, consisting of the entries on the path together with another path next to it. This initial data set contains the squared distances corresponding to a triangulation of an n-gon, together with the squared lengths of $n-3$ extra diagonals. We then obtain the following theorem.

Theorem 1.23 (cf. Theorem 3.94)**.** *A sufficiently generic coherent spherical Cayley-Menger frieze is uniquely determined by the entries lying on the thickening of a traversing path.*

Spherical Heronian friezes and spherical Cayley-Menger friezes are closely related.

Theorem 1.24 (cf. Theorem 3.101)**.**

1. *Given a sufficiently generic spherical Heronian frieze, restricting to the integer-indexed entries (equivalent to forgetting the triangle measurements S^K) yields a spherical Cayley-Menger frieze.*

2. *Given a sufficiently generic coherent spherical Cayley-Menger frieze $\widehat{\mathbf{z}}$, there are exactly two spherical Heronian friezes that extend $\widehat{\mathbf{z}}$. These two friezes differ from each other by a global change in sign.*

Structure of Chapter 3

Sections 3.1-3.4 develop spherical Heronian friezes and their properties. We begin in Section 3.1 with geometric preliminaries including the spherical triangle measurement S^K, Heron's formula, and the Cayley-Menger determinant. We expand in Section 3.2 from spherical triangles to spherical quadrilaterals, establishing a set of algebraic identities satisfied by the measurements associated to a spherical quadrilateral. In Section 3.3 we define spherical Heronian diamonds and friezes, provide examples, and give our first solution to the main problem. The discussion of spherical Heronian friezes continues in Section 3.4 where we establish a version of the Laurent phenomenon.

In Section 3.5 we develop our second solution. We begin with a discussion of the spherical analogue of the Cayley-Menger determinant. We define spherical Cayley-Menger friezes, provide examples, and establish the coherence equation in the geometric setting. In Section 3.6, we establish the relationship between the two kinds of spherical friezes.

CHAPTER 2

Geometric Incarnations of 3-term Relations

Three-term relations of the form $AB+CD = EF$ arise in multiple mathematical contexts, including the Ptolemy equation for a cyclic quadrilateral, Casey's theorem on bitangents, Penner's relation for lambda lengths, and Plücker's identity for the maximal minors of a 2×4 matrix. In this chapter, we explain how these different occurrences of the 3-term relation can be directly obtained from each other.

2.1 Four incarnations of the 3-term relation

Ptolemy, a Greco-Roman astronomer and geometer, lived in the city of Alexandria in the 2nd century CE. His classical treatise Almagest contains the following famous result:

Theorem 2.1 ([Pto14, Book 1, Sec. 10, Lem. 1.1])**.** *Let A_1, A_2, A_3, A_4 be four points arranged counterclockwise on a unit circle* $\mathbf{S}$ *on the Euclidean plane. For $1 \le i < j \le 4$, let d_{ij} denote the distance from A_i to A_j, see Figure 2.1. Then*

$$d_{12}d_{34} + d_{14}d_{23} = d_{13}d_{24}\,. \tag{2.1.1}$$

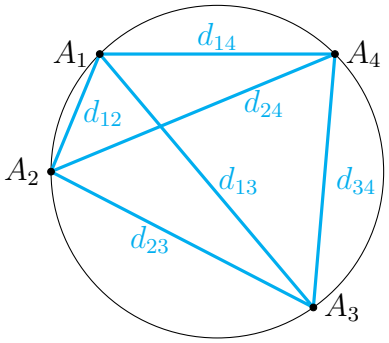


Figure 2.1: Distances between four points on a circle

In 1820s Japan, **Shiraishi Nagatada** (also known as Shiraishi Chōchū) depicted a remarkable generalization of Ptolemy's theorem without providing a proof (see [FR08]). In 1860s Ireland, **John Casey**, at the time a high school teacher, independently published this result:

Theorem 2.2 ([Cas66])**.** *Let H_1, H_2, H_3, H_4 be four circles contained in* $\mathbf{S}$ *that are tangent to* $\mathbf{S}$ *at the points A_1, A_2, A_3, A_4, respectively, see Figure 2.2. For $1 \le i < j \le 4$, let t_{ij} denote the length of a common tangent to H_i and H_j drawn so that both circles lie on the same side. Then*

$$t_{12}t_{34} + t_{14}t_{23} = t_{13}t_{24}\,. \tag{2.1.2}$$

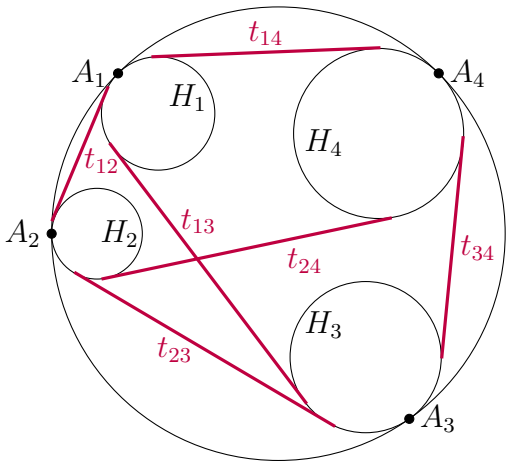


Figure 2.2: Bitangent distances between four circles tangent to a fifth circle

In the degenerate case, when the four circles shrink to points on $\mathbf{S}$, we recover Ptolemy's theorem.

In the late 20th century, the American mathematician **Robert Penner** introduced the notion of lambda length

$$\lambda_{ij} = e^{\delta_{ij}/2}$$

between two horocycles H_i and H_j in the hyperbolic plane; here δ_{ij} is the signed hyperbolic distance between H_i and H_j. He established the following hyperbolic analogue of Ptolemy's theorem:

Theorem 2.3 ([Pen87])**.** *Let A_1, A_2, A_3, A_4 be ideal points on the boundary of the hyperbolic plane. For $1 \le i < j \le 4$, let H_1, H_2, H_3, H_4 be four horocycles centered at A_1, A_2, A_3, A_4, see Figure 2.3. Then the lambda lengths λ_{ij} satisfy*

$$\lambda_{12}\lambda_{34} + \lambda_{23}\lambda_{14} = \lambda_{13}\lambda_{24}\,. \tag{2.1.3}$$

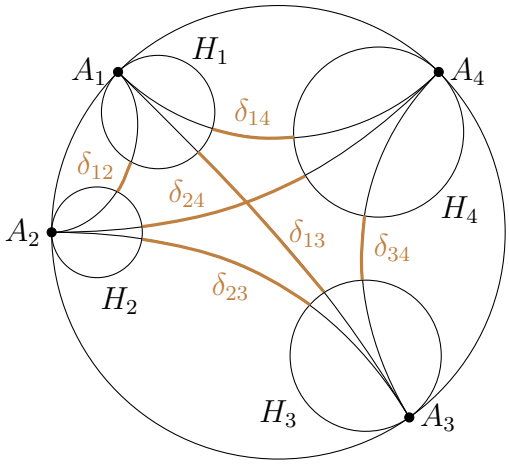


Figure 2.3: Hyperbolic distances between horocycles

Working at the same time as Casey, the German scientist **Julius Plücker** initiated the study of what we now call the Grassmannian of 2-dimensional subspaces of a 4-dimensional vector space. In modern notation, he discovered the following Plücker relation:

Theorem 2.4 ([Plü65, Add. Note, Sec. I, Part 3])**.** *Consider a* 2×4 *matrix*

$$M = \begin{bmatrix} x_1 & x_2 & x_3 & x_4 \\ y_1 & y_2 & y_3 & y_4 \end{bmatrix}.$$

For $1 \leq i < j \leq 4$*, denote*

$$P_{ij} = \det \begin{bmatrix} x_i & x_j \\ y_i & y_j \end{bmatrix}.$$

Then

$$P_{12}P_{34} + P_{14}P_{23} = P_{13}P_{24}\,. \tag{2.1.4}$$

Furthermore, any 6-tuple of complex numbers (P_{ij}) *satisfying* (2.1.4) *can be obtained in this way.*

Many mathematicians have observed the striking similarity between the equations (2.1.1)-(2.1.4). See, e.g., A. Felikson's paper [Fel23] which also discusses connections to frieze patterns and cluster algebras. It is natural to wonder whether the equations (2.1.1)-(2.1.4) can be directly deduced from each other. We will show that this is indeed the case.

2.2 Each equation implies the others

We will employ the following insight.

Observation 2.5. Consider two 6-tuples of complex numbers: $(a_{12}, a_{13}, a_{14}, a_{23}, a_{24}, a_{34})$, and $(b_{12}, b_{13}, b_{14}, b_{23}, b_{24}, b_{34})$. Suppose that there exist nonzero numbers q_1, q_2, q_3, q_4 such that

$$b_{ij} = q_i q_j a_{ij} \quad (\text{for } 1 \leq i < j \leq 4) \ . \tag{2.2.1}$$

The numbers a_{ij} satisfy the 3-term relation

$$a_{12}a_{34} + a_{14}a_{23} = a_{13}a_{24} \tag{2.2.2}$$

if and only if the numbers b_{ij} satisfy the 3-term relation

$$b_{12}b_{34} + b_{14}b_{23} = b_{13}b_{24} \, . \tag{2.2.3}$$

We next describe the measurements that will be cast in the roles of a_{ij}, b_{ij} (see Figure 2.4).

Let $\mathbf{S} \subseteq \mathbb{R}^2$ be the unit circle centered at the origin. Let $A_1, A_2, A_3, A_4 \in \mathbf{S}$ be four points on $\mathbf{S}$ arranged in order counterclockwise. For $1 \leq i \leq 4$, let $0 \leq \alpha_i \leq \pi$ such that $A_i = (\cos 2\alpha_i, \sin 2\alpha_i)$. Let H_1, H_2, H_3, H_4 be four circles tangent to $\mathbf{S}$ on the inside at A_1, A_2, A_3, A_4, as in Figure 2.2. Let r_i be the radius of H_i. For simplicity, we assume that $H_i \cap H_j = \varnothing$ for $1 \leq i, j \leq 4$.

If we change our perspective and regard $\mathbf{S}$ as the Poincaré disk representing the hyperbolic plane, then the H_i become horocycles with centers A_i. Draw the hyperbolic geodesic γ_{ij} from A_i to A_j and denote by δ_{ij} the hyperbolic distance along γ_{ij} between the points $H_i \cap \gamma_{ij}$ and $H_j \cap \gamma_{ij}$.

We now have the following measurements:

- d_{ij} = Euclidean distance between A_i and A_j,
- t_{ij} = length of the exterior bitangent to H_i and H_j,
- $\lambda_{ij} = e^{\delta_{ij}/2}$ = lambda length between H_i and H_j,
- $P_{ij} = \det \begin{bmatrix} \cos\alpha_i & \cos\alpha_j \\ \sin\alpha_i & \sin\alpha_j \end{bmatrix}$.

It turns out that these measurements are related to each other by rescaling:

Proposition 2.6. *In the setting described above,*

$$t_{ij} = \sqrt{1 - r_i}\sqrt{1 - r_j}\, d_{ij} \, , \tag{2.2.4}$$

$$t_{ij} = \lambda_{ij}\sqrt{2r_i}\sqrt{2r_j} \, , \tag{2.2.5}$$

$$d_{ij} = 2P_{ij} \, . \tag{2.2.6}$$

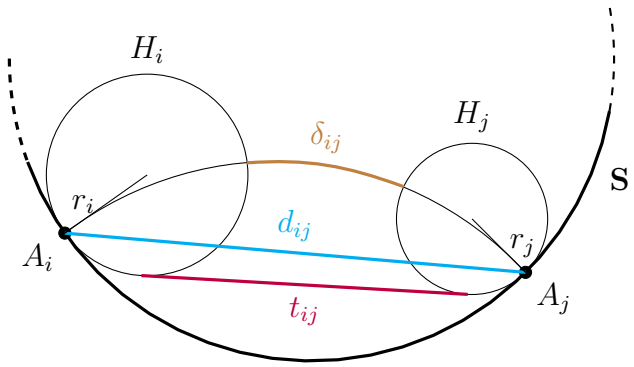


Figure 2.4: The measurements d_{ij}, t_{ij}, and δ_{ij}

We defer the proof of Proposition 2.6 until later.

Remark 2.7. The numbers P_{ij} appearing in (2.2.6) are the 2×2 minors of the matrix

$$\begin{bmatrix} \cos(\alpha_1) & \cos(\alpha_2) & \cos(\alpha_3) & \cos(\alpha_4) \\ \sin(\alpha_1) & \sin(\alpha_2) & \sin(\alpha_3) & \sin(\alpha_4) \end{bmatrix}.$$

This matrix is of a special kind: its columns are unit vectors that lie in the upper half plane and are ordered counterclockwise. Thus, we are not dealing here with the most general form of the 3-term Plücker relation (2.1.4). On the other hand, the general relation (2.1.4) follows from this special case due to

- the invariance of (2.1.4) under arbitrary rescaling of the columns of the matrix, and
- the invariance of (2.1.4) under arbitrary permutations of the column indices $1, 2, 3, 4$ (noting that $P_{ji} = -P_{ij}$).

2.3 The torus action

The solutions of the 3-term relation (2.2.2) form a quadric hypersurface $\Sigma \subset \mathbb{C}^6$. By Observation 2.5, the torus $(\mathbb{C}^*)^4$ acts on Σ by rescaling: an element $(q_1, q_2, q_3, q_4) \in (\mathbb{C}^*)^4$ acts on a 6-tuple $(a_{ij}) \in \Sigma$ by sending

$$a_{ij} \mapsto q_i q_j a_{ij}\,.$$

The action of $(\mathbb{C}^*)^4$ splits the 5-dimensional quadric Σ into 4-dimensional torus orbits.

Two points $(a_{ij}), (b_{ij}) \in \Sigma$ will typically lie in different orbits. In other words, given two 6-tuples (a_{ij}) and (b_{ij}) satisfying (2.2.2)–(2.2.3), there is generally no reason to expect the existence of scalars q_1, q_2, q_3, q_4 such that formulas (2.2.1) hold. It is natural to ask: when do such scalars q_i exist? The answer is given in the following proposition.

Proposition 2.8. *Given two 6-tuples (a_{ij}) and (b_{ij}) of nonzero numbers satisfying* (2.2.2)–(2.2.3)*, the following are equivalent:*

- *there exists a quadruple of scalars (q_i) such that* (2.2.1) *holds;*
- *the numbers a_{ij} and b_{ij} satisfy the relation*

$$\frac{a_{12}a_{34}}{a_{23}a_{14}} = \frac{b_{12}b_{34}}{b_{23}b_{14}}\,. \tag{2.3.1}$$

Proof. It is evident that (2.2.1) implies (2.3.1). It remains to verify the converse implication.

Suppose that (2.2.2)–(2.2.3) and (2.3.1) hold. For $1 \le i < j \le 4$, let us denote $c_{ij} = \frac{b_{ij}}{a_{ij}}$. Equation (2.3.1) implies that

$$c_{12}c_{34} = c_{23}c_{14}\,. \tag{2.3.2}$$

We also have

$$\frac{a_{13}a_{24}}{a_{23}a_{14}} \overset{(2.2.2)}{=} \frac{a_{12}a_{34}}{a_{23}a_{14}} + 1 \overset{(2.3.1)}{=} \frac{b_{12}b_{34}}{b_{23}b_{14}} + 1 \overset{(2.2.3)}{=} \frac{b_{13}b_{24}}{b_{23}b_{14}}\,,$$

implying

$$c_{23}c_{14} = c_{13}c_{24}\,. \tag{2.3.3}$$

We need to find q_1, q_2, q_3, q_4 that satisfy the equations $q_iq_j = c_{ij}$ (cf. (2.2.1)). To this end, choose q_1 so that

$$q_1^2 = \frac{c_{12}c_{13}}{c_{23}}\,, \tag{2.3.4}$$

then set

$$q_2 = \frac{c_{12}}{q_1}\,, \qquad q_3 = \frac{c_{13}}{q_1}\,, \qquad q_4 = \frac{c_{14}}{q_1}\,. \tag{2.3.5}$$

We then have $q_1q_j = c_{1j}$ (for $j = 2, 3, 4$), and moreover

$$\begin{aligned}
q_2q_3 &\overset{(2.3.5)}{=} \frac{c_{12}c_{13}}{q_1^2} \overset{(2.3.4)}{=} c_{23}\,,\\
q_2q_4 &\overset{(2.3.5)}{=} \frac{c_{12}c_{14}}{q_1^2} \overset{(2.3.4)}{=} \frac{c_{14}c_{23}}{c_{13}} \overset{(2.3.3)}{=} c_{24}\,,\\
q_3q_4 &\overset{(2.3.5)}{=} \frac{c_{13}c_{14}}{q_1^2} \overset{(2.3.4)}{=} \frac{c_{14}c_{23}}{c_{12}} \overset{(2.3.2)}{=} c_{34}\,,
\end{aligned}$$

as desired. □

2.4 The cross-ratio

The reader may recognize the expressions appearing in (2.3.1) as cross-ratios of points on the projective line.

Definition 2.9. Let $X_1, X_2, X_3, X_4 \in \mathbb{CP}^1$ be distinct points on the complex projective line represented by the column vectors $\left[\begin{smallmatrix} x_i \\ y_i \end{smallmatrix}\right]$. Their cross-ratio $[X_1, X_2, X_3, X_4]$ is defined by

$$[X_1, X_2, X_3, X_4] = \frac{P_{12}P_{34}}{P_{23}P_{14}}\,, \tag{2.4.1}$$

where we use the notation

$$P_{ij} = \det \begin{bmatrix} x_i & x_j \\ y_i & y_j \end{bmatrix}\,.$$

This notion can be extended to cases where two (but not more) of the X_i coincide.

The reader is encouraged to verify that Definition 2.9 matches the conventional definition of the cross-ratio.

Definition 2.9 and the last statement of Theorem 2.4 allow us to restate Proposition 2.8. In the language of cross-ratios, Proposition 2.8 asserts that for two 2×4 matrices M and N, the following are equivalent:

- the columns of N can be rescaled so that the Plücker coordinates match the Plücker coordinates of M;
- the columns of M and N represent two quadruples of points in $\mathbb{CP}^1$ that have the same cross-ratio.

2.5 Models of the hyperbolic plane

The proof of Proposition 2.6 will utilize three different models of the hyperbolic plane.

2.5.1 The upper half plane

Definition 2.10. Our first model of the hyperbolic plane is the upper half plane

$$\mathcal{U} = \{(x, y) \in \mathbb{R}^2 \ : \ y > 0\}\,,$$

endowed with the Riemannian metric

$$ds^2 = (dx^2 + dy^2)/y^2\,.$$

Identifying $\mathbb{R}^2$ with the complex plane $\mathbb{C}$ identifies $\mathcal{U}$ with the complex numbers with positive imaginary part. The points of the extended real axis $\mathbb{R} \cup \{\infty\}$ are the ideal points of $\mathcal{U}$. Denote by $\overline{\mathcal{U}}$ the union of $\mathcal{U}$ and the ideal points.

Proposition 2.11 (cf. [Pen12], p. 16)**.** *Take two distinct points $W_1, W_2 \in \mathcal{U}$. Let $W_1', W_2' \in \overline{\mathcal{U}}$ be the ideal endpoints of the geodesic connecting W_1 and W_2, see Figure 2.5. Then the hyperbolic distance δ_{12} between W_1 and W_2 is given by the cross-ratio*

$$\delta_{12} = \log[W_1, W_1', W_2, W_2'] \,.$$

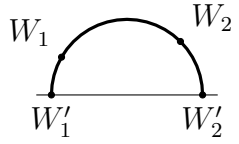


Figure 2.5: The ideal points W_1' and W_2' used to compute the hyperbolic distance between W_1 and W_2

2.5.2 The Poincaré disk

Definition 2.12. Our second model of the hyperbolic plane is the Poincaré disk

$$\mathbb{D} = \{z \in \mathbb{C} \ : \ |z| = x^2 + y^2 < 1\} \,,$$

endowed with the metric

$$ds^2 = 4(dx^2 + dy^2)/(1 - |z|^2)^2 \,.$$

Ideal points lie on the unit circle $\mathbf{S}$.

To move back and forth between the models $\mathcal{U}$ and $\mathbb{D}$, one can apply the mutually inverse isometries known as the Cayley transforms:

$$\begin{aligned} &\mathcal{U} \to \mathbb{D} \,, && \mathbb{D} \to \mathcal{U} \,, \\ &z \mapsto \tfrac{z-i}{z+i} \,, && w \mapsto i\tfrac{1+w}{1-w} \,. \end{aligned}$$

2.5.3 The hyperboloid

Definition 2.13. Minkowski 3-space is $\mathbb{R}^3$ endowed with the indefinite pairing

$$\begin{aligned} \langle \cdot, \cdot \rangle : \mathbb{R}^3 \times \mathbb{R}^3 \to \mathbb{R} \,, \\ \langle (x, y, z), (x', y', z') \rangle \mapsto xx' + yy' - zz' \,. \end{aligned}$$

The upper sheet of a hyperboloid

$$\mathbb{H} = \left\{ u = (x, y, z) \in \mathbb{R}^3 \,:\, \langle u, u \rangle = -1,\, z > 0 \right\},$$

inherits a Riemannian metric from the pairing on Minkowski 3-space, producing a model for the hyperbolic plane.

Identify the closed unit disk $\mathbb{D} \cup \mathbf{S}$ with the horizontal disk at height zero in Minkowski 3-space. Then the following pair of mutually inverse maps give isometries between $\mathbb{D}$ and $\mathbb{H}$:

$$\begin{aligned} \mathbb{H} &\to \mathbb{D}\,, \\ (x, y, z) &\mapsto \overline{(x, y, z)} = \tfrac{1}{1+z}(x, y)\,, \\ \mathbb{D} &\to \mathbb{H}\,, \\ (x, y) &\mapsto \tfrac{1}{1-x^2-y^2}(2x, 2y, 1 + x^2 + y^2)\,. \end{aligned}$$

Definition 2.14. The open positive light cone L^+ is defined by

$$L^+ = \left\{ u = (x, y, z) \in \mathbb{R}^3 \,:\, \langle u, u \rangle = 0,\, z > 0 \right\}.$$

For $u = (x, y, z) \in L^+$ since $\langle u, u \rangle = 0$, we have

$$0 = \langle u, u \rangle = \langle (x, y, z), (x, y, z) \rangle = x^2 + y^2 - z^2\,.$$

Since $z > 0$, we conclude that $\sqrt{x^2 + y^2} = z$.

The map from $\mathbb{H}$ to $\mathbb{D}$ is given by central projection from the point $(0, 0, -1)$. The projection extends to a surjective but not injective natural mapping

$$\begin{aligned} L^+ &\to \mathbf{S}\,, \\ (x, y, z) &\mapsto \overline{(x, y, z)} = \tfrac{1}{\sqrt{x^2+y^2}}(x, y, 0)\,. \end{aligned}$$

2.6 Horocycles and lambda lengths

In order to prove Proposition 2.6, we will need to recall some facts about horocycles.

Definition 2.15. A horocycle H on the hyperbolic plane is a curve of constant curvature such that all perpendicular geodesics are limiting parallel and converge to a single ideal point called the center of H.

In the model of the upper half plane $\mathcal{U}$, a horocycle H is either a Euclidean circle tangent to the real axis or a horizontal straight line parallel to the real axis. In the former case, the point of tangency is the center of H. In the model of Poincaré disk $\mathbb{D}$, a horocycle is a Euclidean circle tangent to $\mathbf{S}$. The point of tangency is the center of H.

There is an isomorphism between points of the upper light cone L^+ and the collection of all horocycles in the hyperbolic plane $\mathbb{H}$, namely

$$\begin{aligned} &L^+ \to \{\text{horocycles in } \mathbb{H}\}\,, \\ &u \mapsto h(u) = \left\{v \in \mathbb{H} \ : \ \langle u, v\rangle = -\tfrac{1}{\sqrt{2}}\right\}\,. \end{aligned}$$

Let $u \in L^+$. Then we can map

$$u \in L^+ \ \mapsto h(u) \in \mathbb{H} \ \xrightarrow{\text{Cayley transform}} \ \overline{h}(u) \in \mathbb{D}\,.$$

The center of the horocycle $\overline{h}(u)$ in $\mathbb{D}$ is

$$\overline{(x,y,z)} = \tfrac{1}{\sqrt{(x^2+y^2)}}(x,y,0)\,, \tag{2.6.1}$$

and the Euclidean radius of $\overline{h}(u)$ in $\mathbb{D}$ is $\frac{1}{1+z\sqrt{2}}$.

Definition 2.16. Let $H_1, H_2 \subset \mathbb{D}$ be horocycles with distinct centers. Let γ be the geodesic that connects these centers. Let δ_{12} be the signed hyperbolic distance along γ between the points $H_1 \cap \gamma$ and $H_2 \cap \gamma$, where the sign of δ_{12} is positive if and only if H_1 and H_2 are disjoint, cf. Figure 2.6. The lambda length between H_1 and H_2 is then defined by $\lambda(H_1, H_2) = \lambda_{12} = \sqrt{e^{\delta}}$.

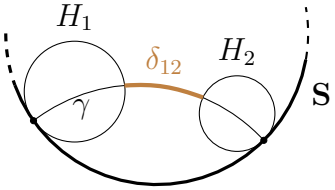


Figure 2.6: The signed hyperbolic distance between two horocycles

Alternatively, let

$$u_1 = (x_1, y_1, z_1),\ u_2 = (x_2, y_2, z_2) \in L^+ \tag{2.6.2}$$

be horocycles that do not lie on a common ray in L^+. The lambda length $\lambda_{12} = \lambda(u_1, u_2)$ is given by $\lambda_{12} = \sqrt{-\langle u_1, u_2\rangle} = \sqrt{-x_1x_2 - y_1y_2 + z_1z_2}$.

2.7 Proof of Proposition 2.6

Proof of (2.2.4). This equation can be deduced from the law of cosines, see, e.g., [Zac42], [FR08, p. 297]. □

Proof of (2.2.5). Consider horocycles $u_1, u_2 \in L^+$, as in (2.6.2), that do not lie on a common ray in L^+. Viewing them as horocycles $H_1 = \overline{h}(u_1), H_2 = \overline{h}(u_2)$ in $\mathbb{D}$, by (2.6.1), they have hyperbolic centers

$$A_1 = \left(\tfrac{x_1}{\sqrt{x_1^2+y_1^2}}, \tfrac{y_1}{\sqrt{x_1^2+y_1^2}}\right), A_2 = \left(\tfrac{x_2}{\sqrt{x_2^2+y_2^2}}, \tfrac{y_2}{\sqrt{x_2^2+y_2^2}}\right).$$

As Euclidean circles, H_1 and H_2 have radii

$$r_1 = \tfrac{1}{1+z_1\sqrt{2}}\,, r_2 = \tfrac{1}{1+z_2\sqrt{2}}\,.$$

Then

$$\begin{aligned}(1-r_1)(1-r_2) &= 1 - \tfrac{1}{1+z_1\sqrt{2}} - \tfrac{1}{1+z_2\sqrt{2}} + \tfrac{1}{(1+z_1\sqrt{2})(1+z_2\sqrt{2})} \\ &= \tfrac{2z_1z_2}{(1+z_1\sqrt{2})(1+z_2\sqrt{2})}.\end{aligned}$$

The Euclidean distance between A_1 and A_2 is

$$\begin{aligned}d_{12} &= \left(\left(\tfrac{x_1}{\sqrt{x_1^2+y_1^2}} - \tfrac{x_2}{\sqrt{x_2^2+y_2^2}}\right)^2 + \left(\tfrac{y_1}{\sqrt{x_1^2+y_1^2}} - \tfrac{y_2}{\sqrt{x_2^2+y_2^2}}\right)^2\right)^{1/2} \\ &= \left(2\left(1 - \tfrac{x_1x_2+y_1y_2}{\sqrt{x_1^2+y_1^2}\sqrt{x_2^2+y_2^2}}\right)\right)^{1/2} \\ &= \left(2\left(1 - \tfrac{x_1x_2+y_1y_2}{z_1z_2}\right)\right)^{1/2} \\ &= \left(2\left(\tfrac{z_1z_2-x_1x_2-y_1y_2}{z_1z_2}\right)\right)^{1/2}.\end{aligned}$$

By equation (2.2.4), the length t_{12} of the bitangent is

$$\begin{aligned}t_{12} &= \left(2\left(\tfrac{z_1z_2-x_1x_2-y_1y_2}{z_1z_2}\right)\left(\tfrac{2z_1z_2}{(1+z_1\sqrt{2})(1+z_2\sqrt{2})}\right)\right)^{1/2} \\ &= 2(-x_1x_2 - y_1y_2 + z_1z_2)^{1/2}((1+z_1\sqrt{2})(1+z_2\sqrt{2}))^{-1/2} \\ &= 2\lambda_{12}\cdot((1+z_1\sqrt{2})(1+z_2\sqrt{2}))^{-1/2} \\ &= \lambda_{12}\sqrt{2r_1}\sqrt{2r_2}.\end{aligned}$$

□

Proof of (2.2.6). Recall that $A_i = (\cos 2\alpha_i, \sin 2\alpha_i)$ and $\alpha_i < \alpha_j$ for $i < j$. We then compute (see Figure 2.7):

$$\begin{aligned} d_{ij} &= 2\sin(\alpha_j - \alpha_i) \\ &= 2(\sin\alpha_j \cos\alpha_i - \cos\alpha_j \sin\alpha_i) \\ &= 2\begin{bmatrix} \cos\alpha_i & \cos\alpha_j \\ \sin\alpha_i & \sin\alpha_j \end{bmatrix} \\ &= 2P_{ij}\,. \end{aligned}$$

□

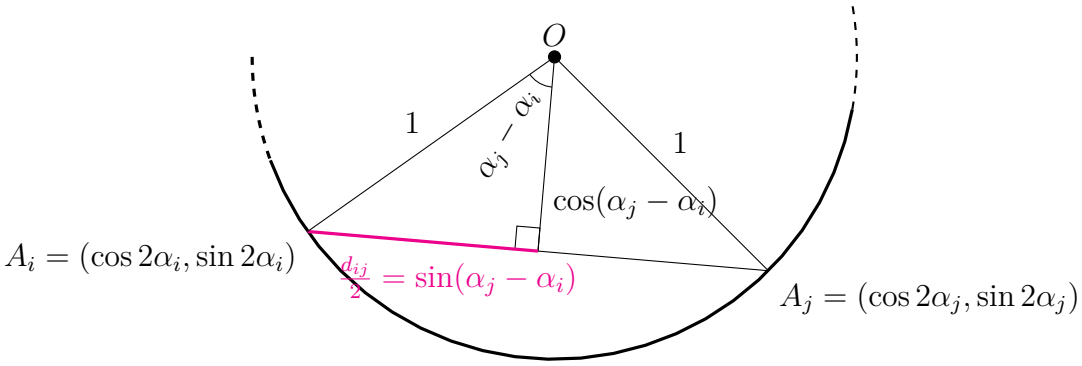


Figure 2.7: Measurements used to calculate d_{ij}

2.8 Generalizations and historical notes

Ptolemy's theorem (Theorem 2.1) can be generalized in multiple directions. In 1872, Darboux [Dar72] shifted the setting to spherical geometry, establishing a relation among pairwise spherical distances between four concyclic points on a sphere; similar results were obtained by Frobenius [Fro75]. In 1912, Kubota [Kub12] found an analogous relation in a hyperbolic setting. Indeed, Observation 2.5 can be used to extend Ptolemy's relation to both spherical and hyperbolic geometry, see Guo and Sonmëz [GS11], the discussion in [Pen12, p.43], and the pictorial explanation on Stothers' remarkable website [Sto].

One can generalize Theorem 2.1 by considering larger collections of concyclic points. A result for hexagons was obtained in the late 19th century by Fuhrmann [Fuh90]. This was further extended by Gregorac [Gre96].

Various authors looked at the converse of Theorem 2.1: four points only lie on a circle if the 3-term relation holds among their pairwise distances. Haantjes [Haa51] gave both spherical and hyperbolic versions of this result; this was later completed by Valentine [Val70b, Val70a].

Casey's relation holds in greater generality than is stated in Theorem 2.2, for any configuration of four circles that are tangent—either internally or externally—to a fifth circle,

as long as one is careful about their choice of bitangents. For a comprehensive summary, see [Gue02].

Various authors have found versions of Casey's theorem in spherical and hyperbolic geometry [AM15, KK16] and in higher dimensions [AA18, MM19]. Kostin [Kos24] extended Fuhrmann's theorem to the hyperbolic plane.

An uninitiated reader may be interested in learning more about Shiraishi Nagatada (or Shiraishi Chōchū) and the practice of hanging sangaku, wooden tablets with geometric figures, on the walls of Shinto shrines and Buddhist temples in Japan. This practice was widespread from the 17th through 20th century, coinciding largely with the Edo period when Japan was closed to trade and intellectual exchange with Europe. An excellent source to learn more is the survey [FR08].

Shiraishi's work Shamei Sanpu [Shi26] contains a large collection of sangaku. Shiraishi was a samurai, a member of nobility. At the time, this elite strata of society included mathematicians who also taught students [SM14].

Cross-ratios appear in Book 7 of Pappus' Collection, which drew heavily on now lost works of Euclid [Jon86]. Like Ptolemy, both Euclid and Pappus lived and worked in Alexandria, around 300 BCE and 300 CE respectively. The modern notion of a cross-ratio crystallized during the first half of the 19th century in the work of Lazare Carnot, Jean-Victor Poncelet, Michel Chasles, and August Möbius. The cross-ratio plays a central role in the foundations of projective geometry as developed by Karl von Staudt, Arthur Cayley, and Felix Klein. Klein also used the cross-ratio to define the metric on hyperbolic space, see, e.g., [LRM96, Proposition 2.11].

Theorems 2.1-2.4 underlie areas of active current research, such as the study of cluster algebras and frieze patterns. Frieze patterns are arrays of numbers that satisfy a certain local algebraic relation. This relation can be interpreted as an instance of any of the four incarnations (2.1.1)–(2.1.4) of the 3-term relation $AB + CD = EF$. When H. S. M. Coxeter [Cox71] introduced frieze patterns, he observed their connection to cross-ratios and to the Pentagramma mirificum of Gauss and Napier.

As shown by Coxeter and Conway [Cox71, CC73], frieze patterns can be studied from a combinatorial perspective that utilizes triangulations of a polygon. This construction leads to at least two geometric interpretations of friezes. First, Penner's Theorem 2.3 can be used to realize frieze patterns (and more generally, cluster algebras associated with bordered oriented surfaces) via lambda lengths for triangulations of ideal hyperbolic polygons [FT18, Fel23] (resp., triangulations of the surface) decorated by horocycles. Second, equation (2.2.5) and Casey's formula allow us to realize Coxeter-Conway friezes via bitangent distances between four circles tangent to a fifth circle.

CHAPTER 3

Spherical Friezes

3.1 Measurements associated to spherical triangles

In this chapter, we develop the theory of spherical friezes whose brief outline was given in Section 1.3.

Let $V_{\mathbb{R}} \cong \mathbb{R}^3$, a three-dimensional real Euclidean space, with a scalar product

$$\begin{aligned} \langle\,,\rangle : V_{\mathbb{R}} \times V_{\mathbb{R}} &\to \mathbb{R}\,, \\ (x, y) &\mapsto \langle x, y\rangle\,, \end{aligned}$$

that is symmetric, bilinear, and positive definite. Define a trilinear skew-symmetric volume form

$$\begin{aligned} [\,] : V_{\mathbb{R}} \times V_{\mathbb{R}} \times V_{\mathbb{R}} &\to \mathbb{R}\,, \\ (x, y, z) &\mapsto \begin{bmatrix} x & y & z \end{bmatrix}\,. \end{aligned}$$

In Cartesian coordinates, if $x = \left[\begin{smallmatrix} x_1 \\ x_2 \\ x_3 \end{smallmatrix}\right]$, $y = \left[\begin{smallmatrix} y_1 \\ y_2 \\ y_3 \end{smallmatrix}\right]$, and $z = \left[\begin{smallmatrix} z_1 \\ z_2 \\ z_3 \end{smallmatrix}\right]$, then

$$\langle x, y\rangle = x_1y_1 + x_2y_2 + x_3y_3\,, \quad \text{and} \quad \begin{bmatrix} x & y & z \end{bmatrix} = \det \left[\begin{smallmatrix} x_1 & y_1 & z_1 \\ x_2 & y_2 & z_2 \\ x_3 & y_3 & z_3 \end{smallmatrix}\right]\,.$$

This construction can be complexified, producing a three-dimensional complex vector space $V = V_{\mathbb{C}}$ endowed with both a scalar product and a volume form given by the same formulas. While the reader can consider the results of this paper in the context of $V_{\mathbb{R}} \cong \mathbb{R}^3$ to aid understanding, we will generally work in $V = V_{\mathbb{C}}$.

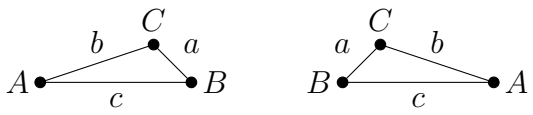
Definition 3.1. We will implicitly identify V with an affine space that has a distinguished point O, the origin. For two points $A, B \in V$, we denote by $\overrightarrow{AB}$ a vector from A to B and by $x(A, B)$ the scalar product

$$x(A, B) = \langle \overrightarrow{AB}, \overrightarrow{AB}\rangle\,.$$

Note that $x(A, B) = x(B, A)$. In $V_{\mathbb{R}} = \mathbb{R}^3$, the quantity $x(A, B)$ is the square of the Euclidean distance from A to B. For points $A_1, A_2, \ldots$, we denote $x_{ij} = x(A_i, A_j)$.

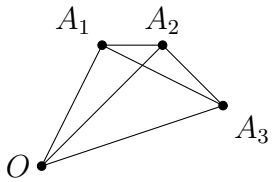
Let $\mathbf{S} \subseteq V$ be a "complexified" sphere of positive real radius centered at O, or more precisely, the set of points $A \in V$ such that $x(A, O) = R^2$. Let $K = \frac{1}{R^2}$. One can view $\mathbf{S}$ as the complexification of a space of constant Gaussian curvature K. All points of interest to us will lie on $\mathbf{S}$ with the exception of O. Let $\mathrm{Aut}(\mathbf{S})$ denote the group of orientation-preserving isometries of $\mathbf{S}$.

We will work with triangulations of polygons on $\mathbf{S}$ (cf. Definitions 3.29-3.31). As shown below, up to the action of $\mathrm{Aut}(\mathbf{S})$, there are two triangles on $\mathbf{S}$ with the squared side distances a, b, c. We will need an additional measurement that distinguishes such triangles from each other.



In two-dimensional real Euclidean space, a natural way to distinguish triangles is by their signed oriented area. There is no consistent way to extend this notion to the three-dimensional space V, but there are a few related measurements one can take given a triangle on the sphere $\mathbf{S} \subseteq V$. We will use the following skew-symmetric measurement S^K that is invariant under cyclic permutations of the vertices of a triangle.

Definition 3.2. For $A_1, A_2, A_3 \in \mathbf{S}$, consider the Euclidean tetrahedron $OA_1A_2A_3$ with vertices O, A_1, A_2, A_3, as shown below:



The signed Euclidean volume V of $OA_1A_2A_3$ is given by

$$V(OA_1A_2A_3) = \tfrac{1}{6}\left[\overrightarrow{OA_1}\ \overrightarrow{OA_2}\ \overrightarrow{OA_3}\right]. \tag{3.1.1}$$

Define the measurement

$$S^K(A_1, A_2, A_3) = \tfrac{12}{R} V(OA_1A_2A_3). \tag{3.1.2}$$

When convenient, for $A_i, A_j, A_k \in \mathbf{S}$ we will abbreviate $S^K_{ijk} = S^K(A_i, A_j, A_k)$. The measurement S^K is sensitive to the specified ordering of points: when the points A_i, A_j, A_k are permuted, S^K changes its sign depending on whether the permutation is odd or even.

Remark 3.3. Let $OA_1A_2A_3$ be a tetrahedron in $V_{\mathbb{R}}$. Let h be the unsigned distance from O to the plane $(A_1A_2A_3)$. The unsigned volume of $OA_1A_2A_3$ is given by

$$\text{unsigned volume of } OA_1A_2A_3 \;\; = \tfrac{1}{3} \cdot (\text{unsigned area of triangle } A_1A_2A_3) \cdot h\,. \tag{3.1.3}$$

When points A_1, A_2, A_3 are close together on $\mathbf{S}$, the radius R is a good approximation of height h. Equation (3.1.3) motivates our use of $\frac{3}{R}V(OA_1A_2A_3)$ in lieu of the signed area of the triangle $A_1A_2A_3$. The factor of 4 in equation 3.1.2 is explained in Remark 3.9.

Remark 3.4. Informally, S^K is a spherical analogue for the rescaled signed area of a triangle $A_1A_2A_3$. When $R \to \infty$ ($K \to 0$), the measurement $S^K(A_1, A_2, A_3)$ defined by (3.1.2) converges to

$$4 \cdot (\text{signed area of the triangle } A_1A_2A_3) = 2\left[\overrightarrow{A_1A_2}\ \overrightarrow{A_1A_3}\right],$$

(cf. [FS21, 2.2]).

One can measure volumes in an n-dimensional Euclidean space using the $n \times n$ Cayley-Menger determinant, which we define next.

Definition 3.5 ([Ber77, Section 9.7.3])**.** Let $A_1, A_2, A_3 \in V$. Denote $x_{ij} = x(A_i, A_j)$. The associated Cayley-Menger determinant is given by

$$M^0_3(x_{12}, x_{13}, x_{23}) = \det \begin{bmatrix} 0 & 1 & 1 & 1 \\ 1 & 0 & x_{12} & x_{13} \\ 1 & x_{12} & 0 & x_{23} \\ 1 & x_{13} & x_{23} & 0 \end{bmatrix}.$$

The Cayley-Menger determinant M^0_k associated to a collection of k points in a Euclidean space is defined analogously. (The superscript 0 in our notation is explained in Remark 3.72.)

Proposition 3.6 ([Ber77, Section 10.6.5])**.** *Consider a simplex $A_1 \cdots A_{n+1}$ in $\mathbb{R}^n$, with volume V. Then*

$$V^2 = \frac{(-1)^{n+1}}{(n!)^2 \cdot 2^n} M^0_{n+1}(x_{12}, x_{13}, \ldots, x_{23}, x_{24}, \ldots, x_{n,n+1})\,. \tag{3.1.4}$$

Remark 3.7. Cayley obtained this formula for $n \leq 4$ and used it to derive an algebraic relation amongst the distances between $n+1$ points in an $(n-1)$-dimensional Euclidean space. Menger extended Cayley's result to compute the volume of simplices in any dimension [LL15].

The $n = 3$ case of (3.1.4) is a classical result (e.g. [Tod86, Section 161]) that [Dö65, Section 68] attributes to Euler. The $n = 2$ case can be viewed as a restatement of the well-known Heron's formula, see below. As discussed in [Hea21], while Heron published it in his work Metrica sometime before 250 CE, this was a collection of both new and previously known results and Archimedes knew Heron's formula two centuries prior to Heron.

Theorem 3.8 (Heron's Formula)**.** *Let $A_1, A_2, A_3 \in \mathbb{R}^2$. Denote $x_{ij} = x(A_i, A_j)$. For each pair $1 \leq i < j \leq 3$, select a sign $\pm$ and set*

$$y = \pm\sqrt{x_{12}}\,, \quad z = \pm\sqrt{x_{13}}\,, \quad w = \pm\sqrt{x_{23}}\,, \quad s = \tfrac{y+z+w}{2}\,.$$

Regardless of the choices made, we then have

$$(\text{area of } A_1A_2A_3)^2 = s(s-y)(s-z)(s-w)\,.$$

It is instructive to deduce this classical result from Proposition 3.6:

Proof. By Proposition 3.6,

$$\begin{aligned}(4 \cdot \text{area of } A_1A_2A_3)^2 &= -M_3^0(x_{12}, x_{13}, x_{23})\,, \\ &= -x_{12}^2 - x_{13}^2 - x_{23}^2 + 2x_{12}x_{13} + 2x_{12}x_{23} + 2x_{13}x_{23}\,, \\ &= -y^4 - z^4 - w^4 + 2y^2z^2 + 2y^2w^2 + 2z^2w^2\,, \\ &= (y+z+w)(-y+z+w)(y-z+w)(y+z-w)\,.\end{aligned} \tag{3.1.5}$$

□

Remark 3.9. The factor of 4 in equation (3.1.5) motivates the appearance of the same factor in the definition of S^K.

We will show that our measurement S^K satisfies a spherical version of Heron's formula. In order to state this formula, we introduce the following notation.

Definition 3.10. For $a, b, c \in \mathbb{C}$, define

$$H^K(a, b, c) = -a^2 - b^2 - c^2 + 2ab + 2ac + 2bc - Kabc\,.$$

Proposition 3.11 (Spherical Heron's Formula, cf. Remark 3.73)**.** *Let $A_1, A_2, A_3 \in \mathbf{S}$. Denote $x_{ij} = x(A_i, A_j)$. Then*

$$H^K(x_{12}, x_{13}, x_{23}) = \Big(S^K(A_1, A_2, A_3)\Big)^2\,.$$

Proof. Note that $x(O, A_i) = R^2$ for $i = 1, 2, 3$. Using Proposition 3.6 with $A_4 = O$, we get:

$$(S^K(A_1, A_2, A_3))^2 = \left(\tfrac{12V(OA_1A_2A_3)}{R}\right)^2 = \tfrac{1}{2R^2} M_4^0(x_{12}, x_{13}, R^2, x_{23}, R^2, R^2)\,.$$

Therefore (recall that $K = \frac{1}{R^2}$),

$$\begin{aligned}(S^K(A_1, A_2, A_3))^2 &= \tfrac{1}{2R^2} \det \begin{bmatrix} 0 & 1 & 1 & 1 & 1 \\ 1 & 0 & x_{12} & x_{13} & R^2 \\ 1 & x_{12} & 0 & x_{23} & R^2 \\ 1 & x_{13} & x_{23} & 0 & R^2 \\ 1 & R^2 & R^2 & R^2 & 0 \end{bmatrix}\,, \\ &= -x_{12}^2 - x_{13}^2 - x_{23}^2 + 2x_{12}x_{13} + 2x_{12}x_{23} + 2x_{13}x_{23} - Kx_{12}x_{13}x_{23}\,, \\ &= H^K(x_{12}, x_{13}, x_{23})\,. \end{aligned}$$

□

A spherical triangle ABC is uniquely determined, up to the action of $\mathrm{Aut}(\mathbf{S})$, by its squared side distances a, b, c together with the additional data of $S^K(A, B, C)$:

Lemma 3.12. *Let $A, C \in \mathbf{S}$ with $x(A, C) = b \notin \left\{0, \frac{4}{K}\right\}$. Let $a, c, p \in \mathbb{C}$ be such that*

$$p^2 = H^K(a, b, c)\,. \tag{3.1.6}$$

Then there exists a unique point $B \in \mathbf{S}$ with $x(B, C) = a$, $x(A, B) = c$, and $S^K(A, B, C) = p$.

Proof. Let $A = \begin{bmatrix} u' \\ u'' \\ u''' \end{bmatrix}$, $C = \begin{bmatrix} v' \\ v'' \\ v''' \end{bmatrix}$. Since $A, C \in \mathbf{S}$, we have

$$(u')^2 + (u'')^2 + (u''')^2 = R^2\,, \qquad \text{and} \qquad (v')^2 + (v'')^2 + (v''')^2 = R^2\,. \tag{3.1.7}$$

The condition $x(A, C) = b$ gives $(u' - v')^2 + (u'' - v'')^2 + (u''' - v''')^2 = b$. Combining these facts, we see that

$$u'v' + u''v'' + u'''v''' = R^2 - \tfrac{b}{2}\,. \tag{3.1.8}$$

We seek a point $B = \begin{bmatrix} w' \\ w'' \\ w''' \end{bmatrix} \in \mathbf{S}$ with $w', w'', w''' \in \mathbb{C}$ that satisfies the conditions

$$\begin{aligned} (w')^2 + (w'')^2 + (w''')^2 &= R^2\,, \\ (u' - w')^2 + (u'' - w'')^2 + (u''' - w''')^2 &= a\,, \qquad (3.1.9) \\ (v' - w')^2 + (v'' - w'')^2 + (v''' - w''')^2 &= c\,. \qquad (3.1.10) \end{aligned}$$

Combining these conditions and simplifying, equations (3.1.9)-(3.1.10) translate into

$$u'w' + u''w'' + u'''w''' = R^2 - \tfrac{a}{2}\,, \tag{3.1.11}$$

$$v'w' + v''w'' + v'''w''' = R^2 - \tfrac{c}{2}\,. \tag{3.1.12}$$

To achieve $S^K(A,B,C)=p$ we need

$$p=\tfrac{2}{R}\det\begin{bmatrix} u' & v' & w' \\ u'' & v'' & w'' \\ u''' & v''' & w''' \end{bmatrix}. \tag{3.1.13}$$

The system of three linear equations (3.1.11)-(3.1.13) in w', w'', w''' can be represented with the matrix

$$\left[\begin{array}{ccc|c} u' & u'' & u''' & R^2-\frac{a}{2} \\ v' & v'' & v''' & R^2-\frac{c}{2} \\ \frac{2}{R}(u''v'''-v''u''') & \frac{2}{R}(u'''v'-u'v''') & \frac{2}{R}(u'v''-v'u'') & p \end{array}\right]; \tag{3.1.14}$$

the system will have a single solution if the determinant of the left 3×3 submatrix is non-zero. Up to scaling by $R/2$, the Laplace expansion along the bottom row of the submatrix is

$$\Delta := (u'v''-v'u'')^2+(u'''v'-u'v''')^2+(u''v'''-v''u''')^2\,.$$

Let us verify $\Delta\neq 0$ under the conditions given. From equations (3.1.7) we deduce:

$$R^4=(u'v')^2+(u''v'')^2+(u'''v''')^2+2(u'u''v'v''+u'u'''v'v'''+u''u'''v''v''')+\Delta\,.$$

Recalling equation (3.1.8), this implies

$$R^4=\left(R^2-\tfrac{b}{2}\right)^2+\Delta\,. \tag{3.1.15}$$

Since $b\notin\left\{0,\frac{4}{K}\right\}$, we conclude that the system of equations represented by (3.1.14) has a unique solution, namely

$$\begin{aligned}
w' &= \tfrac{1}{\Delta}\Big(\left(R^2-\tfrac{a}{2}\right)(v''(u'v''-u''v')+v'''(u'v'''-u'''v')) \\
&\qquad -\left(R^2-\tfrac{c}{2}\right)(u''(u'v''-u''v')+u'''(u'v'''-u'''v'))+\tfrac{Rp}{2}(u''v'''-u'''v'')\Big), \\
w'' &= \tfrac{1}{\Delta}\Big(\left(R^2-\tfrac{a}{2}\right)(v'(u''v'-u'v'')+v'''(u''v'''-u'''v''))) \\
&\qquad -\left(R^2-\tfrac{c}{2}\right)(u'(u''v'-u'v'')+u'''(u''v'''-u'''v''))+\tfrac{Rp}{2}(u'''v'-u'v''')\Big), \\
w''' &= \tfrac{1}{\Delta}\Big(\left(R^2-\tfrac{a}{2}\right)(v'(u'''v'-u'v''')+v''(u'''v''-u''v''')) \\
&\qquad -\left(R^2-\tfrac{c}{2}\right)(u'(u'''v'-u'v''')+u''(u'''v''-u''v'''))+\tfrac{Rp}{2}(u'v''-u''v')\Big).
\end{aligned}$$

It remains to verify that $(w')^2+(w'')^2+(w''')^2=R^2$.

Expanding, making use of equations (3.1.7)-(3.1.8), and simplifying, we obtain

$$(w')^2 + (w'')^2 + (w''')^2 = \tfrac{R^2}{\Delta}\left(R^2 b + \tfrac{p^2}{4} + \tfrac{a^2}{4} + \tfrac{c^2}{4} - \tfrac{ab}{2} - \tfrac{ac}{2} - \tfrac{bc}{2} + \tfrac{abc}{4R^2}\right).$$

We are now able to substitute for p^2 using the given condition (3.1.6). We simplify the resulting expression using equation (3.1.15) to complete the proof:

$$(w')^2 + (w'')^2 + (w''')^2 = \tfrac{R^2}{\Delta}\left(R^2 b - \tfrac{b^2}{4}\right) = R^2\,. \qquad \square$$

Remark 3.13. The condition $b \neq 0$ in Lemma 3.12 prevents points A and C from being coincident. In the real setting, the condition $b \neq \frac{4}{K} = (2R)^2$ prohibits A and C from being antipodal on the sphere. This prohibition is necessary: for antipodal A and C, there are infinitely many points B satisfying the conditions in Lemma 3.12.

Lemma 3.14. *Let $a, b, c \in \mathbb{C}$ with at least one of a, b, c nonzero and not equal to $\frac{4}{K}$. If $p^2 = H^K(a, b, c)$, then there exist points $A, B, C \in \mathbf{S}$ such that*

$$x(B,C) = a\,, \quad x(A,C) = b\,, \quad x(A,B) = c\,, \quad \text{and} \quad S^K(A,B,C) = p\,.$$

Moreover, such a triple (A, B, C) is unique up to the action of $\mathrm{Aut}(\mathbf{S})$.

Proof. Without loss of generality, we can assume that $b \notin \left\{0, \frac{4}{K}\right\}$. Let $A, C \in \mathbf{S}$ such that $x(A, C) = b$. Then there exists a unique point $B \in \mathbf{S}$ such that $x(B, C) = a$, $x(A, B) = c$, and $S^K(A, B, C) = p$ by Lemma 3.12. $\square$

3.2 Spherical quadrilaterals

Moving towards spherical polygons, in this section we will establish key algebraic relations satisfied by the squared side distances and S^K measurements formed by four points on the sphere $\mathbf{S}$.

Example 3.15. A spherical quadrilateral $A_1A_2A_3A_4$ can be subdivided into two spherical triangles in two different ways. Each triangle (e.g., $A_1A_2A_3$) gives rise to a tetrahedron (say, $OA_1A_2A_3$) as shown in Figure 3.1 below. The associated measurements are:

$$\begin{aligned}
&a = x_{14}\,, \quad b = x_{12}\,, \quad c = x_{23}\,, \quad d = x_{34}\,, \quad e = x_{13}\,, \quad f = x_{24}\,,\\
&g = x(O, A_1)\,, \quad h = x(O, A_2)\,, \quad i = x(O, A_3)\,, \quad j = x(O, A_4)\,,\\
&p = S^K(A_1, A_2, A_3)\,, \quad q = S^K(A_1, A_3, A_4)\,, \qquad (3.2.1)\\
&r = S^K(A_1, A_2, A_4)\,, \quad s = S^K(A_2, A_3, A_4)\,. \qquad (3.2.2)
\end{aligned}$$

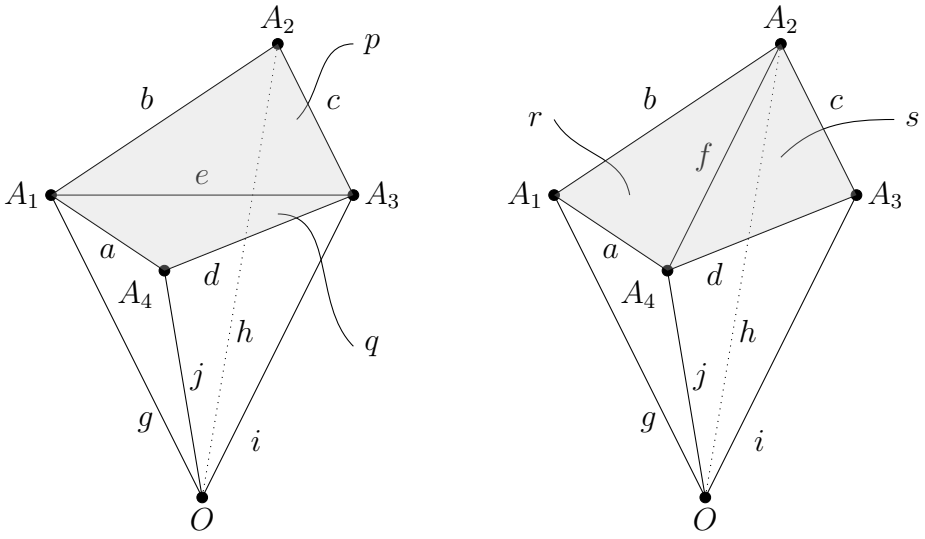


Figure 3.1: Measurements associated to triangulations of a spherical quadrilateral.

We will derive our first type of relation amongst the measurement data for a spherical quadrilateral from the following elementary lemma.

Lemma 3.16 (cf. [Wey46, Chapter III, Section 17, the J_3 relation])**.** *Let $\overrightarrow{v_1}, \ldots, \overrightarrow{v_{d+1}}$ be vectors in a d-dimensional space W equipped with a volume form*

$$\begin{aligned} [\,] : W^d &\to \mathbb{R}\,, \\ (\overrightarrow{w_1}, \ldots, \overrightarrow{w_d}) &\mapsto \left[\overrightarrow{w_1} \;\cdots\; \overrightarrow{w_d}\right]\,. \end{aligned}$$

Let $\widehat{\overrightarrow{v_i}}$ indicate that we omit $\overrightarrow{v_i}$ when computing the volume form. Then

$$\sum_{i=1}^{d+1} (-1)^{i+1} \left[\overrightarrow{v_1} \;\cdots\; \widehat{\overrightarrow{v_i}} \;\cdots\; \overrightarrow{v_{d+1}}\right] \overrightarrow{v_i} = 0\,. \tag{3.2.3}$$

Proof. Let $v_{1,j}, v_{2,j}, \ldots, v_{d+1,j}$ be the jth coordinates of vectors $\overrightarrow{v_1}, \ldots, \overrightarrow{v_{d+1}}$ respectively. Form the $d \times (d+1)$-matrix of column vectors $\overrightarrow{v_1}, \overrightarrow{v_2}, \ldots, \overrightarrow{v_{d+1}}$. Select a row j and duplicate it, placing it above to form a $(d+1) \times (d+1)$-matrix. The resulting matrix is singular because it has two identical rows. Laplace expansion then gives

$$\begin{bmatrix} v_{1,j} & v_{2,j} & \ldots & v_{d+1,j} \\ \overrightarrow{v_1} & \overrightarrow{v_2} & \ldots & \overrightarrow{v_{d+1}} \end{bmatrix} = \sum_{i=1}^{d+1} (-1)^{i+1} \left[\overrightarrow{v_1} \;\cdots\; \widehat{\overrightarrow{v_i}} \;\cdots\; \overrightarrow{v_{d+1}}\right] v_{i,j} = 0\,. \tag{3.2.4}$$

As this works for any row j we get the claim. □

Remark 3.17. Taking scalar products with an arbitrary vector in equation (3.2.3) yields an algebraic relation. E.g., if $\overrightarrow{x}, \overrightarrow{y}, \overrightarrow{z}, \overrightarrow{w}$ are vectors in a 2-dimensional Euclidean space, then we have

$$\left[\overrightarrow{x}\ \overrightarrow{y}\right]\langle\overrightarrow{z},\overrightarrow{w}\rangle - \left[\overrightarrow{x}\ \overrightarrow{z}\right]\langle\overrightarrow{y},\overrightarrow{w}\rangle + \left[\overrightarrow{y}\ \overrightarrow{z}\right]\langle\overrightarrow{x},\overrightarrow{w}\rangle = 0\,.$$

Proposition 3.18. *In the setting of Example 3.15, depicted in Figure 3.1, the following identities hold:*

$$p+q = r+s+\tfrac{K}{2}(ap+bq-er)\,, \tag{3.2.5}$$
$$p+q = r+s+\tfrac{K}{2}(fp-cr-bs)\,, \tag{3.2.6}$$
$$p+q = r+s+\tfrac{K}{2}(dp+cq-es)\,, \tag{3.2.7}$$
$$p+q = r+s+\tfrac{K}{2}(fq-dr-as)\,. \tag{3.2.8}$$

Proof. Take, e.g., $\overrightarrow{g}$ as shorthand for the vector $\overrightarrow{OA_1}$. Let V_{ijk} be the volume of the tetrahedron $OA_iA_jA_k$.

By Lemma 3.16 and the fact that the determinant of a matrix of three column vectors is six times the volume of the tetrahedron they define (equation (3.1.1)), we get

$$6V_{234}\overrightarrow{g} - 6V_{134}\overrightarrow{h} + 6V_{124}\overrightarrow{i} - 6V_{123}\overrightarrow{j} = 0\,.$$

Multiply by $2/R$ to get

$$s\overrightarrow{g} - q\overrightarrow{h} + r\overrightarrow{i} - p\overrightarrow{j} = 0\,. \tag{3.2.9}$$

As in Remark 3.17, take scalar products of equation 3.2.9 with $\overrightarrow{g}, \overrightarrow{h}, \overrightarrow{i}, \overrightarrow{j}$ respectively. Then use the identities of the form

$$\langle\overrightarrow{i},\overrightarrow{j}\rangle = R^2 - \frac{d}{2}$$

to obtain

$$\begin{aligned}
p(2-Ka) + q(2-Kb) - r(2-Ke) - 2s &= 0\,,\\
p(2-Kf) + 2q - r(2-Kc) - s(2-Kb) &= 0\,,\\
p(2-Kd) + q(2-Kc) - 2r - s(2-Ke) &= 0\,,\\
2p + q(2-Kf) - r(2-Kd) - s(2-Ka) &= 0\,.
\end{aligned}$$

Rearranging yields the claim. □

Remark 3.19. Taking $R \to \infty$ (equivalently, $K \to 0$), each of equations (3.2.5)-(3.2.8) becomes

$$p + q = r + s.$$

For configurations in $V_{\mathbb{R}}$ with $K = 0$, this statement reflects the fact that in a triangulation of a quadrilateral, the areas of the two triangles add up to the area of the quadrilateral.

Corollary 3.20. *In the setting of Example 3.15, depicted in Figure 3.1, the following relations hold:*

$$\begin{aligned}
a(p+s) &= q(f-b) + r(e-d)\,, \\
b(s+q) &= p(f-a) + r(e-c)\,, \\
c(q+r) &= p(f-d) + s(e-b)\,, \\
d(r+p) &= q(f-c) + s(e-a)\,, \\
e(r-s) &= p(a-d) + q(b-c)\,, \\
f(p-q) &= r(c-d) + s(b-a)\,.
\end{aligned} \tag{3.2.10}$$

Proof. Each of these relations can be obtained by subtracting one equation in Proposition 3.18 from another and rearranging. □

Remark 3.21. Any three equations in Corollary 3.20 imply the rest. Note that equation (3.2.10) recovers [FS21, (2.19)].

The final identities that we will establish for spherical quadrilaterals are analogues of the following classical result.

Theorem 3.22 (Bretschneider's Formula)**.** *Let V be 2-dimensional Euclidean space. As in Example 3.15, let $A_1, A_2, A_3, A_4 \in V$, and define $a, b, c, d, e, f, p, q, r, s$. Then*

$$4ef = (p+q)^2 + (a-b+c-d)^2 = (r+s)^2 + (a-b+c-d)^2\,.$$

Remark 3.23. In 1842, Bretschneider [Bre42] and Strehlke [Str42] each published proofs that in the Euclidean planar version ($V = V_{\mathbb{R}}$ and $K = 0$) of Example 3.15 above, we have

$$(p+q)^2 = (s-a)(s-b)(s-c)(s-d) - abcd\cos^2\left(\tfrac{\alpha+\gamma}{2}\right)\,,$$

where $s = \frac{a+b+c+d}{2}$ and α and γ are the angles between sides labeled by a and b and c and d respectively. The version appearing in Theorem 3.22 above and used in [FS21] seems to be due to Coolidge [Coo39]. Coolidge's formulation generalizes a similar result known as

Brahmagupta's formula (6th century CE) for the area of a cyclic quadrilateral; see [Ayo07] for an exposition of Brahmagupta and Bretschneider's formulas and related results. Of note, Heron's formula (Theorem 3.8) can be regarded as a degenerate case of Brahmagupta's formula (see [JG20]), and hence a special case of Bretschneider's formula.

Bretschneider's formula has been proved in many different ways. One common method is to represent the sides and diagonals of a quadrilateral by vectors and to relate the area of the quadrilateral to the cross product of the vectors representing the diagonals. We will provide a proof based on the following classical fact. The method of this proof will then be used to establish a spherical version.

Lemma 3.24 ([Mui82, Sections 67-68])**.** *Let* $\overrightarrow{u_1}, \dots, \overrightarrow{u_n}, \overrightarrow{v_1}, \dots, \overrightarrow{v_n} \in V$*. Then*

$$\det \begin{bmatrix} \langle \overrightarrow{u_1}, \overrightarrow{v_1} \rangle & \dots & \langle \overrightarrow{u_1}, \overrightarrow{v_n} \rangle \\ \vdots & \ddots & \vdots \\ \langle \overrightarrow{u_n}, \overrightarrow{v_1} \rangle & \dots & \langle \overrightarrow{u_n}, \overrightarrow{v_n} \rangle \end{bmatrix} = \begin{bmatrix} \overrightarrow{u_1} & \cdots & \overrightarrow{u_n} \end{bmatrix} \begin{bmatrix} \overrightarrow{v_1} & \cdots & \overrightarrow{v_n} \end{bmatrix} . \tag{3.2.11}$$

Remark 3.25. The determinant on the left-hand side of equation (3.2.11) is commonly called a Gram determinant (see, e.g., [Ber77, Section 8.11.5]). The identity (3.2.11) appears in [Tur60, Chapter IV, Section 6], is the first relation listed for SL_n in [PV94, p. 255], and is deemed a "well-known relation" by Weyl [Wey46, p. 53].

Proof of Theorem 3.22. Use the shorthand $\overrightarrow{a}$ (respectively, $\overrightarrow{b}$, $\overrightarrow{e}$) for the vector $\overrightarrow{A_1A_4}$ (respectively, $\overrightarrow{A_1A_2}$, $\overrightarrow{A_1A_3}$). By Lemma 3.24,

$$\det \begin{bmatrix} 2\langle \overrightarrow{a}, \overrightarrow{b} \rangle & 2\langle \overrightarrow{a}, \overrightarrow{e} \rangle \\ 2\langle \overrightarrow{e}, \overrightarrow{b} \rangle & 2\langle \overrightarrow{e}, \overrightarrow{e} \rangle \end{bmatrix} = 2 \begin{bmatrix} \overrightarrow{a} & \overrightarrow{e} \end{bmatrix} \cdot 2 \begin{bmatrix} \overrightarrow{b} & \overrightarrow{e} \end{bmatrix} .$$

First note that the oriented area of the (flat) triangle $A_1A_2A_3$ is equal to $\frac{1}{2} \begin{bmatrix} \overrightarrow{b} & \overrightarrow{e} \end{bmatrix}$, implying $p = 2 \begin{bmatrix} \overrightarrow{b} & \overrightarrow{e} \end{bmatrix}$. Similarly $q = -2 \begin{bmatrix} \overrightarrow{a} & \overrightarrow{e} \end{bmatrix}$. Then using the identities analogous to

$$2\langle \overrightarrow{a}, \overrightarrow{b} \rangle = a + b - f ,$$

we get

$$\det \begin{bmatrix} a+b-f & a+e-d \\ b+e-c & 2e \end{bmatrix} = -qp .$$

Therefore

$$2ef - be - ce + e^2 - ae - de + ab - ac - bd + dc = qp , \tag{3.2.12}$$

which implies, by virtue of Heron's formula:

$$\begin{aligned}(p+q)^2 &= p^2+q^2+2pq \\ &= (-b^2-c^2-e^2+2bc+2be+2ce)+(-a^2-d^2-e^2+2ad+2ae+2de) \\ &\quad +2(2ef-be-ce+e^2-ae-de+ab-ac-bd+dc) \qquad (3.2.13) \\ &= 4ef-(a-b+c-d)^2\,. \qquad \square\end{aligned}$$

We next obtain the following spherical analogues of Bretschneider's formula. In the case $K=0$, both equations recover Bretschneider's formula.

Theorem 3.26 (Spherical Analogues of Bretschneider's Formula)**.** *In the setting of Example 3.15, the following two equations hold:*

$$4ef\left(1-\tfrac{Ke}{4}\right) = (p+q)^2+(a-b+c-d)^2-Ke(a-b)(c-d)\,, \qquad (3.2.14)$$

$$4ef\left(1-\tfrac{Kf}{4}\right) = (r+s)^2+(a-b+c-d)^2-Kf(a-d)(c-b)\,. \qquad (3.2.15)$$

Proof. We follow the general plan of the above proof of Theorem 3.22.

By Lemma 3.24,

$$\det\begin{bmatrix}\langle\overrightarrow{g},\overrightarrow{g}\rangle & \langle\overrightarrow{g},\overrightarrow{i}\rangle & \langle\overrightarrow{g},\overrightarrow{j}\rangle \\ \langle\overrightarrow{h},\overrightarrow{g}\rangle & \langle\overrightarrow{h},\overrightarrow{i}\rangle & \langle\overrightarrow{h},\overrightarrow{j}\rangle \\ \langle\overrightarrow{i},\overrightarrow{g}\rangle & \langle\overrightarrow{i},\overrightarrow{i}\rangle & \langle\overrightarrow{i},\overrightarrow{j}\rangle\end{bmatrix} = \begin{bmatrix}\overrightarrow{g} & \overrightarrow{h} & \overrightarrow{i}\end{bmatrix}\cdot\begin{bmatrix}\overrightarrow{g} & \overrightarrow{i} & \overrightarrow{j}\end{bmatrix}\,.$$

Manipulating scalar products and recalling definitions, this becomes

$$\begin{aligned}\det\begin{bmatrix}g & \frac{g+i-e}{2} & \frac{g+j-a}{2} \\ \frac{h+g-b}{2} & \frac{h+i-c}{2} & \frac{h+j-f}{2} \\ \frac{i+g-e}{2} & i & \frac{i+j-d}{2}\end{bmatrix} &= 6V_{123}\cdot 6V_{134}\,, \\ &= \tfrac{R}{2}S^K_{123}\cdot\tfrac{R}{2}S^K_{134}\,.\end{aligned}$$

Noting that $g,i,h,j=R^2$, we deduce

$$4K\cdot\det\begin{bmatrix}\frac{1}{K} & \frac{1}{K}-\frac{e}{2} & \frac{1}{K}-\frac{a}{2} \\ \frac{1}{K}-\frac{b}{2} & \frac{1}{K}-\frac{c}{2} & \frac{1}{K}-\frac{f}{2} \\ \frac{1}{K}-\frac{e}{2} & \frac{1}{K} & \frac{1}{K}-\frac{d}{2}\end{bmatrix} = pq\,.$$

Computing the determinant and simplifying, we get

$$ab - ac - bd + cd - ae - be - ce - de + e^2 + 2ef + \tfrac{K}{2}(ace + bde - e^2 f) = pq\,. \tag{3.2.16}$$

Using this in a calculation analogous to (3.2.13) (but with the formulas (3.2.1)-(3.2.2) for p^2 and q^2) produces equation (3.2.14).

Equation (3.2.15) can be derived in a similar way. □

The following collection of identities will prove useful later.

Proposition 3.27. *Let $A_1, A_2, A_3, A_4 \in \mathbf{S}$ and consider the spherical quadrilateral $A_1A_2A_3A_4$ with measurements $a, b, c, d, e, f, p, q, r, s$ as in Example 3.15. Then*

$$p^2 = H^K(b, c, e) = -b^2 - c^2 - e^2 + 2bc + 2be + 2ce - Kbce\,, \tag{3.2.17}$$

$$q^2 = H^K(a, d, e) = -a^2 - d^2 - e^2 + 2ad + 2ae + 2de - Kade\,, \tag{3.2.18}$$

$$r^2 = H^K(a, b, f) = -a^2 - b^2 - f^2 + 2ab + 2af + 2bf - Kabf\,, \tag{3.2.19}$$

$$s^2 = H^K(c, d, f) = -c^2 - d^2 - f^2 + 2cd + 2cf + 2df - Kcdf\,, \tag{3.2.20}$$

$$p + q = r + s + \tfrac{K}{2}(ap + bq - er)\,, \tag{3.2.21}$$

$$4ef\left(1 - \tfrac{Ke}{4}\right) = (p + q)^2 + (a - b + c - d)^2 - Ke(a - b)(c - d)\,, \tag{3.2.22}$$

$$e(r - s) = p(a - d) + q(b - c)\,. \tag{3.2.23}$$

Proof. Equations (3.2.17), (3.2.18), (3.2.19), and (3.2.20) are all instances of equation (3.11). Equation (3.2.21) is equation (3.2.5). Equation (3.2.22) is equation (3.2.14). Equation (3.2.23) is equation (3.2.10). □

Remark 3.28. Specializing $K = 0$ recovers [FS21, (2.13)-(2.19)].

3.3 Spherical Heronian friezes

We established that the data of three squared distances x_{ij} together with an associated S^K measurement is sufficient to determine a spherical triangle (cf. Lemma 3.14). In this section, we consider a more general question: Which measurement data are sufficient to determine a spherical polygon? Some definitions and results in this section are spherical counterparts of those in [FS21, Sections 2, 3].

Definition 3.29. For $n \geq 3$, a labeled spherical polygon (or n-gon) in $\mathbf{S}$ is an ordered n-tuple of points

$$P = (A_1, \ldots, A_n) \in \mathbf{S}^n.$$

For such a polygon, for distinct $i, j, k \in \{1, \ldots, n\}$, we collect the measurements $x_{ij} = x_{ij}(P)$ and $S^K_{ijk} = S^K_{ijk}(P) = S^K(A_i, A_j, A_k)$ and form the tuple

$$\mathbf{xS}(P) = (x_{ij}) \sqcup (S^K_{ijk}).$$

Note that by Proposition 3.11 these measurements satisfy the equations

$$(S^K_{ijk})^2 = H^K(x_{ij}, x_{jk}, x_{ik}). \tag{3.3.1}$$

Definition 3.30. Let G be an undirected graph on n vertices $v_1, \ldots, v_n$ with $2n-3$ edges, of which a distinguished size n set, without loss of generality

$$(v_1, v_2), (v_2, v_3), \ldots, (v_{n-1}, v_n), (v_n, v_1),$$

form a cycle. The $n-3$ edges of G that are not in the distinguished cycle are called diagonals. We call G a triangulated cycle, or refer to G as a triangulation, if there exists an embedding of G into the real plane such that the distinguished cycle is represented by a convex n-gon (with $v_1, \ldots, v_n$ appearing in clockwise order) and the diagonals are represented by pairwise non-crossing diagonals.

Definition 3.31. A triangulated spherical polygon $T = (P, G)$ is a spherical polygon P together with a choice of triangulation G of the underlying cycle. For such an object, we consider the subcollection of measurements $\mathbf{xS}_G(P) \subset \mathbf{xS}(P)$, which contains all the measurements x_{ij} and S^K_{ijk} that correspond to the sides, diagonals, and triangles that appear in the triangulation G.

Proposition 3.32. *Let G be a triangulated cycle with vertices $v_1, \ldots, v_n$ as in Definition 3.30. Let $\mathbf{xS}_G = (x_{ij}) \sqcup (S^K_{ijk})$ be a tuple of complex numbers such that*

- *the numbers $x_{ij} \in \mathbb{C} - \{0, \frac{4}{K}\}$, for $i < j$, are labeled by the edges $\{v_i, v_j\}$ present in G, and*
- *the numbers S^K_{ijk}, $i < j < k$, are labeled by the triangles (v_i, v_j, v_k) in G.*

Assume that equation (3.3.1) *holds for each $i < j < k$:*

$$(S^K_{ijk})^2 = H^K(x_{ij}, x_{ik}, x_{jk}).$$

Then there exists a spherical n-gon P on $\mathbf{S}$ such that $\mathbf{xS}_G(P) = \mathbf{xS}_G$. Moreover, the polygon P is unique up to the action of $\mathrm{Aut}(\mathbf{S})$. *In particular, all measurements in $\mathbf{xS}(P)$ are uniquely determined by $\mathbf{xS}_G(P)$.*

Proof. We proceed by induction on the number of vertices in G. If G has one triangle, we can apply Lemma 3.14. Assume the claim holds for $k < n$ and consider G with n vertices. Then G has $n-2$ triangles, so one triangle must include two edges from the distinguished cycle. Apply Lemmas 3.12 and 3.14 to this triangle. The rest of G has less than n vertices in its distinguished cycle, and only shares one edge with the triangle we have constructed. By induction we get the claim. □

We will next write formulas expressing the measurements for a spherical polygon P in terms of the initial data associated to a triangulation of the vertices of P. We begin with the case of a quadrilateral, then proceed to the more general case. We will use the following object to organize the measurement data of a quadrilateral.

Definition 3.33. Let $K \in \mathbb{C}$. A spherical Heronian diamond is an ordered 10-tuple of numbers $(a, b, c, d, e, f, p, q, r, s)$ satisfying equations (3.2.17)-(3.2.23). We display the entries in a diamond shape as shown on the right in Figure 3.2. Explicitly,

- a, c, e, f are placed at the corners of the diamond;
- p, q, r, s are placed at the midpoints of the sides of the diamond;
- the dashed line going Southeast (resp. Southwest) is labeled d (resp. b).

The entries are arranged so that the four "measurements" associated with each side of the diamond (e.g., a, d, e, q) satisfy the corresponding spherical Heron equation (e.g., equation (3.2.18)).

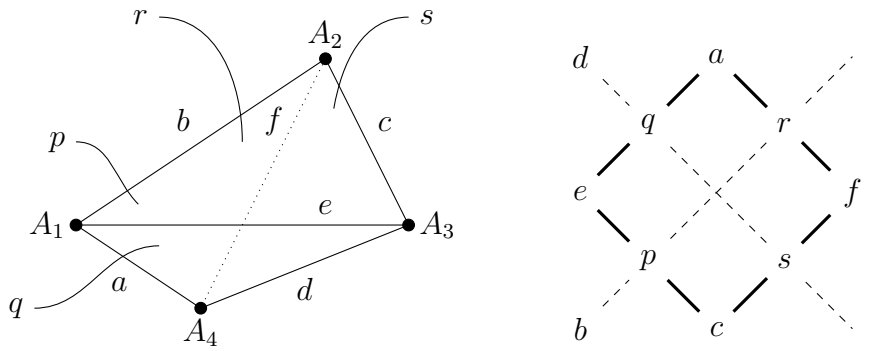


Figure 3.2: Left: A spherical quadrilateral $A_1A_2A_3A_4$ as discussed in Example 3.15. Right: A spherical Heronian diamond.

Remark 3.34. A spherical quadrilateral gives rise to a spherical Heronian diamond. Conversely, for any spherical Heronian diamond $(a, b, c, d, e, f, p, q, r, s)$ such that $a, b, c, d, e, f \notin \{0, \frac{4}{K}\}$, Proposition 3.32 implies that there exists a unique spherical quadrilateral $A_1A_2A_3A_4$ associated to it, as in Example 3.15.

A priori, a spherical Heronian diamond is a purely algebraic object, an ordered 10-tuple of numbers that satisfy certain relations. We will next derive formulas to express three of these numbers (f, r, s) in terms of the others. When applied in the geometric context, these formulas will allow us to express the ten measurements $\mathbf{xS}(P)$ of a spherical quadrilateral in terms of the seven measurements $\mathbf{xS}_G(P)$ associated to its triangulation.

Proposition 3.35. *Let (a, b, c, d, e, p, q) be a 7-tuple of complex numbers satisfying equations* (3.2.17)-(3.2.18)*, with $e \notin \left\{0, \frac{4}{K}\right\}$. Then there exist unique $f, r, s \in \mathbb{C}$ such that the 10-tuple $(a, b, c, d, e, f, p, q, r, s)$ is a spherical Heronian diamond. Specifically*

$$f = \frac{(p+q)^2 + (a-b+c-d)^2 - Ke(a-b)(c-d)}{4e\left(1 - \frac{Ke}{4}\right)}, \tag{3.3.2}$$

$$r = \frac{p\left(e + a - d - \frac{Kae}{2}\right) + q\left(e - c + b - \frac{Kbe}{2}\right)}{2e\left(1 - \frac{Ke}{4}\right)}, \tag{3.3.3}$$

$$s = \frac{p\left(e - a + d - \frac{Kde}{2}\right) + q\left(e + c - b - \frac{Kce}{2}\right)}{2e\left(1 - \frac{Ke}{4}\right)}. \tag{3.3.4}$$

(The condition $e \notin \{0, \frac{4}{K}\}$ ensures that the denominators of equations (3.3.2)-(3.3.4) *do not vanish.)*

Proof. Define f, r, s as in equations (3.3.2), (3.3.3), and (3.3.4). To verify that the resulting tuple $(a, b, c, d, e, f, p, q, r, s)$ is a spherical Heronian diamond we need to verify equations (3.2.19)-(3.2.23). (Equations (3.2.17)-(3.2.18) hold by assumption.)

Equations (3.2.19) and (3.2.20) can be checked with standard software, as follows. For each of the equations (3.2.17), (3.2.18), (3.3.2), (3.3.3), and (3.3.4), identify a polynomial that vanishes when the equation holds. For example, the equation (3.2.17)

$$p^2 = -b^2 - c^2 - e^2 + 2bc + 2be + 2ce - Kbce$$

corresponds to the polynomial

$$p^2 - (-b^2 - c^2 - e^2 + 2bc + 2be + 2ce - Kbce). \tag{3.3.5}$$

Collect these five polynomials and use them to generate an ideal I. Then, for example,

equation (3.2.19) is obtained by checking that

$$e^2(Ke-4)^2(r^2-(-a^2-b^2-f^2+2ab+2af+2bf-Kabf))\in I. \tag{3.3.6}$$

We can check for ideal membership by reducing the polynomial (3.3.6) with respect to a Gröbner basis B (for example with lexicographic monomial order). Note that the polynomial (3.3.5) does not lie in I: the factors e^2 and $(Ke-4)^2$ in (3.3.6) are required for the argument to work.

Equation (3.3.2) can be slightly rearranged to get equation (3.2.22). Equations (3.2.21)-(3.2.23) can be verified manually, by plugging in the definitions of r and s.

To show the uniqueness of f, r, s, it suffices to deduce (3.3.2)-(3.3.4) from the equations of a spherical Heronian diamond. Again, equation (3.2.22) can be slightly rearranged to obtain equation (3.3.2). To get r, we use equation (3.2.10). Replacing s with the expression obtained from (3.2.21), we get

$$er = p(a-d)+q(b-c)+e\left(p+q-K\left(\tfrac{ap+bq-er}{2}\right)\right).$$

Simplifying, we obtain (3.3.3). Formula (3.3.4) is established analogously. □

Remark 3.36. By Proposition 3.35, Definitions 3.33 and 1.18 are equivalent to each other.

Let P be a spherical quadrilateral with squared side distances a, b, c, d. Proposition 3.35 gives formulas to express the squared distance f and the S^K measurements r, s in terms of a, b, c, d, the squared distance e, and the S^K measurements p, q.

The following example shows an application of Theorem 3.35.

Example 3.37. Given the five spherical distances shown in Figure 3.3, let us compute the unknown spherical distance from Minneapolis to Miami. For this calculation we will assume that the surface of the Earth is a sphere whose great circles have length $40,000\,\text{km}$. Then $R = \frac{4\cdot 10^4}{2\cdot\pi}\,\text{km}$ and therefore $K = \frac{\pi^2}{4\cdot 10^8}\,\text{km}^{-2}$.

We begin by converting spherical distances into squared Euclidean distances. Let $|AB|$ be the spherical distance between points $A, B \in \mathbf{S}$. The squared Euclidean distance between A and B (cf. (3.1)) is given by

$$x(A,B) = 2R^2\left(1-\cos\left(\tfrac{|AB|}{R}\right)\right).$$

Applying this formula to the values in Figure 3.3, we get the values of a, b, c, d, e shown in Figure 3.4. Let f denote the squared Euclidean distance between Minneapolis and Miami.

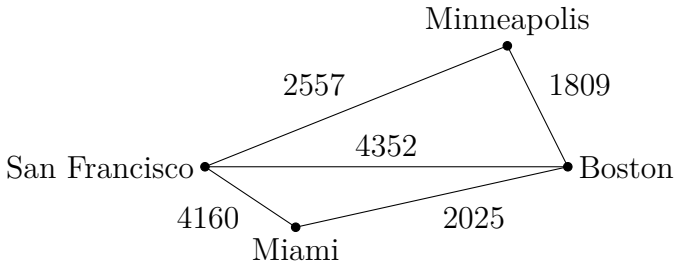


Figure 3.3: Spherical distances (in km) between four American cities [Swa].

Let

$$p = S^K(\text{San Francisco, Minneapolis, Boston}),$$
$$q = S^K(\text{San Francisco, Boston, Miami}).$$

Then $p^2 = H^K(b, c, e)$ and $q^2 = H^K(a, d, e)$ with H^K given by equation (3.10). Taking positive square roots, we obtain the quantities p, q shown in Figure 3.4.

We can now use equation (3.3.2) to compute the spherical distance F from Minneapolis to Miami:

$$f = \frac{(p+q)^2 + (a-b+c-d)^2 - Ke(a-b)(c-d)}{4e\left(1 - \frac{Ke}{4}\right)} = 57600370 \text{ km}^2,$$
$$F = R \arccos\left(1 - \tfrac{57600370 \text{ km}^2}{2R^2}\right) = 2414 \text{ km}.$$

We note that in spite of making several simplifications and approximations, our calculation achieved a remarkably accurate result: the actual spherical distance from Miami to Minneapolis is 2415 km, see [Swa].

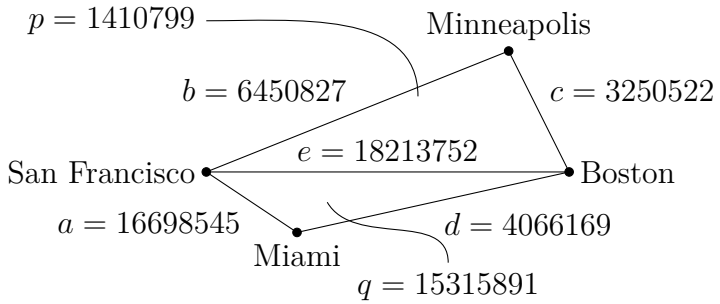


Figure 3.4: Squared Euclidean distances between the four cities (in km^2).

We next discuss the symmetries of the notion of a spherical Heronian diamond.

Proposition 3.38. *Let $(a, b, c, d, e, f, p, q, r, s)$ be a spherical Heronian diamond. Then*

1. *$(c, d, a, b, e, f, q, p, s, r)$ is a spherical Heronian diamond;*
2. *if $e \notin \left\{0, \frac{4}{K}\right\}$ then $(a, d, c, b, f, e, s, r, q, p)$ is a spherical Heronian diamond.*

Proposition 3.38 implies that flipping a spherical Heronian diamond horizontally or vertically produces another spherical Heronian diamond.

Proof. To prove the first claim, we interchange $a \leftrightarrow c$, $b \leftrightarrow d$, $p \leftrightarrow q$, and $r \leftrightarrow s$. These switches correspond to a vertical reflection of the spherical Heronian diamond across the center horizontal axis. We need to show equations (3.2.17)-(3.2.23) hold for the new tuple $(c, d, a, b, e, f, q, p, s, r)$. The swaps cause equations (3.2.17) and (3.2.18) and equations (3.2.19) and (3.2.20) to be exchanged, and equations (3.2.22)-(3.2.23) are unaffected. Equation (3.2.21) with these values is

$$p + q = r + s + \tfrac{K}{2}(cq + dp - es) \ ,$$

but since equation (3.2.23) holds we can substitute $e(s-r) - q(c-b) + ap$ for dp and simplify to achieve

$$p + q = r + s + \tfrac{K}{2}(ap + bq - er) \ ,$$

which holds by assumption. So $(c, d, a, b, e, f, q, p, s, r)$ again satisfies the conditions of Proposition 3.27 and therefore by definition is a spherical Heronian diamond.

Now interchange $b \leftrightarrow d$, $e \leftrightarrow f$, $p \leftrightarrow s$ and $q \leftrightarrow r$. This corresponds to a horizontal reflection of the spherical Heronian diamond $(a, b, c, d, e, f, p, q, r, s)$. Again equations (3.2.17)-(3.2.20) are interchanged.

Equations (3.2.21), (3.2.22) and (3.2.23) become

$$s + r = q + p + \tfrac{K}{2}(as + dr - fq) \ , \tag{3.3.7}$$

$$4ef\left(1 - \tfrac{K}{4}f\right) = (s + r)^2 + (a - d + c - b)^2 - Kf(a - d)(c - b) \, , \tag{3.3.8}$$

$$f(q - p) = s(a - b) + r(d - c) \, , \tag{3.3.9}$$

and we need to show that as long as $e \notin \{0, \frac{4}{K}\}$ and $(a, b, c, d, e, f, p, q, r, s)$ is a spherical Heronian diamond, these equations hold. We can write each of the equations (3.2.17)-(3.2.23) in the form $F(a, b, c, d, e, f, p, q, r, s) = 0$ where F is a polynomial. We then collect these seven polynomials and form the ideal I that they generate. We similarly write each of the

equations (3.3.7)-(3.3.9) in the form $G = 0$. It then suffices to show that the polynomials

$$\begin{gathered}\left(s + r - q - p - K\left(\tfrac{as+dr-fq}{2}\right)\right) \cdot e(Ke - 4)\,, \\ \left(4ef\left(1 - K\tfrac{f}{4}\right) - (s+r)^2 - (a-d+c-b)^2 + Kf(a-d)(c-b)\right) \cdot e(Ke-4)\,, \\ (f(q-p) - s(a-b) - r(d-c)) \cdot e(Ke-4)\end{gathered}$$

lie in the ideal I. (Here we rely on the condition $e \notin \{0, \frac{4}{K}\}$.) This can be confirmed with standard software. □

Remark 3.39. By the symmetry of swapping, if a tuple $(c, d, a, b, e, f, q, p, s, r)$ is a spherical Heronian diamond, then by bullet 1 of Proposition 3.38, the tuple $(a, b, c, d, e, f, p, q, r, s)$ is also a spherical Heronian diamond.

Corollary 3.40. *In a spherical Heronian diamond $(a, b, c, d, e, f, p, q, r, s)$, once the components a, b, c, d are fixed, the values e, p, q determine f, r, s uniquely (as long as $e \notin \{0, \frac{4}{K}\}$), and vice versa (as long as $f \notin \{0, \frac{4}{K}\}$).*

Proof. Fix a, b, c, d. The fact that e, p, q with $e \notin \{0, \frac{4}{K}\}$ determines f, r, s is the content of Proposition 3.35 (as applied to the 7-tuple (a, b, c, d, e, p, q)).

In reverse, by the second bullet of Proposition 3.38, if $(a, b, c, d, e, f, p, q, r, s)$ is a spherical Heronian diamond then $(a, d, c, b, f, e, s, r, q, p)$ is a spherical Heronian diamond. Assuming that $f \notin \{0, \frac{4}{K}\}$ and applying Proposition 3.35 we see that e, p, q are determined uniquely by the 7-tuple (a, d, c, b, f, s, r). Since a, b, c, d are fixed, as long as $f \notin \{0, \frac{4}{K}\}$, the measurements f, r, s determine e, p, q uniquely. □

The following lemmas and corollary deal with cases corresponding in the geometric setting to various degenerate quadrilaterals.

Lemma 3.41. *Let $b, c, d, e, f, p, s \in \mathbb{C}$ and $a = q = r = 0$. The corresponding tuple $(0, b, c, d, e, f, p, 0, 0, s)$ is a spherical Heronian diamond if and only if*

$$p^2 = H^K(b, c, e)\,, \quad d = e\,, \quad f = b\,, \quad \text{and} \quad s = p\,. \tag{3.3.10}$$

Proof. Assume the tuple $(0, b, c, d, e, f, p, 0, 0, s)$ is a spherical Heronian diamond. Then equations (3.2.17)-(3.2.18) and (3.2.21) give us the following, which together imply (3.3.10):

$$\begin{aligned} p^2 &= H^K(b, c, e)\,, \\ 0 &= H^K(0, d, e) = -(d-e)^2\,, \\ 0 &= H^K(0, f, b) = -(f-b)^2\,, \\ p &= s\,. \end{aligned}$$

Conversely, assume that (3.3.10) hold. Then equations (3.2.17)-(3.2.19) are immediate. To show $s^2 = H^K(c, f, d)$ (equation (3.2.20)), we note that

$$s^2 = p^2 = H^K(b, c, e) = H^K(f, c, d)\,.$$

Since $f = b$, we have the following, which rearranges to equation (3.2.22):

$$p^2 = H^K(b, c, e) = -b^2 - c^2 - e^2 + 2bc + 2be + 2ce + Kebc + 4e(f - b) + Ke^2(b - f)\,.$$

Utilizing $p = s$ and $e = d$, we conclude $-es = -pd$ (equations (3.2.21), (3.2.23)). □

Lemma 3.42. *Let $a, b, d, e, f, q, r \in \mathbb{C}$ and $c = p = s = 0$. The corresponding tuple $(a, b, 0, d, e, f, 0, q, r, 0)$ is a spherical Heronian diamond if and only if*

$$q^2 = H^K(a, d, e)\,, \tag{3.3.11}$$

$$b = e\,, \tag{3.3.12}$$

$$f = d\,, \tag{3.3.13}$$

$$r = q\,. \tag{3.3.14}$$

Proof. Argue similarly to Lemma 3.41 above, or note

$$(a, b, 0, d, e, f, 0, q, r, 0)$$

is a spherical Heronian diamond if and only if

$$(0, d, a, b, e, f, q, 0, 0, r)$$

is a spherical Heronian diamond (see Remark 3.39); then apply Lemma 3.41. □

The lemmas above and Corollary 3.40 imply the following corollary.

Corollary 3.43. *Let $a, b, c, d, e, f, p, q, r, s \in \mathbb{C}$. If the tuple $(0, b, c, d, e, f, p, 0, 0, s)$ is a spherical Heronian diamond, then the values e, b, p determine f, d, s uniquely, and vice versa. If $(a, b, 0, d, e, f, 0, q, r, 0)$ is a spherical Heronian diamond, then the values d, e, q determine b, f, r uniquely, and vice versa.*

We will now apply what we know about spherical quadrilaterals to the case of a spherical polygon.

Proposition 3.44. *Let $P = A_1 \dots A_n$ be a spherical polygon on $\mathbf{S}$. For any four vertices A_i, A_j, A_k, A_l, we can arrange the ten measurements $\mathbf{xS}(P) = (x_{ij}) \sqcup (S^K(A_i, A_j, A_k))$ to form a Heronian diamond as pictured on the right in Figure 3.5.*

In particular, by Proposition 3.27, the measurements $\mathbf{xS}(P) = (x_{ij}) \sqcup (S^K(A_i, A_j, A_k))$ *satisfy the following identities, where we use the shorthand* $S^K_{ijk} = S^K(A_i, A_j, A_k)$*:*

$$\begin{aligned}
(S^K_{ijk})^2 &= H^K(x_{ij}, x_{jk}, x_{ik})\,, \qquad (3.3.15)\\
S^K_{ijk} + S^K_{ikl} &= S^K_{ijl} + S^K_{jkl} + \tfrac{K}{2}\left(x_{il}S^K_{ijk} + x_{ij}S^K_{ikl} - x_{ik}S^K_{jkl}\right)\,,\\
4x_{ik}x_{jl}\left(1 - \tfrac{Kx_{ik}}{4}\right) &= (S^K_{ijk} + S^K_{ikl})^2 + (x_{il} - x_{ij} + x_{jk} - x_{kl})^2 - Kx_{ik}(x_{il} - x_{ij})(x_{jk} - x_{kl})\,,\\
x_{ik}(S^K_{ijl} - S^K_{jkl}) &= S^K_{ijl}(x_{il} - x_{kl}) + S^K_{ijk}(x_{ij} - x_{jk})\,.
\end{aligned}$$

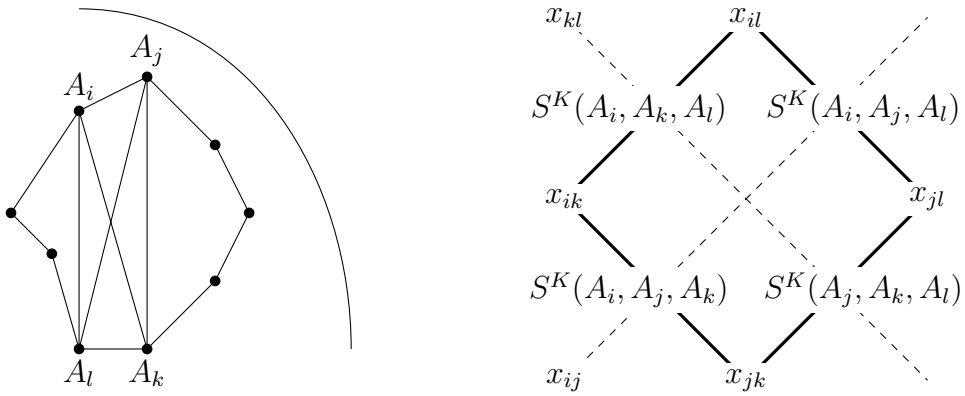


Figure 3.5: Left: In a spherical polygon, any four vertices A_i, A_j, A_k, A_l form a spherical quadrilateral. Right: The corresponding spherical Heronian diamond.

We next define a spherical Heronian frieze, a tessellation of a planar region by spherical Heronian diamonds that collects and organizes the measurement data for a spherical polygon. Spherical Heronian friezes generalize to arbitrary values of K the (Euclidean) Heronian friezes introduced by Fomin and Setiabrata [FS21].

We begin by defining an indexing set for a spherical Heronian frieze.

Definition 3.45. For $n \geq 4$, let

$$I_n^{SH} = \left\{\left(i + \tfrac{1}{2}, j\right), \left(i, j + \tfrac{1}{2}\right), (i,j)\right\}_{\substack{0 \leq j-i \leq n \\ i,j \in \mathbb{Z}}} \cup \left\{\left(i + \tfrac{1}{2}, \diagup\right)\right\}_{i \in \mathbb{Z}} \cup \left\{\left(\diagdown, j + \tfrac{1}{2}\right)\right\}_{j \in \mathbb{Z}}.$$

Our notation uses the symbols $\diagup$ and $\diagdown$, which represent lines headed Northeast and Southeast respectively.

To visually represent I_n^{SH}, rotate the usual coordinate axes in $\mathbb{R}^2$ by $\pi/4$ clockwise, so that the points $(i,j) \in \mathbb{Z}^2$ satisfying the inequalities $0 \leq j - i \leq n$ would lie inside a horizontal strip. See a depiction of I_6^{SH} in Figure 3.6. We call elements of I_n^{SH} with two numerical coordinates nodes. We classify a node (i,j) as interior if $1 \leq j - i \leq n-1$, so that (i,j) lies in the interior of the horizontal strip.

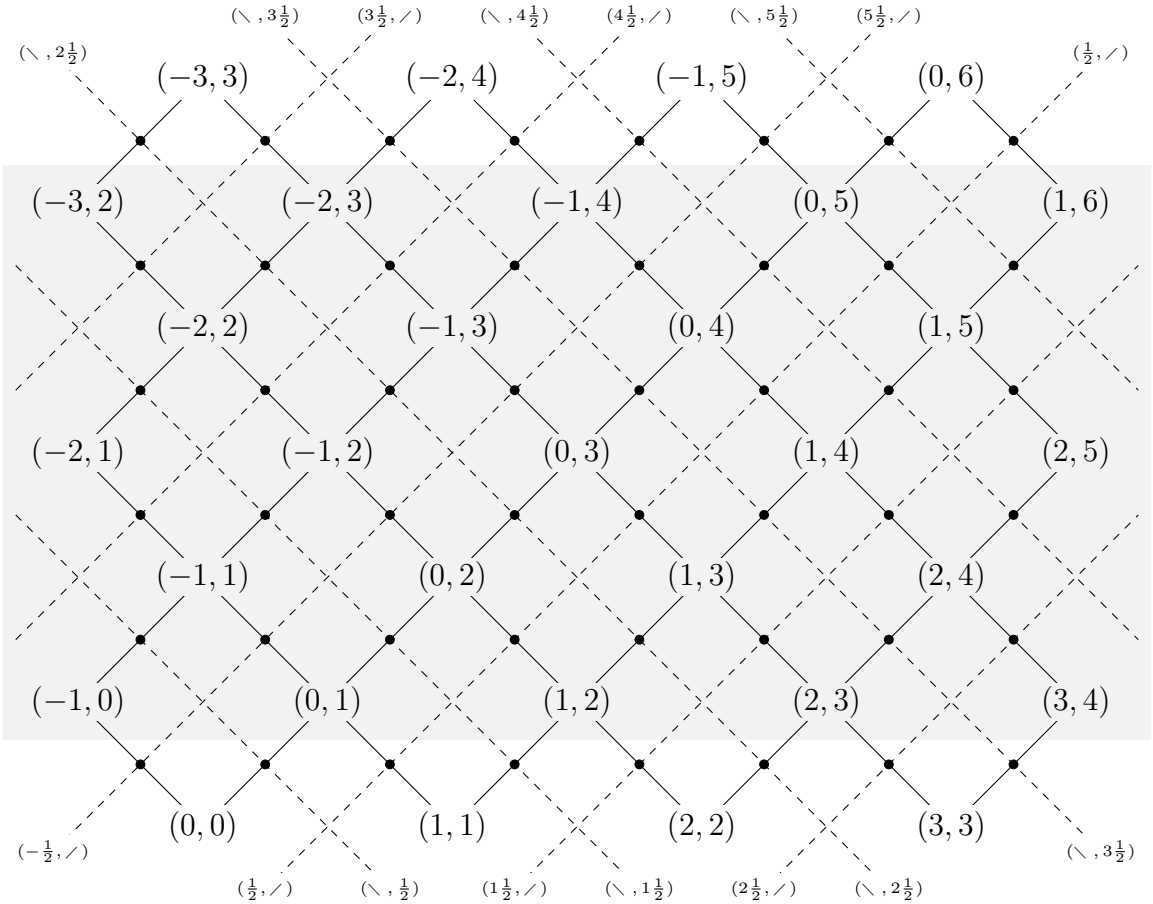


Figure 3.6: A portion of the index set I_6^{SH}, it extends infinitely to the right and left. For the points of the form $\left(i+\frac{1}{2}, j\right)$ and $\left(i, j+\frac{1}{2}\right)$ (indicated with black filled-in circles), the labels are not shown. Interior nodes lie in the gray shaded region. The dashed lines have labels of the form $(i+\frac{1}{2}, \diagup)$ or $(\diagdown, j+\frac{1}{2})$.

Definition 3.46. For $K \in \mathbb{C}$, and $n \geq 4$, a spherical Heronian frieze of order n (e.g., Figure 3.7) is an array $\mathbf{z} = (z_\alpha)_{\alpha \in I_n^{SH}}$ of complex numbers indexed by I_n^{SH} (Definition 3.45) such that each full diamond of numbers is a spherical Heronian diamond. Specifically, for an interior node $(i,j) \in \mathbb{Z}^2$, the tuple

$$\left(z_{(i,j+1)}, z_{(i+\frac{1}{2},\diagup)}, z_{(i+1,j)}, z_{(\diagdown,j+\frac{1}{2})}, z_{(i,j)}, z_{(i+1,j+1)}, z_{(i+\frac{1}{2},j)}, z_{(i,j+\frac{1}{2})}, z_{(i+\frac{1}{2},j+1)}, z_{(i+1,j+\frac{1}{2})}\right)$$

forms a Heronian diamond of the form shown in Figure 3.2. Additionally, at the boundary of the frieze, we impose the following conditions:

$$z_{(i,i)} = z_{(i,i+n)} = z_{(i,i+\frac{1}{2})} = z_{(i,i+n-\frac{1}{2})} = 0 \quad (i \in \mathbb{Z}). \tag{3.3.16}$$

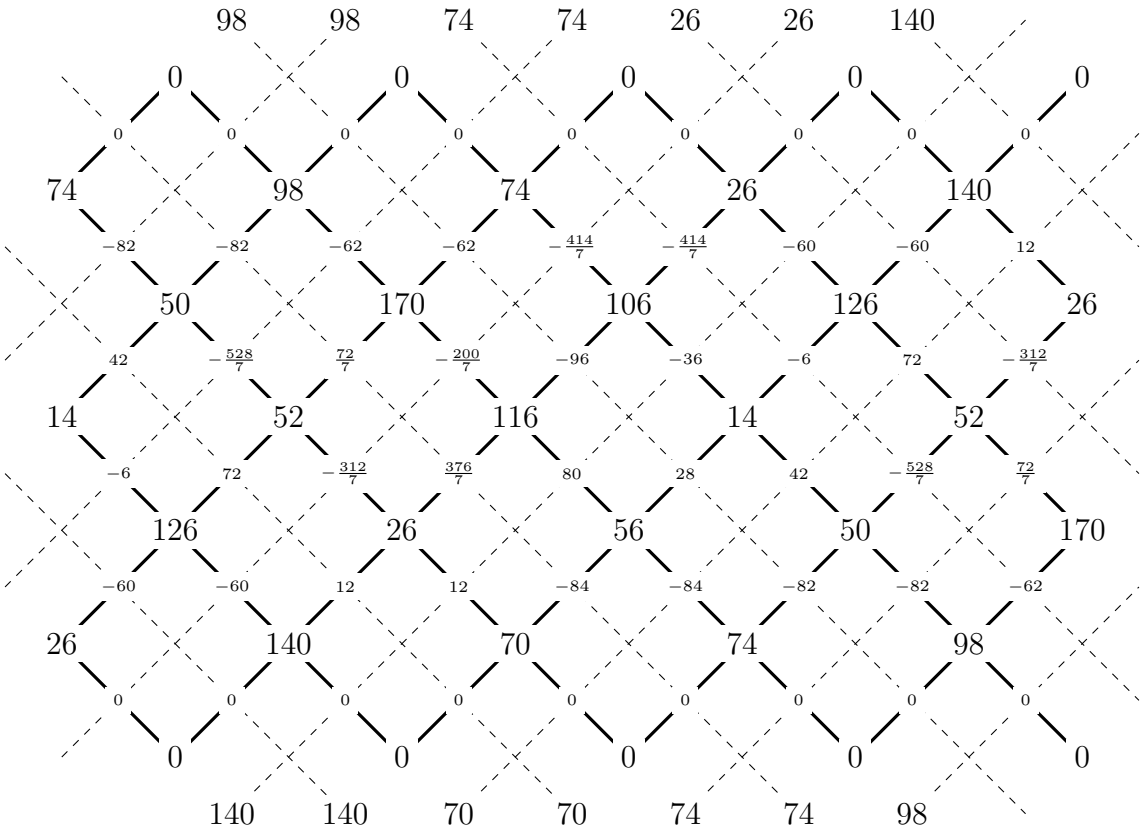


Figure 3.7: A spherical Heronian frieze of order 6. This frieze corresponds to a hexagon on a sphere with radius 7.

Remark 3.47. Let $\mathbf{z}$ be a spherical Heronian frieze. Consider, for example, the points with first coordinate 0: $(0,0),(0,\frac{1}{2}),(0,1),(0,1+\frac{1}{2}),(0,2),\ldots$ In our visualization they form a straight line of alternating integer and half-integer points traveling in the Northeast direction. Crossing this line perpendicularly at each half-integer point are the lines indexed by $(\diagdown, j+\frac{1}{2})$.

The entry $z_{(0,j+\frac{1}{2})}$ at a half-integer point satisfies a Heron relation (equation (3.3.15)) together with the integer entries located immediately Northeast and immediately Southwest of it, and the entry associated with the line $(\diagdown, j+\frac{1}{2})$.

Definition 3.48. Let $P = A_1 \ldots A_n$ be a spherical polygon on $\mathbf{S}$. Define $\mathbf{z} = \mathbf{z}(P)$, a spherical Heronian frieze of order n, by setting

$$\begin{aligned} z_{(i,j)} &= x_{\langle i\rangle\langle j\rangle}\,, \\ z_{(i+\frac{1}{2},j)} &= S^K_{\langle i\rangle\langle i+1\rangle\langle j\rangle}\,, \\ z_{(i,j+\frac{1}{2})} &= S^K_{\langle i\rangle\langle j\rangle\langle j+1\rangle}\,, \\ z_{(i+\frac{1}{2},\diagdown)} &= x_{\langle i\rangle\langle i+1\rangle}, \\ z_{(\diagup,j+\frac{1}{2})} &= x_{\langle j\rangle\langle j+1\rangle}\,, \end{aligned}$$

where $\langle m\rangle$ denotes the unique integer k in $\{1,\ldots,n\}$ satisfying $m \equiv k \pmod{n}$.

Condition (3.3.16) on the boundary holds because for any $i \in \mathbb{Z}$ we have

$$x_{ii} = S^K_{\langle i\rangle\langle i\rangle\langle i+1\rangle} = S^K_{\langle i\rangle\langle i+1\rangle\langle i+1\rangle} = 0.$$

In words, we put the S^K measurements of triangles at each half integer point, e.g., $(i+\frac{1}{2}, j)$. At the integer points directly above and below, we surround a particular S^K triangle measurement with the squared side lengths of the triangle. There is one perpendicular line passing through the half integer point, which we label with the third side of the triangle.

As we move up and to the right along a line we alternate between integer and half-integer points, i.e., side length and S^K triangle measurements. Each step along the line represents a small movement, from a side to an adjacent triangle, to another side of the triangle, to another adjacent triangle, slowly walking through the polygon.

Note that, by design, the only S^K triangle measurements that appear in a frieze correspond to triangles that share a side with the polygon.

Example 3.49. The frieze in Figure 3.7 corresponds to a hexagon considered up to oriented isometry on the sphere of radius 7 (curvature $K = 1/49$) centered at the origin. It is depicted in Figure 3.8.

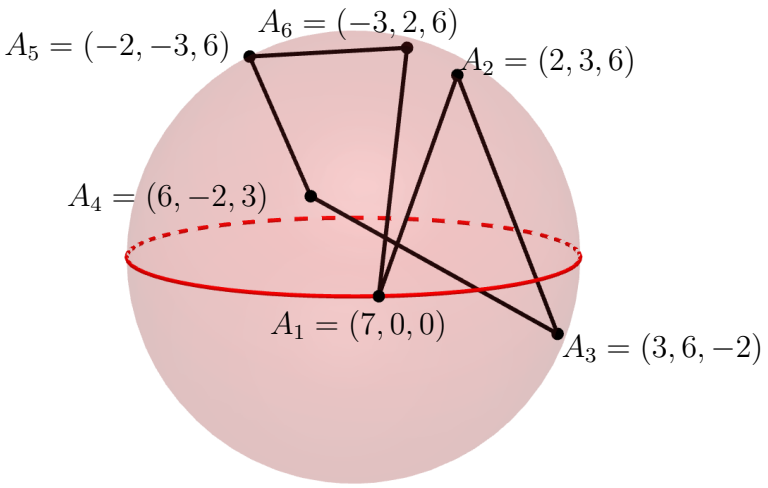


Figure 3.8: The vertices of the spherical hexagon $A_1A_2A_3A_4A_5A_6$ lie on the sphere of radius 7 centered at the origin in $\mathbb{R}^3$.

For a spherical Heronian frieze arising from a spherical polygon, the interior nodes $z_{(i,i+1)}$ and $z_{(i,i+n-1)}$ along the top and bottom of the frieze correspond to the squared distances $x_{\langle i\rangle\langle i+1\rangle}$ and $x_{\langle i\rangle\langle i+n-1\rangle}$ respectively—the squared side lengths of the polygon. These quantities also appear as the dashed lines that run through multiple spherical Heronian diamonds. We don't need this geometric interpretation, however, to get the following purely algebraic result.

Proposition 3.50. *Let* $\mathbf{z} = (z_\alpha)_{\alpha \in I_n^{SH}}$ *be a spherical Heronian frieze of order* n*. Then*

$$\begin{aligned} z_{(i,i+1)} &= z_{(i+\frac{1}{2},\diagup)} = z_{(\diagdown,i+\frac{1}{2})} \qquad (i \in \mathbb{Z})\,, \\ z_{(i,i+n-1)} &= z_{(i-\frac{1}{2},\diagup)} = z_{(\diagdown,i+n-\frac{1}{2})} \qquad (i \in \mathbb{Z})\,. \end{aligned}$$

Proof. Looking at the spherical Heronian diamond with $z_{(i,i+1)}$ on the far left (in the position e in Figure 3.2), we see condition (3.3.16) ensures the bottom entries are all zero. In other words,

$$z_{(i+1,i+1)} = z_{(i+\frac{1}{2},i+1)} = z_{(i+1,i+\frac{3}{2})} = 0\,.$$

This means that Lemma 3.42 applies and we get $z_{(i,i+1)} = z_{(i+\frac{1}{2},\diagup)}$ (by (3.3.12)). The other results can be proved similarly. □

Remark 3.51. A spherical polygon P with n vertices has a finite number of sides, diagonals, and triangulations. As in the Euclidean case [FS21, (3.15)-(3.17)], a spherical Heronian

frieze $\mathbf{z}(P)$ of order n arising from P is thus periodic. Specifically, $\mathbf{z}(P)$ must satisfy

$$\begin{aligned} z_{(i,j)} &= x_{\langle i\rangle\langle j\rangle} = z_{(i+n,j+n)}\,, \\ z_{(i+\frac{1}{2},\diagup)} &= x_{\langle i\rangle\langle i+1\rangle} = z_{(i+\frac{1}{2}+n,\diagup)}\,, \\ z_{(\diagdown,j+\frac{1}{2})} &= x_{\langle j\rangle\langle j+1\rangle} = z_{(\diagdown,j+\frac{1}{2}+n)}\,. \end{aligned}$$

In particular, because of the symmetry of the measurements (see Definition 3.1 and Definition 3.2), for $i, j \in \mathbb{Z}$ we must have glide symmetry (cf. Figure 3.9 and 3.10):

$$\begin{aligned} z_{(i,j)} &= x_{\langle i\rangle\langle j\rangle} = x_{\langle j\rangle\langle i\rangle} = z_{(j,i+n)}\,, \\ z_{(i+\frac{1}{2},j)} &= S^K_{\langle i\rangle\langle i+1\rangle\langle j\rangle} = S^K_{\langle j\rangle\langle i\rangle\langle i+1\rangle} = z_{(j,i+\frac{1}{2}+n)}\,, \\ z_{(i,j+\frac{1}{2})} &= S^K_{\langle i\rangle\langle j\rangle\langle j+1\rangle} = S^K_{\langle j\rangle\langle j+1\rangle\langle i\rangle} = z_{(j+\frac{1}{2},i+n)}\,. \end{aligned}$$

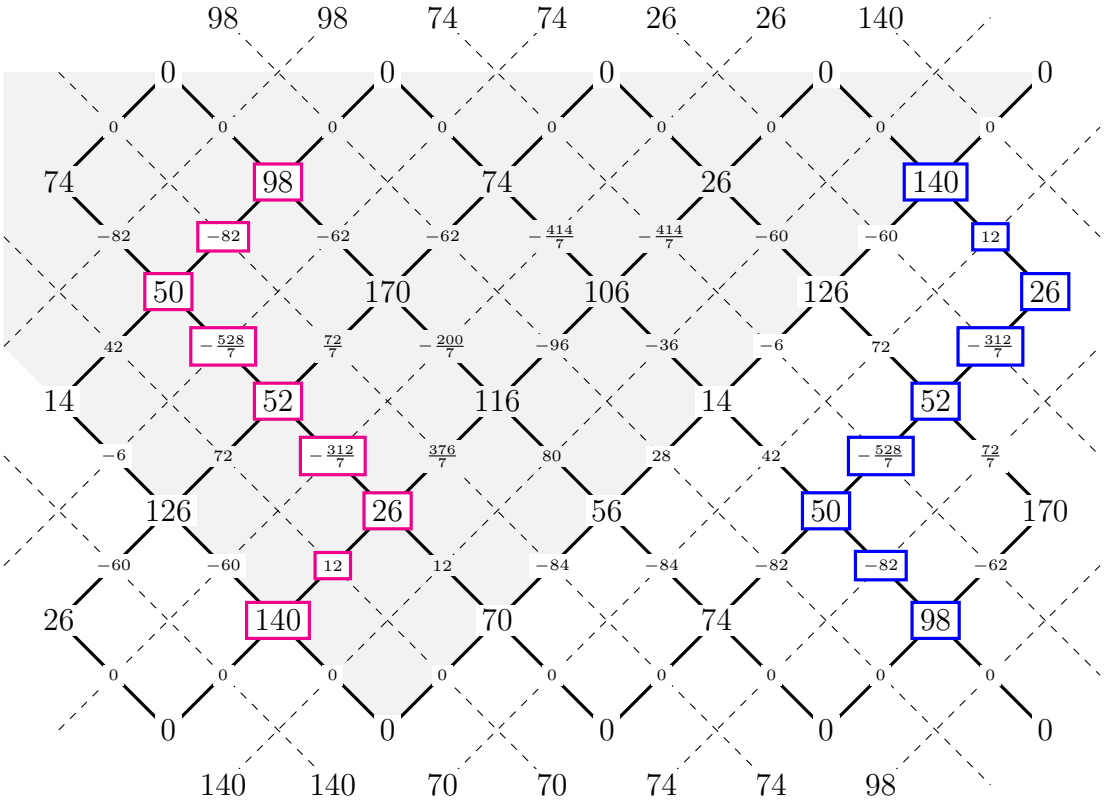


Figure 3.9: The same spherical Heronian frieze as in Figure 3.7, this time illustrating the glide symmetry. To see it, flip the gray shaded region upside down and paste it to the right of its original location. The blue and magenta highlighted entries form two separate traversing paths. Thanks to the glide symmetry, their entries form identical sets. Both paths correspond to the triangulation shown in Figure 3.10.

We will next show that, like in the Euclidean case, a small amount of data determines the entire spherical Heronian frieze through a propagation recurrence. This propagation requires careful selection of initial data. One suitable choice is the set of entries along a traversing path. The following statements mirror those in [FS21].

Definition 3.52. A traversing path in a spherical Heronian frieze of order n is an ordered collection

$$\pi = ((i_1, j_1), \ldots, (i_{2n-3}, j_{2n-3}), l_1, \ldots, l_{n-2})$$

of $3n-5$ indices in I_n^{SH} that can be viewed as stepping stones on a shortest path from the lower to the upper boundary of the frieze (see Figure 3.9). We require that the first point is of the form $(i_1, j_1) = (k, k+1)$ for some $k \in \mathbb{Z}$ (a point almost on the bottom boundary); similarly $(i_{2n-3}, j_{2n-3}) = (m, m+n-1)$ for some $m \in \mathbb{Z}$ (just below the top boundary). In particular, all (i_k, j_k) are interior nodes. The $l_1, \ldots, l_{n-2}$ are the dashed lines that intersect this shortest path. See, for example, the magenta or blue outlined entries in Figure 3.7.

Remark 3.53. If a spherical Heronian frieze $\mathbf{z}(P)$ arises from a spherical polygon P, then the path π corresponds to a triangulation of P. For example, the highlighted magenta and blue traversing paths in Figure 3.7 both correspond to the triangulation shown in Figure 3.10 of the polygon shown in Figure 3.8.

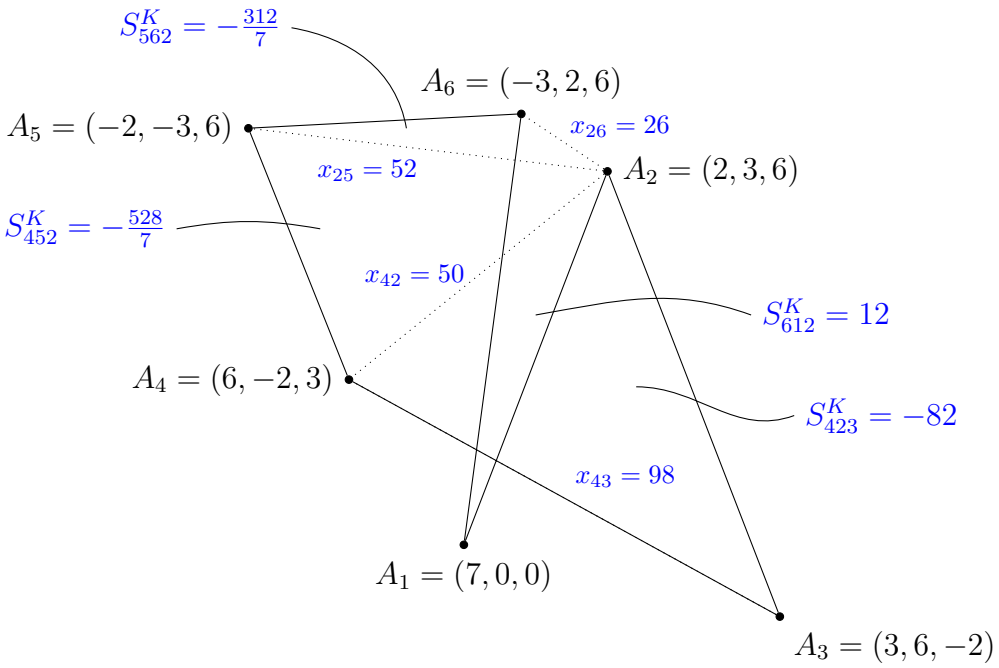


Figure 3.10: Frieze entries for the hexagon $A_1A_2A_3A_4A_5A_6$ from Figure 3.8. These frieze entries lie on the traversing path shown in Figure 3.9.

To see the correspondence, start at $(i_1, j_1) = (k, k+1)$ at which we have $z_{(k,k+1)} = x_{\langle k\rangle\langle k+1\rangle}$. Imagine two ants sitting at the boundary of polygon P: ant Alice at vertex A_k and ant Bob at vertex A_{k+1}. As we move up along π to (i_2, j_2), we get to, e.g., $(k, k+1+\frac{1}{2})$ with $z_{(k,k+1+\frac{1}{2})}$ corresponding to $S^K_{\langle k\rangle\langle k+1\rangle\langle k+2\rangle}$ and we include the associated triangle $A_kA_{k+1}A_{k+2}$ in our triangulation. Then we move to $(k, k+2)$ with $z_{(k,k+2)}$. Bob moves to vertex A_{k+2} of P.

Proceed similarly. As we continue on the path π, Alice moves to the vertex corresponding to the first coordinate, and Bob to the vertex corresponding to the second coordinate. Note that since only one number changes at each step in an alternating fashion, the triangles form a zigzagging triangulation of P and the only triangles we include have one side along the boundary of P.

The lines $l_1, \ldots, l_{n-2}$ are not needed to pass from a traversing path to a triangulation of P. They will be needed in the algebraic result (Corollary 3.54) below.

Since the traversing path gives a triangulation of the polygon, by Proposition 3.32 we can recover all the measurements of the polygon, hence the entire frieze.

Corollary 3.54. *Let $(z_\alpha)_{\alpha\in I_n^{SH}}$ be a spherical Heronian frieze of order n such that*

$$z_{(i,j)} \notin \left\{0, \tfrac{4}{K}\right\} \text{ for any } (i,j) \in \mathbb{Z}^2 \text{ with } 2 \le j-i \le n-2\,. \tag{3.3.17}$$

Then starting from a single traversing path π, we can recover the entire frieze.

Proof. Starting with the entries adjacent to π, apply Corollary 3.40 and Corollary 3.43 filling in all remaining values uniquely. Recall that we need to know that all the diamonds in the frieze are spherical Heronian in order to apply these corollaries. □

While Corollary 3.54 is a purely algebraic result, it has a geometric underpinning:

Corollary 3.55. *Let $\mathbf{z}$ be a spherical Heronian frieze of order n satisfying condition* (3.3.17)*. Then there exists a unique n-gon P such that $\mathbf{z} = \mathbf{z}(P)$.*

Proof. Select a traversing path π. The data of π satisfies the requirements to apply Proposition 3.32 and construct a unique triangulated spherical polygon P whose spherical Heronian frieze $\mathbf{z}(P)$ agrees with $\mathbf{z}$ along π. By Corollary 3.54, the rest of $\mathbf{z}(P)$ frieze is determined uniquely by π and so must agree with $\mathbf{z}$. □

Proposition 3.56. *Let π be a traversing path. Denote by $\mathbf{z}_-$ a collection of complex numbers assigned to the indices in π which satisfy the appropriate spherical Heron equations. If the values in $\mathbf{z}_-$ at the integer nodes of π lie in $\mathbb{C} - \{0, \frac{4}{K}\}$ then there exists a unique spherical Heronian frieze that agrees with π.*

Proof. Using the ideas in Remark 3.53, construct a triangulated cycle G matching π. By Proposition 3.32, there exists a unique n-gon P such that the measurements along π are precisely $\mathbf{xS}_G(P)$. Construct the frieze $\mathbf{z}(P)$. It will agree with π and by Corollary 3.54 above, the frieze is unique. □

Remark 3.57. Proposition 3.56 provides formulas for solving the original question in spherical distance geometry, namely the propagation formulas (equations (3.3.2)-(3.3.4)) applied iteratively. We will say more about these formulas in Section 3.4.

The geometric results in Corollary 3.55 and Remark 3.51 give us this algebraic conclusion:

Theorem 3.58. *Let* $\mathbf{z}$ *be a spherical Heronian frieze satisfying condition* (3.3.17)*. Then* $\mathbf{z}$ *is periodic and possesses glide symmetry.*

3.4 Rational expressions for spherical Heronian friezes

To propagate outwards from an initial data set in a frieze we apply the propagation formulas iteratively. We will next show that the resulting expressions for the entries of the frieze are structurally simpler than one might expect: they satisfy a form of Laurentness, with predictable denominators.

Let $\mathbf{z}_\pi$ be the initial data associated with a traversing path π in a spherical Heronian frieze $\mathbf{z}$. Define

$$D(\pi) = \left\{ x_{ij} \left(1 - \tfrac{Kx_{ij}}{4}\right) \;\middle|\; (i,j) \text{ an integer node of } \pi \text{ with } 2 \le i-j \le n-2 \right\}.$$

Proposition 3.59. *If all elements of* $D(\pi)$ *are nonzero, then each entry of* $\mathbf{z}$ *can be written as a rational function in terms of* $\mathbf{z}_\pi$ *whose numerator is a polynomial with integer coefficients and whose denominator is a monomial in the elements of* $D(\pi)$*.*

The rest of this section is devoted to the proof of Proposition 3.59.

Remark 3.60. Let $\mathbf{z}(P)$ be a spherical Heronian frieze arising from a spherical polygon P. The integer nodes (i,j) of π with $2 \le i-j \le n-2$ index the squared distances of the diagonals of P. An element $x_{ij}\left(1 - \frac{Kx_{ij}}{4}\right)$ vanishes precisely when the vertices A_i, A_j of P are either coincident or antipodal (cf. Remark 3.13).

We will need additional terminology, some of which also appeared in [FS21].

Definition 3.61. Let $n \ge 4$. Number the vertices of an n-cycle in order $1, 2, \ldots$. Consider two distinct diagonals $\{i,j\}$ and $\{k,l\}$, with $i<j$ and $k<l$. We say that these diagonals cross if $i<k<j<l$ or $k<i<l<j$. We say that a diagonal $\{i,j\}$ crosses a triangle (k,l,m) if it crosses at least one diagonal side of the triangle.

Definition 3.62. Fix a triangulation G of an n-cycle. For an edge $\{i, j\}$ or a triple (i, j, k), let $\gamma(G, i, j)$ (resp. $\gamma(G, i, j, k)$) denote the trimming of G with respect to $\{i, j\}$ (resp. (i, j, k)), defined as the induced subgraph of G with vertex set

$$\{i, j\} \bigcup \{l, k \mid \text{diagonal } \{l, k\} \text{ crosses edge } \{i, j\} \text{ (resp. triangle } (i, j, k))\}.$$

If $G = \tau(G, i, j)$ (resp., $G = \tau(G, i, j, k)$), we say that G is trimmed with respect to $\{i, j\}$ (resp. (i, j, k)). See Figure 3.11.

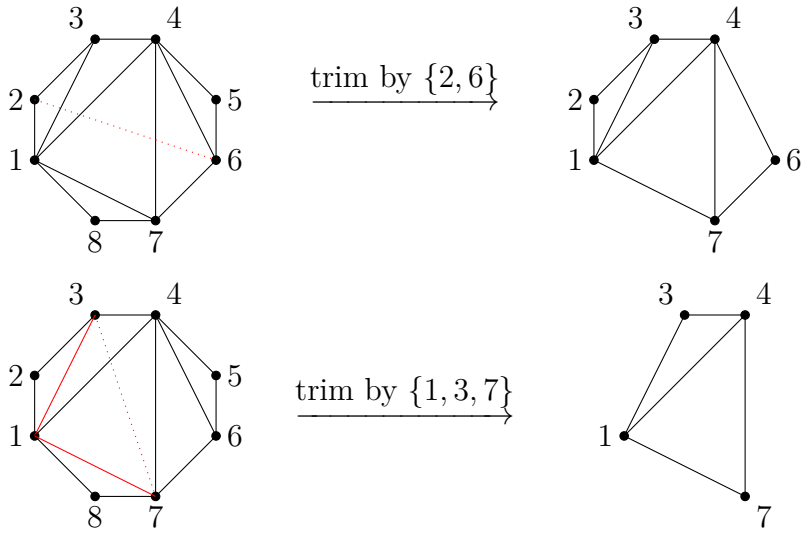


Figure 3.11: The trimmings of triangulation G with respect to diagonal $\{2, 6\}$ and triangle $\{1, 3, 7\}$ respectively.

Remark 3.63. Trimming a triangulation always returns a subgraph that is itself a triangulation, typically with fewer edges and vertices than the original one. Loosely speaking, trimming snips off a few extraneous triangles. For example, the trimming of a triangulation G with respect to a diagonal or triangle that appears in G is just the diagonal or triangle itself. A triangulated n-gon trimmed with respect to $\{i, j\}$ has no diagonals incident to vertices i or j. As a tool, trimming is most impactful with respect to a pair of vertices or a triangle that is not a subgraph of the triangulation.

In particular, trimming a triangulation of an n-cycle produces a triangulation of an $(n - k)$-cycle ($k \geq 0$) by thin triangles, each of which shares a side with the $(n - k)$-cycle. Performing such a trimming can be used strategically to remove distracting pieces of the polygon whose measurements are irrelevant for computation.

Definition 3.64. Let G be a triangulated n-cycle. We call G a thin triangulation if each of its triangles shares a side with the n-cycle (we will refer to such triangles as thin). Notably, any traversing path in a spherical Heronian frieze corresponds to a triangulation by thin triangles.

Definition 3.65. Let $\{i,j\}$ be a diagonal in a triangulation G. There is a unique diagonal $\{k,l\}$ such that the following collection of diagonals is still a triangulation:

$$G' = \mu_{ij}(G) = G \cup \{k,l\} - \{i,j\}\,.$$

We refer to this operation as flipping $\{i,j\}$ to $\{k,l\}$.

Definition 3.66. For (P,G) a triangulated polygon, let $D(G)$ denote the set of diagonals appearing in G. Define

$$\mathbf{x}_{D(G)}(P) = \left\{ x_{ij}\left(1 - \tfrac{Kx_{ij}}{4}\right) \;\middle|\; \{i,j\} \in D(G) \right\}.$$

Note that the elements of $\mathbf{x}_{D(G)}$ are the type of factors that appear in the denominators of the equations for propagation in the frieze (cf. Proposition 3.35).

Towards a proof of Proposition 3.59, we will next show that, in the case that a triangulated n-gon G is trimmed with respect to a diagonal $\{i,j\}$ (resp. a triple (i,j,k)), the corresponding measurement x_{ij} (resp. S^K_{ijk}) can be expressed as a rational function in $\mathbf{xS}_G(P)$ whose denominator is a monomial in the elements of $\mathbf{x}_{D(G)}(P)$. Our inductive arguments in the following propositions will involve flipping a diagonal. We will require the following technical lemma, which handles the case that a new triangulation produced by flipping is no longer trim with respect to $\{i,j\}$ (resp. (i,j,k)) (cf. Figure 3.12).

Lemma 3.67. *Let G be a triangulated cycle and $e \in D(G)$. Flip e to get edge f and $G' = \mu_e(G)$. Pick $\{i,j\} \notin D(G)$ so that G is trimmed with respect to $\{i,j\}$, but G' is not. Trim G' with respect to $\{i,j\}$ to get $G'' = \tau(G',i,j)$. Assume that the measurement x_{ij} can be written as a rational function in $\mathbf{xS}_{G''}(P)$ whose denominator is a monomial in the elements of $\mathbf{x}_{D(G'')}(P)$. Then x_{ij} can be written as a rational function in $\mathbf{xS}_G(P)$ whose denominator is a monomial in the elements of $\mathbf{x}_{D(G)}(P)$. The same statement holds for (i,j,k) and S^K_{ijk} in place of $\{i,j\}$ and x_{ij}.*

Proof. For both results we can apply the same proof method as [FS21]. Using the assumption, write $x_{ij} = Q/S$ with numerator Q a polynomial in $\mathbf{xS}_{G''}(P)$ and denominator S a monomial in $\mathbf{x}_{D(G'')}(P)$.

We are already close to the goal, since $D(G'') \subset D(G)$ and $\mathbf{xS}_{G''}(P)$ only contains a few measurements not present in $\mathbf{xS}_G(P)$. In particular, $\mathbf{xS}_{G''}(P) \setminus \mathbf{xS}_G(P)$ contains x_f and two measurements of the form S^K_{fgh}, for two triangles of G with f as a side. Use equations (3.3.2)-(3.3.4) to write these three measurements as rational functions in $\mathbf{xS}_G(P)$ each with denominator a scalar multiple of $x_e\left(1-\frac{Kx_e}{4}\right) \in \mathbf{x}_{D(G)}(P)$.

Substitute the new values back into Q (as needed) to get Q'. The expression Q' is a rational function in $\mathbf{xS}_G(P)$ with denominator a monomial in $x_e\left(1-\frac{Kx_e}{4}\right)$. Substituting back into x_{ij} we have now written $x_{ij} = Q'/S$, a rational function in $\mathbf{xS}_G(P)$ whose denominator is a monomial in

$$\left\{x_e\left(1-\tfrac{Kx_e}{4}\right)\right\} \cup \mathbf{x}_{D(G)''}(P) = \mathbf{x}_{D(G)}(P).$$

The result for (i,j,k) and S^K_{ijk} follows similarly. □

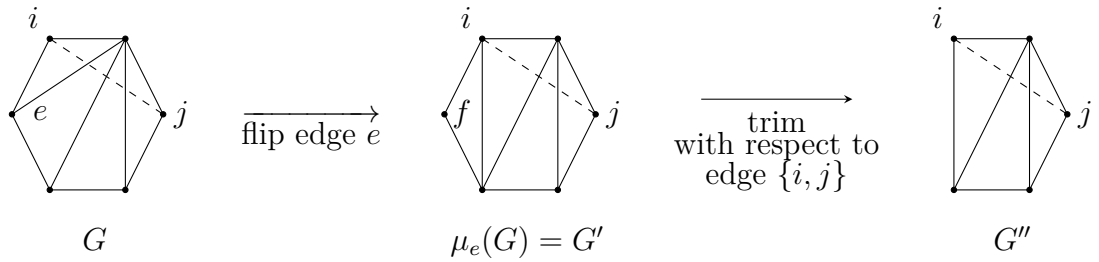


Figure 3.12: The procedure described in Lemma 3.67.

Proposition 3.68. *Let G be a triangulated n-gon trimmed with respect to diagonal $\{i,j\}$. Then x_{ij} can be expressed as a rational function in $\mathbf{xS}_G(P)$ whose denominator is a monomial in the elements of $\mathbf{x}_{D(G)}(P)$.*

Proof. As in the analogous proof in [FS21] we induct on n. When $n = 4$, use our spherical analogue of Bretschneider's formula (3.2.14). Let $n > 4$. There are no diagonals in G incident to i (see Remark 3.63), so edge $e = \{i-1, i+1\}$ (working modulo n) must be a diagonal of G. Flip the diagonal e to get a new triangulation G'. Since G' contains a diagonal incident to i, it is not trimmed with respect to $\{i,j\}$. Compute G'', the trimming of G' with respect to e. Since G'' has fewer vertices than G, apply the induction hypothesis. We get the conditions of Lemma 3.67, which then proves the claim. □

Proposition 3.69. *Let G be a triangulated n-gon that is trimmed with respect to the triple (i,j,k). Then S^K_{ijk} can be expressed as a rational function in $\mathbf{xS}_G(P)$ whose denominator is a monomial in the elements of $\mathbf{x}_{D(G)}(P)$.*

Proof. Again, we induct on n, following the general outline of the proof of the analogous result in [FS21]. When $n = 4$, the result is due to equation (3.3.3) or (3.3.4) (both of whom return rational functions in $\mathbf{xS}_G(P)$ with denominator a monomial in $\mathbf{x}_D(G)(P)$).

Let $n = 5$. All triangulations are the same up to cyclic renumbering of vertices, so without loss of generality assume triangulation G has diagonals $\{1, 3\}$ and $\{1, 4\}$. These diagonals must cut across the triangle (i, j, k), so 2 and 5 must be two of the components of the triple. Using Lemma 3.67 with $e = \{1, 3\}$ and $(i, j, k) = (1, 2, 5)$ (resp., $(2, 4, 5)$), we can see that S^K_{125} (resp. S^K_{245}) can be written as a rational function in $\mathbf{xS}_G(P)$ with denominator a monomial in $\mathbf{x}_{D(G)}(P)$. The case for S^K_{235} is similar.

Consider the case where $n = 6$ and G is the triangulation with diagonals $\{1, 3\}$, $\{3, 5\}$, and $\{1, 5\}$ (see Figure 3.13). While G is not trimmed with respect to any of the triangles

$$(2, 3, 4), (4, 5, 6), (1, 2, 6), (3, 4, 6), (2, 3, 6), (1, 3, 6), (3, 5, 6),$$

each is inside of a sub-quadrilateral or sub-pentagon of G that is triangulated by diagonals of G, and so by induction the claim holds. For example, $\{1, 2, 3, 4, 5\}$ is triangulated by the diagonals of G and is trimmed with respect to $(2, 3, 4)$. The table below shows each triangle and the subpolygon that is trimmed with respect to that triangle:

triangle	trimmed with respect to
$(1, 3, 6)$, $(3, 5, 6)$	$\{1, 3, 5, 6\}$
$(2, 3, 4)$	$\{1, 2, 3, 4, 5\}$
$(4, 5, 6)$, $(3, 4, 6)$	$\{1, 3, 4, 5, 6\}$
$(1, 2, 6)$, $(2, 3, 6)$	$\{1, 2, 3, 5, 6\}$

Additionally, note that since the sub-quadrilateral $\{1, 3, 5, 6\}$ is trimmed with respect to $\{3, 6\}$ by Proposition 3.68, the side length x_{36} can also be written in the desired form.

The 6-gon G with diagonals $\{1, 3\}, \{3, 5\}, \{1, 5\}$ is only trimmed with respect to the triangle $(2, 4, 6)$. In this case, starting with G, we flip edges until we arrive at a triangulation that contains the triangle $(2, 4, 6)$ (see the sequence of flips in Figure 3.13).

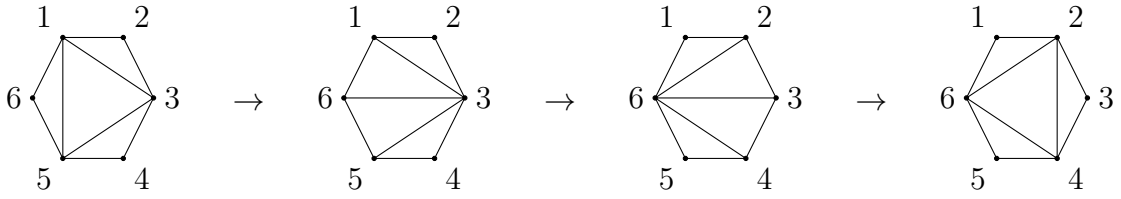


Figure 3.13: Using flips to derive an identity for S^K_{246}.

With each flip we use equation (3.2.21) to write a new identity. Flipping the edge $\{1,5\}$ we get

$$S^K_{135} + S^K_{156} = S^K_{136} + S^K_{356} + \frac{x_{35}S^K_{156} + x^K_{56}S^K_{135} - x_{15}S^K_{356}}{2}. \tag{3.4.1}$$

Flipping edge $\{1,3\}$ we get

$$S^K_{123} + S^K_{136} = S^K_{126} + S^K_{236} + \frac{x_{16}S^K_{123} + x_{12}S^K_{136} - x_{13}S^K_{126}}{2}. \tag{3.4.2}$$

Flipping edge $\{3,5\}$ we get

$$S^K_{356} + S^K_{345} = S^K_{456} + S^K_{346} + \frac{x_{45}S^K_{356} + x_{56}S^K_{345} - x_{35}S^K_{456}}{2}. \tag{3.4.3}$$

Finally, flipping edge $\{3,6\}$ we get

$$S^K_{346} + S^K_{236} = S^K_{234} + S^K_{246} + \frac{x_{23}S^K_{346} + x_{34}S^K_{236} - x_{36}S^K_{234}}{2}. \tag{3.4.4}$$

Summing and making use of equations (3.4.1)-(3.4.4) we achieve the identity

$$\begin{aligned} S^K_{156} + S^K_{123} + S^K_{345} + S^K_{135} = \\ S^K_{246} + S^K_{234} + S^K_{126} + S^K_{456} + \frac{x_{35}(S^K_{156} - S^K_{456}) + x_{56}(S^K_{135} + S^K_{345}) + (x_{45} - x_{15})S^K_{356}}{2} \\ + \frac{x_{16}S^K_{123} + x_{12}S^K_{136} - x_{13}S^K_{126} + x_{23}S^K_{346} + x_{34}S^K_{236} - x_{36}S^K_{234}}{2}. \end{aligned}$$

Since we have shown that every component of this identity (with the exception of S^K_{246}) can be written as a rational function in $\mathbf{xS}_G(P)$ with denominator a monomial in $\mathbf{x}_{D(G)}(P)$, this must be the case for S^K_{246} as well. (Note that a much cleaner identity holds in the case $K = 0$, see [FS21].)

The remaining inductive cases will be handled generally. Suppose triangulation G has edge $e \in D(G)$ incident to vertex i. Since G is trimmed with respect (i,j,k), we can assume e crosses $\{j,k\}$. Similarly, were G to have a diagonal incident to j, it would have to cross $\{i,k\}$. But such a diagonal would also cross e. Therefore, G has no diagonal incident to j and $f = \{j-1, j+1\} \in D(G)$. The triangulation $G' = \mu_f(G)$ is not trimmed with respect to (i,j,k) so by Lemma 3.67 and the induction hypothesis, S^K_{ijk} can be written as a rational function in $\mathbf{xS}_G(P)$ with denominator a monomial in $\mathbf{x}_{D(G)}(P)$.

Consider the case where triangulation G has no diagonals incident to i, j, or k. Then $D(G)$ must include diagonals $\{i-1, i+1\}$, $\{j-1, j+1\}$, and $\{k-1, k+1\}$ (modulo n). Let G' be the triangulation achieved by flipping $\{i-1, i+1\}$ to $\{i, v\}$ for the appropriate $v \in \{1, \ldots, n\}$. If $\{i, v\}$ does not cross $\{j,k\}$, then Lemma 3.67 and the induction hypothesis apply.

If $\{i, v\}$ crosses $\{j, k\}$, then so do $\{i-1, v\}, \{i+1, v\}$ which are edges of the original triangulation. First assume that

$$\{\{i-1, v\}, \{i+1, v\}\} \neq \{\{j-1, j+1\}, \{k-1, k+1\}\}. \tag{3.4.5}$$

Then flipping one of $\{j-1, j+1\}, \{k-1, k+1\}$ will result in an untrimmed triangulation (with respect to (i, j, k)), trim it down and then apply Lemma 3.67 and the induction hypothesis to the smaller polygon. In the case that (3.4.5) holds, we must have $n = 6$, with the triangulation given by $\{3, 4, 5\}$ and $(i, j, k) = (2, 4, 6)$, which we handled above. □

Proof of Proposition 3.59. Proposition 3.56 proves that $\mathbf{z}_\pi$, the collection of numbers associated with a traversing path π, can be uniquely extended to a spherical Heronian frieze $\mathbf{z}$ via the construction of a triangulated polygon (P, G) associated to π. Propositions 3.68 and 3.69 above show that the elements of $\mathbf{z}$ are all rational functions with denominators coming from $D(\pi)$. □

3.5 Spherical Cayley-Menger friezes

We now present our second solution to the original spherical distance geometry question. In this solution, our initial data set consists entirely of squared distances x_{ij}. It involves the squared distances associated to a particular triangulation of a polygon, along with a few extra squared distances (the "bracing" edges). The measurements S^K are not used at all.

Proposition 3.6 implies a coplanarity test for $n+1$ points in n-dimensional Euclidean space: if the points $A_1, \ldots, A_{n+1} \in \mathbb{R}^n$ lie on a hyperplane, then the Cayley-Menger determinant $M^0_{n+1}(x_{12}, \ldots, x_{n,n+1})$ vanishes. We will need a similar test for cosphericity, this time utilizing a spherical Cayley-Menger determinant. The papers [Aud11] and [BG43] give different developments of the spherical Cayley-Menger determinant. We most closely follow the development in [Tao19], cf. Theorem 3.71.

Lemma 3.70 below will allow us to express scalar products in terms of the squared distances. We will use the following shorthand: for a point $A \in \mathbf{S}$, we will write $\overrightarrow{A}$ instead of $\overrightarrow{OA}$.

Lemma 3.70. *For $A, B \in \mathbf{S}$, denote $x_{A,B} = x(A, B)$. Then*

$$\langle \overrightarrow{A}, \overrightarrow{B} \rangle = \tfrac{1}{K}\left(1 - \tfrac{K}{2} x_{A,B}\right). \tag{3.5.1}$$

Proof. Using the vector form of the law of cosines, we have

$$\langle \overrightarrow{B} - \overrightarrow{A}, \overrightarrow{B} - \overrightarrow{A} \rangle = \langle \overrightarrow{B}, \overrightarrow{B} \rangle + \langle \overrightarrow{A}, \overrightarrow{A} \rangle - 2\langle \overrightarrow{A}, \overrightarrow{B} \rangle \,. \tag{3.5.2}$$

Since $A, B \in \mathbf{S}$, we have

$$\begin{aligned} \langle \overrightarrow{A}, \overrightarrow{A} \rangle = \langle \overrightarrow{B}, \overrightarrow{B} \rangle = R^2 = \tfrac{1}{K} \,, \\ \langle \overrightarrow{B} - \overrightarrow{A}, \overrightarrow{B} - \overrightarrow{A} \rangle = x_{A,B} \,. \end{aligned}$$

So equation (3.5.2) becomes $x_{A,B} = \frac{2}{K} - 2\langle \overrightarrow{A}, \overrightarrow{B} \rangle$, which rearranges to (3.5.1). □

Theorem 3.71 (cf. [Aud11, BG43, Tao19])**.** *Let $m \geq 4$ and $A_1, \ldots, A_m \in \mathbf{S} \subset \mathbb{C}^3$. Denote $x_{ij} = x(A_i, A_j)$. Then the spherical Cayley-Menger determinant vanishes:*

$$M_m^K(x_{12}, \ldots, x_{m-1,m}) = \begin{bmatrix} \frac{K}{2} & 1 & \cdots & 1 \\ 1 & 0 & \cdots & x_{1m} \\ \vdots & \vdots & \ddots & \vdots \\ 1 & x_{m1} & \cdots & 0 \end{bmatrix} = 0 \,.$$

Remark 3.72. The notation M_m^K reflects that this is a computation associated to a collection of m points on a sphere with curvature K.

Remark 3.73. The spherical Cayley-Menger determinant M_3^K associated to a triple of points on $\mathbf{S}$ is closely related to the spherical Heron formula (cf. Proposition 3.11):

$$\begin{aligned} -M_3^K(x_{12}, x_{13}, x_{23}) &= -x_{12}^2 - x_{13}^2 - x_{23}^2 + 2x_{12}x_{13} + 2x_{12}x_{23} + 2x_{13}x_{23} - Kx_{12}x_{13}x_{23} \,, \\ &= H^K(x_{12}, x_{13}, x_{23}) \,, \\ &= (S^K(A_1, A_2, A_3))^2 \,. \end{aligned}$$

Proof of Theorem 3.71. Let M be the matrix with column vectors A_i. Its rank is at most 3. The product $M^T M$ is the $m \times m$ Gram matrix (cf. Remark 3.25)

$$M^T M = \begin{bmatrix} \langle A_1, A_1 \rangle & \langle A_1, A_2 \rangle & \cdots & \langle A_1, A_m \rangle \\ \langle A_2, A_1 \rangle & \langle A_2, A_2 \rangle & \cdots & \langle A_2, A_m \rangle \\ \vdots & \cdots & \ddots & \vdots \\ \langle A_m, A_1 \rangle & \langle A_m, A_2 \rangle & \cdots & \langle A_m, A_m \rangle \end{bmatrix} , \tag{3.5.3}$$

which has rank at most 3. Since $m \geq 4$, the determinant of $M^T M$ must vanish.

We now use the condition that our points lie on a sphere with curvature K. Applying the identity (3.5.1) to (3.5.3), we get:

$$
\begin{aligned}
0 &= \det \begin{bmatrix} \frac{1}{K} & \frac{1}{K}\left(1-\frac{K}{2}x_{12}\right) & \cdots & \frac{1}{K}\left(1-\frac{K}{2}x_{1m}\right) \\ \frac{1}{K}\left(1-\frac{K}{2}x_{12}\right) & \frac{1}{K} & \cdots & \frac{1}{K}\left(1-\frac{K}{2}x_{2m}\right) \\ \vdots & \cdots & \ddots & \vdots \\ \frac{1}{K}\left(1-\frac{K}{2}x_{1m}\right) & \frac{1}{K}\left(1-\frac{K}{2}x_{2m}\right) & \cdots & \frac{1}{K} \end{bmatrix}, \\
&= \left(-\tfrac{1}{K}\right)^m \det \begin{bmatrix} -1 & \frac{K}{2}x_{12}-1 & \cdots & \frac{K}{2}x_{1m}-1 \\ \frac{K}{2}x_{12}-1 & -1 & \cdots & \frac{K}{2}x_{2m}-1 \\ \vdots & \cdots & \ddots & \vdots \\ \frac{K}{2}x_{1m}-1 & \frac{K}{2}x_{2m}-1 & \cdots & -1 \end{bmatrix}, \\
&= \left(-\tfrac{1}{2}\right)^m \left(\tfrac{K}{2}\right)^{-(m+1)} \det \begin{bmatrix} \frac{K}{2} & 1 & 1 & \cdots & 1 \\ 0 & -1 & \frac{K}{2}x_{12}-1 & \cdots & \frac{K}{2}x_{1m}-1 \\ 0 & \frac{K}{2}x_{12}-1 & -1 & \cdots & \frac{K}{2}x_{2m}-1 \\ \vdots & \vdots & \cdots & \ddots & \vdots \\ 0 & \frac{K}{2}x_{1m}-1 & \frac{K}{2}x_{2m}-1 & \cdots & -1 \end{bmatrix}, \\
&= \left(-\tfrac{1}{2}\right)^m \left(\tfrac{K}{2}\right)^{-(m+1)} \det \begin{bmatrix} \frac{K}{2} & 1 & 1 & \cdots & 1 \\ \frac{K}{2} & 0 & \frac{K}{2}x_{12} & \cdots & \frac{K}{2}x_{1m} \\ \frac{K}{2} & \frac{K}{2}x_{12} & 0 & \cdots & \frac{K}{2}x_{2m} \\ \vdots & \vdots & \cdots & \ddots & \vdots \\ \frac{K}{2} & \frac{K}{2}x_{1m} & \frac{K}{2}x_{2m} & \cdots & 0 \end{bmatrix}, \\
&= \left(-\tfrac{1}{2}\right)^m \left(\tfrac{2}{K}\right) \det \begin{bmatrix} \frac{K}{2} & 1 & 1 & \cdots & 1 \\ 1 & 0 & x_{12} & \cdots & x_{1m} \\ 1 & x_{12} & 0 & \cdots & x_{2m} \\ \vdots & \vdots & \cdots & \ddots & \vdots \\ 1 & x_{1m} & x_{2m} & \cdots & 0 \end{bmatrix},
\end{aligned}
$$

which implies the claim. □

Remark 3.74. Let $K \in \mathbb{C}$. Let $(a,b,c,d,e,f,p,q,r,s) \in \mathbb{C}^{10}$ be a spherical Heronian diamond (cf. Definition 3.33) such that $e, f \notin \left\{0, \frac{4}{K}\right\}$. There exists a unique quadrilateral $A_1A_2A_3A_4$ on $\mathbf{S}$ with the measurements (a,b,c,d,e,f,p,q,r,s) by Proposition 3.32. Ergo, the spherical Cayley-Menger determinant $M_4^K(a,b,c,d,e,f)$ should vanish.

To verify this directly, write each of the seven equations (3.2.17)-(3.2.23) in the form $F(a,b,c,d,e,f,p,q,r,s) = 0$ where F is a polynomial. Let I be the ideal generated by these polynomials. One can check, with standard software, that

$$M_4^K(a,b,c,d,e,f)e(eK-4)$$

lies in the ideal I. Since $e \notin \{0, \frac{4}{K}\}$ we conclude that $M_4^K(a,b,c,d,e,f) = 0$.

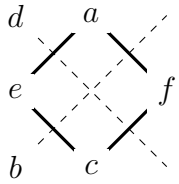
Remark 3.75. In the limit $K \to 0$ (moving towards Euclidean space), the entry in the top left corner of the spherical Cayley-Menger determinant goes to 0, recovering the Euclidean Cayley-Menger determinant.

Some of the following definitions generalize those found in [FS21, Section 5].

Definition 3.76. A spherical Cayley-Menger diamond is a 6-tuple (a,b,c,d,e,f) of complex numbers such that

$$M_4^K(a,b,c,d,e,f) = 0.$$

We organize these numbers in a diamond shape as shown below.



Note that every spherical quadrilateral gives rise to a spherical Cayley-Menger diamond.

Remark 3.77. The definition of $M_4^K(a,b,c,d,e,f)$ implies that we can swap rows and columns to see that if (a,b,c,d,e,f) is a spherical Cayley-Menger diamond, then the tuples (c,d,a,b,e,f), (a,d,c,b,f,e), (f,d,e,b,a,c), and so on, are spherical Cayley-Menger diamonds as well.

Definition 3.78. For $n \geq 4$, define the indexing set

$$I_n^{SCM} = \left\{(i,j) \in \mathbb{Z}^2\right\}_{0 \leq j-i \leq n} \cup \left\{\left(i+\tfrac{1}{2}, \diagup\right)\right\}_{i \in \mathbb{Z}} \cup \left\{\left(\diagdown, j+\tfrac{1}{2}\right)\right\}_{j \in \mathbb{Z}},$$

a subset of the indexing set for a spherical Heronian frieze (cf. Definition 3.45).

As before, the coordinates that use symbols $\diagup$ or $\diagdown$ represent lines. Elements with two numerical coordinates are nodes. When $1 \leq i - j \leq n - 1$, the node (i, j) is interior. We visually represent the set I_n^{SCM} on the usual $\mathbb{R}^2$ coordinate plane rotated $\pi/4$ clockwise (see Figure 3.14).

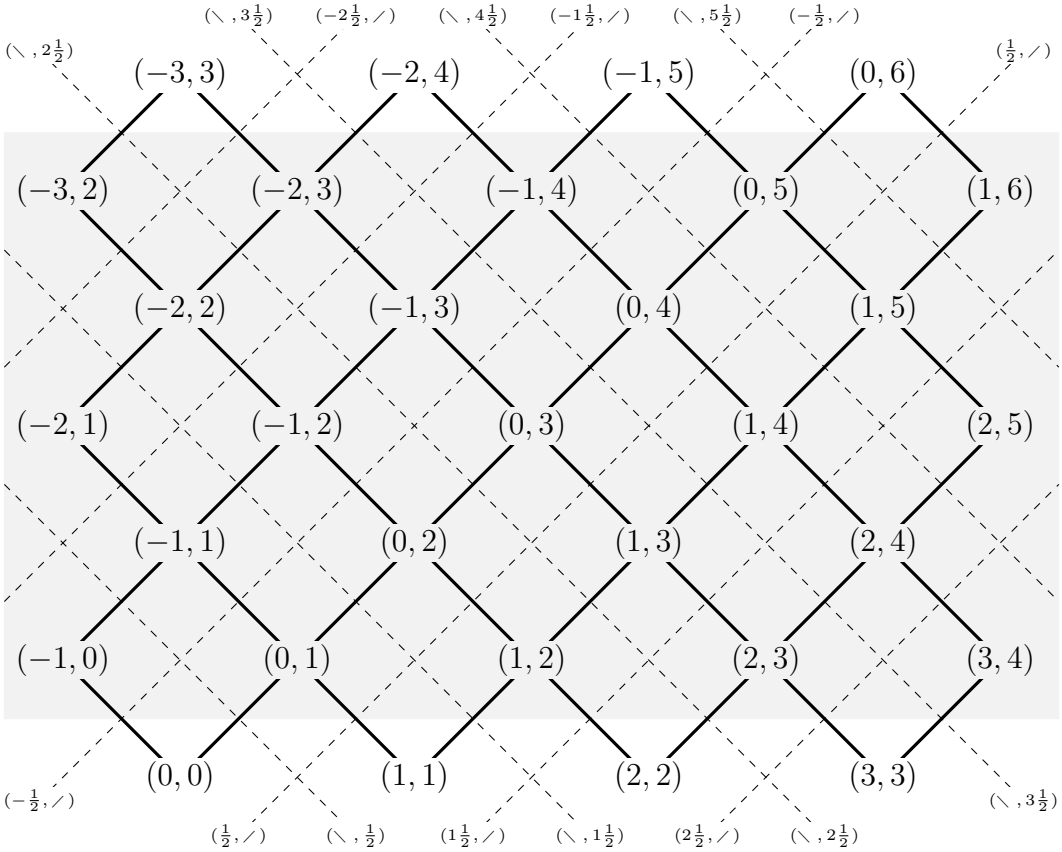


Figure 3.14: A visualization of a portion of the index set I_6^{SCM}. The set extends to the right and left. All nodes in the grey shaded region are interior.

Definition 3.79. For $n \geq 4$, a spherical Cayley-Menger frieze of order n (see, e.g., Figure 3.15) is an array $\widehat{\mathbf{z}} = (z_\alpha)_{\alpha \in I_n^{SCM}}$ of complex numbers indexed by I_n^{SCM} (cf. Definition 3.78) such that each diamond of numbers:

$$\begin{array}{ccccc} & & (\diagdown, j+\frac{1}{2}) & & (i, j+1) \\ & & & \diagup \quad \diagdown & \\ & & (i,j) & & (i+1, j+1) \\ & & & \diagdown \quad \diagup & \\ (i+\frac{1}{2}, \diagup) & & & & (i+1, j) \end{array}$$

is a spherical Cayley-Menger diamond.

More concretely, for an interior node $(i,j) \in \mathbb{Z}^2$, the tuple denoted

$$\diamondsuit_{i,j}(\widehat{\mathbf{z}}) = \left(z_{(i,j+1)}, z_{(i+\frac{1}{2},\diagup)}, z_{(i+1,j)}, z_{(\diagdown,j+\frac{1}{2})}, z_{(i,j)}, z_{(i+1,j+1)}\right).$$

forms a spherical Cayley-Menger diamond with $M_4^K\left(\diamondsuit_{i,j}(\widehat{\mathbf{z}})\right) = 0$. Along the boundary of the frieze, for $i \in \mathbb{Z}$ we require that

$$z_{(i,i)} = z_{(i,i+n)} = 0 \quad \text{(bottom and top rows)}, \tag{3.5.4}$$

$$z_{(i,i+1)} = z_{(i+\frac{1}{2},\diagup)} = z_{(\diagdown,i+\frac{1}{2})}, \tag{3.5.5}$$

$$z_{(i,i+n-1)} = z_{(i-\frac{1}{2},\diagup)} = z_{(\diagdown,i+n-\frac{1}{2})}. \tag{3.5.6}$$

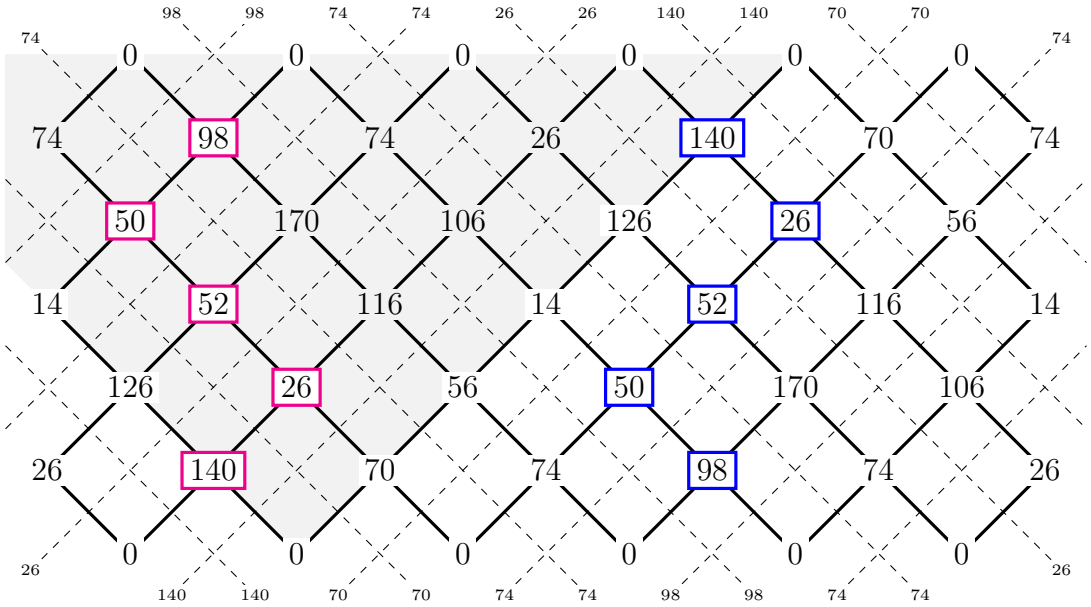


Figure 3.15: A portion of a spherical Cayley-Menger frieze $\mathbf{z}$ of order 6. This frieze corresponds to the hexagon on a sphere with radius 7 in Figure 3.8, the same polygon that gives rise to the spherical Heronian frieze in Figure 3.7. To visualize the glide symmetry, flip the gray shaded region upside down and paste it to the right of its original location. The blue and magenta entries form two separate traversing paths, their entries form identical sets.

Definition 3.80. A traversing path in a spherical Cayley-Menger frieze (cf. Definition 3.52) is an ordered collection

$$\pi = ((i_1,j_1),\ldots,(i_{n-1},j_{n-1}),l_1,\ldots,l_{n-2})$$

of $2n-3$ indices in I_n^{SCM} that consists of elements on a shortest path connecting the lower and upper boundaries of the frieze.

To be more precise, we require that the first point is of the form $(i_1, j_1) = (k, k+1)$ for some $k \in \mathbb{Z}$ (a point almost on the bottom boundary); similarly $(i_{n-1}, j_{n-1}) = (m, m+n-1)$ for some $m \in \mathbb{Z}$ (just below the top boundary). In particular, all (i_k, j_k) are interior nodes. The $l_1, \ldots, l_{n-2}$ are the dashed lines that intersect this shortest path.

Remark 3.81. A spherical polygon P gives rise to a spherical Cayley-Menger frieze $\widehat{\mathbf{z}} = \widehat{\mathbf{z}}(P)$. To visualize the layout of the frieze, again start with two ants standing together at vertex k of the polygon. Correspondingly, the entry at vertex (k, k) in the bottom row is 0, indicating the squared distance between the ants.

As we move along a traversing path upwards in the frieze (now without entries at the half-integer points), each new node corresponds to one of the ants moving to an adjacent vertex of the polygon according to the index on the node. The value at each node always shows the squared distance between the two ants. The squared distance along the side of the polygon that an ant traverses to get to a new vertex is the label on the line $(\diagdown, j + \frac{1}{2})$ or $(i + \frac{1}{2}, \diagup)$ that perpendicularly intersects the traversing path on its way to the next node.

There is an impediment to recovering the entire spherical Cayley-Menger frieze from solely the data associated to a traversing path. When viewed as a polynomial in a single variable x_{ij}, the spherical Cayley-Menger determinant has degree 2. Hence, given $a, b, c, d, e \in \mathbb{C}$, there are generically two values of f, satisfying $M_4^K(a, b, c, d, e, f) = 0$.

To enable propagation, we are going to derive a coherence condition, an additional relation amongst the entries of a spherical Cayley-Menger frieze that holds whenever a frieze arises from a spherical polygon.

Definition 3.82. We use notation for the partial derivatives of the spherical Cayley-Menger polynomial $M_4^K(a, b, c, d, e, f)$ with respect to its 6 variables as shown in Figure 3.16. The arrows in the notation reflect the location of the arguments in a spherical Cayley-Menger diamond. For example,

$$\begin{aligned}\partial_{\rightarrow} M_4^K(a, b, c, d, e, f) &= \frac{\partial M_4^K}{\partial f}(a, b, c, d, e, f) \\ &= 2\left((a-d)(c-b) + e\left(a+b+c+d-e-2f - \tfrac{K}{2}(ac - bd + ef)\right)\right).\end{aligned}$$

The other five partial derivatives of $M_4^K(a, b, c, d, e, f)$ can be obtained by evaluating the expression on the right hand side for various permutations of a, b, c, d, e, f. Note, for example, that a vertical reflection of the spherical Cayley-Menger diamond (swapping $a \leftrightarrow c$ and $b \leftrightarrow d$) leaves the expression unchanged.

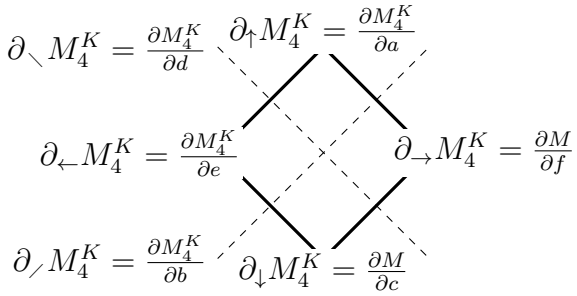


Figure 3.16: Notation for partial derivatives of $M_4^K(a,b,c,d,e,f)$.

Lemma 3.83. *For (a,b,c,d,e,f), a spherical Cayley-Menger diamond, we have:*

$$\begin{aligned}
(\partial_{\rightarrow} M_4^K(a,b,c,d,e,f))^2 &= 4H^K(b,c,e)H^K(a,d,e)\,, \qquad (3.5.7)\\
(\partial_{\uparrow} M_4^K(a,b,c,d,e,f))^2 &= 4H^K(b,c,e)H^K(c,d,f)\,,\\
(\partial_{\downarrow} M_4^K(a,b,c,d,e,f))^2 &= 4H^K(a,b,f)H^K(a,d,e)\,,\\
(\partial_{\leftarrow} M_4^K(a,b,c,d,e,f))^2 &= 4H^K(a,b,f)H^K(c,d,f)\,,\\
(\partial_{\diagdown} M_4^K(a,b,c,d,e,f))^2 &= 4H^K(b,c,e)H^K(a,b,f)\,,\\
(\partial_{\diagup} M_4^K(a,b,c,d,e,f))^2 &= 4H^K(c,d,f)H^K(a,d,e)\,.
\end{aligned}$$

Proof. We will show equation (3.5.7) holds, the others can be derived similarly. One can manually verify the following polynomial identity, which holds for any $a,b,c,d,e,f \in \mathbb{C}$:

$$\begin{aligned}
(\partial_{\rightarrow} M_4^K(a,b,c,d,e,f))^2 = \\
-8e\left(1-\tfrac{Ke}{4}\right) M_4^K(a,b,c,d,e,f) + 4H^K(b,c,e)H^K(a,d,e)\,. \qquad (3.5.8)
\end{aligned}$$

As $M_4^K(a,b,c,e,d,e,f) = 0$, we get equation (3.5.7). □

When a spherical Cayley-Menger diamond arises from a spherical quadrilateral, Lemma 3.83 can be strengthened to a geometric statement.

Proposition 3.84. *Consider a spherical quadrilateral $P = A_1A_2A_3A_4$. Let*

$$\mathbf{x} = (x_{14}, x_{12}, x_{23}, x_{34}, x_{13}, x_{24}) = (a,b,c,d,e,f)$$

denote the corresponding spherical Cayley-Menger diamond. Then

$$\begin{aligned}
\partial_{\leftarrow} M_4^K(\mathbf{x}) &= -2S_{124}^K S_{234}^K\,, & \partial_{\rightarrow} M_4^K(\mathbf{x}) &= -2S_{123}^K S_{134}^K\,, \qquad (3.5.9)\\
\partial_{\diagup} M_4^K(\mathbf{x}) &= 2S_{134}^K S_{234}^K\,, & \partial_{\diagdown} M_4^K(\mathbf{x}) &= 2S_{123}^K S_{124}^K\,, \qquad (3.5.10)\\
\partial_{\uparrow} M_4^K(\mathbf{x}) &= 2S_{123}^K S_{234}^K\,, & \partial_{\downarrow} M_4^K(\mathbf{x}) &= 2S_{124}^K S_{134}^K\,. \qquad (3.5.11)
\end{aligned}$$

Proof. Denoting $p = S^K_{123}$ and $q = S^K_{134}$, the relation $\partial_{\rightarrow} M^K_4(\mathbf{x}) = -2S^K_{123}S^K_{134}$ is the equation (3.2.16). The other relations (3.5.9)-(3.5.11) can be proved similarly, by applying Lemma 3.24 to appropriate collections of vectors. □

Remark 3.85. Specializing $K = 0$ in the equations (3.5.9)-(3.5.11) recovers their analogues obtained in [FS21]. For example, (3.2.12) is obtained by setting $K = 0$ in the relation $\partial_{\rightarrow} M^K_4(\mathbf{x}) = -2S^K_{123}S^K_{134}$. For proof, Fomin and Setiabrata cite [KPSZ17], which references [Dzi00, 40] and [Ham02]. The proof method in [KPSZ17] is to apply the partial derivative directly to the Cayley-Menger matrix, perform row and column operations, reinterpret as a cross product, and then use the Binet-Cauchy formula.

Neither our proof of Proposition 3.84, nor the proof in [KPSZ17], give a geometric explanation for the equations (3.5.9)-(3.5.11), in particular for the appearance of partial derivatives of $M^K_4(\mathbf{x})$. We next attempt to provide such an explanation.

The polynomial $M^K_4(\mathbf{x})$ is quadratic in f: we have $M^K_4(\mathbf{x}) = Af^2 + Bf + C$ for some $A, B, C \in \mathbb{C}$. Therefore

$$\partial_{\rightarrow} M^K_4(\mathbf{x}) = \tfrac{\partial}{\partial f} M^K_4(\mathbf{x}) = 2Af + B\,.$$

Denote $D = B^2 - 4AC$, the discriminant of $M^K_4(\mathbf{x})$. Rewriting

$$M^K_4(\mathbf{x}) = \tfrac{(2Af+B)^2 - (B^2-4AC)}{4A}\,,$$

and recalling that $M^K_4(\mathbf{x}) = 0$, we conclude that

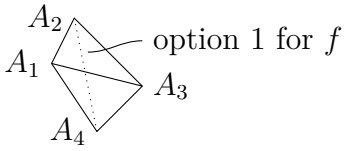
$$\left(\tfrac{\partial}{\partial f} M^K_4(\mathbf{x})\right)^2 = D\,.$$

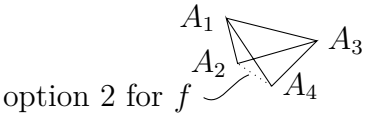
By Proposition 3.84, it follows that

$$D = \left(\tfrac{\partial}{\partial f} M^K_4(\mathbf{x})\right)^2 = 4(S^K_{123})^2 (S^K_{134})^2\,.$$

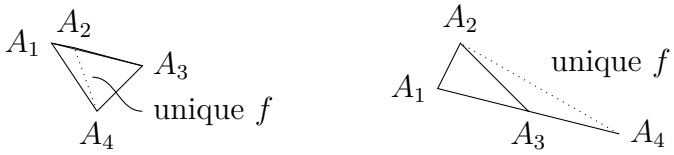
Thus $D = 0$ when either $S^K_{123} = 0$ or $S^K_{134} = 0$.

This can be interpreted geometrically as follows. The discriminant D vanishes when $M^K_4(\mathbf{x}) = 0$ has a double root, i.e., when both solutions for f are the same. Fixing a, b, c, d, e, we get two solutions for f related to each other by reflecting the triangle $A_1A_2A_3$ across the line A_1A_3 (or by reflecting $A_1A_3A_4$ across A_1A_3):





The two options for f coincide with each other if and only if either A_2 or A_4 lie on a great circle of $\mathbf{S}$ passing through A_1 and A_3. This would make either $A_1A_2A_3$ or $A_1A_3A_4$ a "degenerate" triangle, with S^K_{123} or S^K_{134} vanishing:



Proposition 3.86. *Consider four interlocking spherical Cayley-Menger diamonds as depicted in Figure 3.17:*

$$\begin{aligned}
\mathbf{x}_1 &= (x_{15}, x_{12}, x_{24}, x_{45}, x_{14}, x_{25}), \\
\mathbf{x}_2 &= (x_{16}, x_{12}, x_{25}, x_{56}, x_{15}, x_{26}), \\
\mathbf{x}_3 &= (x_{25}, x_{23}, x_{34}, x_{45}, x_{24}, x_{35}), \\
\mathbf{x}_4 &= (x_{26}, x_{23}, x_{35}, x_{56}, x_{25}, x_{36}).
\end{aligned}$$

Then

$$\left(\partial_{\leftarrow} M_4^K(\mathbf{x}_1)\partial_{\rightarrow} M_4^K(\mathbf{x}_4)\right)^2 = \left(\partial_{\uparrow} M_4^K(\mathbf{x}_2)\partial_{\downarrow} M_4^K(\mathbf{x}_3)\right)^2.$$

If the four Cayley-Menger diamonds correspond to a hexagon $P = A_1A_2\cdots A_6$, then

$$\partial_{\leftarrow} M_4^K(\mathbf{x}_1)\partial_{\rightarrow} M_4^K(\mathbf{x}_4) = \partial_{\uparrow} M_4^K(\mathbf{x}_2)\partial_{\downarrow} M_4^K(\mathbf{x}_3). \tag{3.5.12}$$

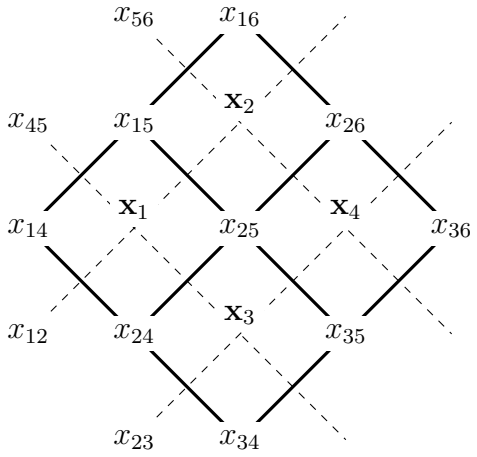


Figure 3.17: Four interlocking Cayley-Menger diamonds.

Proof. We use the shorthand $H^K_{ijk} = H^K(x_{ij}, x_{ik}, x_{jk})$. Using Lemma 3.83 with each diamond gives us

$$\begin{aligned}(\partial_{\leftarrow} M_4^K(\mathbf{x}_1))^2 &= 4H^K_{125}H^K_{245}\,,\\ (\partial_{\rightarrow} M_4^K(\mathbf{x}_4))^2 &= 4H^K_{235}H^K_{256}\,,\\ (\partial_{\uparrow} M_4^K(\mathbf{x}_2))^2 &= 4H^K_{125}H^K_{256}\,,\\ (\partial_{\downarrow} M_4^K(\mathbf{x}_3))^2 &= 4H^K_{235}H^K_{245}\,.\end{aligned}$$

So

$$\left(\partial_{\leftarrow} M_4^K(\mathbf{x}_1)\partial_{\rightarrow} M_4^K(\mathbf{x}_4)\right)^2 = 16H^K_{125}H^K_{245}H^K_{256}H^K_{235} = \left(\partial_{\uparrow} M_4^K(\mathbf{x}_2)\partial_{\uparrow} M_4^K(\mathbf{x}_3)\right)^2.$$

If the diamonds correspond to a hexagon $P = A_1A_2\cdots A_6$ then by Proposition 3.84

$$\begin{aligned}\partial_{\leftarrow} M_4^K(\mathbf{x}_1) &= -2S^K_{125}S^K_{245}\,,\\ \partial_{\rightarrow} M_4^K(\mathbf{x}_4) &= -2S^K_{235}S^K_{256}\,,\\ \partial_{\uparrow} M_4^K(\mathbf{x}_2) &= 2S^K_{125}S^K_{256}\,,\\ \partial_{\downarrow} M_4^K(\mathbf{x}_3) &= 2S^K_{235}S^K_{245}\,,\end{aligned}$$

implying

$$\partial_{\leftarrow} M_4^K(\mathbf{x}_1)\partial_{\rightarrow} M_4^K(\mathbf{x}_4) = 4S^K_{125}S^K_{245}S^K_{256}S^K_{235} = \partial_{\uparrow} M_4^K(\mathbf{x}_2)\partial_{\downarrow} M_4^K(\mathbf{x}_3)\,. \qquad \square$$

Remark 3.87. By Proposition 3.86, for any four interlocking Cayley-Menger diamonds in a frieze $\widehat{\mathbf{z}}$, e.g. for $(i,j) \in \mathbb{Z}^2$ with $2 \le j-i \le n-2$, we get

$$\left(\partial_{\leftarrow} M_4^K\left(\diamondsuit_{i-1,j-1}(\widehat{\mathbf{z}})\right)\partial_{\rightarrow} M_4^K\left(\diamondsuit_{i,j}(\widehat{\mathbf{z}})\right)\right)^2 = \left(\partial_{\uparrow} M_4^K\left(\diamondsuit_{i-1,j}(\widehat{\mathbf{z}})\right)\partial_{\downarrow} M_4^K\left(\diamondsuit_{i,j-1}(\widehat{\mathbf{z}})\right)\right)^2,$$

and therefore

$$\partial_{\leftarrow} M_4^K\left(\diamondsuit_{i-1,j-1}(\widehat{\mathbf{z}})\right)\partial_{\rightarrow} M_4^K\left(\diamondsuit_{i,j}(\widehat{\mathbf{z}})\right) = \pm\partial_{\uparrow} M_4^K\left(\diamondsuit_{i-1,j}(\widehat{\mathbf{z}})\right)\partial_{\downarrow} M_4^K\left(\diamondsuit_{i,j-1}(\widehat{\mathbf{z}})\right).$$

Definition 3.88. We call a spherical Cayley-Menger frieze coherent if for all $i,j \in \mathbb{Z}^2$ with $2 \le j-i \le n-2$ the following coherence condition is satisfied:

$$\partial_{\leftarrow} M_4^K\left(\diamondsuit_{i-1,j-1}(\widehat{\mathbf{z}})\right)\partial_{\rightarrow} M_4^K\left(\diamondsuit_{i,j}(\widehat{\mathbf{z}})\right) = \partial_{\uparrow} M_4^K\left(\diamondsuit_{i-1,j}(\widehat{\mathbf{z}})\right)\partial_{\downarrow} M_4^K\left(\diamondsuit_{i,j-1}(\widehat{\mathbf{z}})\right). \qquad (3.5.13)$$

Theorem 3.89. *For any polygon $P = A_1A_2\cdots A_n$ on $\mathbf{S}$, the spherical Cayley-Menger frieze $\widehat{\mathbf{z}}(P)$ is coherent.*

Proof. This is a direct corollary of Proposition 3.86, see identity (3.5.12). $\square$

Lemma 3.90. *Let*

$$\begin{aligned}\mathbf{x}_2 &= (x_{16}, x_{12}, x_{25}, x_{56}, x_{15}, x_{26})\,,\\ \mathbf{x}_3 &= (x_{25}, x_{23}, x_{34}, x_{45}, x_{24}, x_{35})\,,\\ \mathbf{x}_4 &= (x_{26}, x_{23}, x_{35}, x_{56}, x_{25}, x_{36})\end{aligned}$$

be three spherical Cayley-Menger diamonds arranged as in Figure 3.17. Assume that

$$x_{25}\left(x_{25} - \tfrac{4}{K}\right) H^K(x_{24}, x_{25}, x_{45}) H^K(x_{12}, x_{15}, x_{25}) \neq 0\,. \tag{3.5.14}$$

Let $x_{14} \in \mathbb{C}$ be such that for $\mathbf{x}_1 = (x_{15}, x_{12}, x_{24}, x_{45}, x_{14}, x_{25})$, the coherence condition holds:

$$\partial_{\leftarrow} M_4^K(\mathbf{x}_1)\partial_{\rightarrow} M_4^K(\mathbf{x}_4) = \partial_{\uparrow} M_4^K(\mathbf{x}_2)\partial_{\downarrow} M_4^K(\mathbf{x}_3)\,. \tag{3.5.15}$$

Then the tuple $\mathbf{x}_1$ is also a spherical Cayley-Menger diamond, i.e. $M_4^K(\mathbf{x}_1) = 0$.

Proof. We use the shorthand $H_{ij}^K = H^K(x_{ij}, x_{ik}, x_{jk})$. By Lemma 3.83, we get

$$\left(\partial_{\uparrow} M_4^K(\mathbf{x}_2)\partial_{\downarrow} M_4^K(\mathbf{x}_3)\right)^2 = 16 H_{245}^K H_{125}^K H_{256}^K H_{235}^K\,. \tag{3.5.16}$$

From equation (3.5.8), we get

$$\begin{aligned}&\left(\partial_{\leftarrow} M_4^K(\mathbf{x}_1)\partial_{\rightarrow} M_4^K(\mathbf{x}_4)\right)^2\\ &\qquad = \left(4 H_{245}^K H_{125}^K - 8 x_{25} M_4^K(\mathbf{x}_1)\left(1 - \tfrac{K x_{25}}{4}\right)\right) 4 H_{256}^K H_{235}^K\\ &\qquad = 16 H_{245}^K H_{125}^K H_{256}^K H_{235}^K + 8K x_{25}\left(x_{25} - \tfrac{4}{K}\right) H_{256}^K H_{235}^K M_4^K(\mathbf{x}_1)\,.\end{aligned} \tag{3.5.17}$$

Combining (3.5.15), (3.5.16), and (3.5.17), we conclude that

$$8K x_{25}\left(x_{25} - \tfrac{4}{K}\right) H_{256}^K H_{235}^K M_4^K(\mathbf{x}_1) = 0\,.$$

By assumption (3.5.14), this implies that we must have $M_4^K(\mathbf{x}_1) = 0$, so $\mathbf{x}_1$ is a spherical Cayley-Menger diamond. □

Proposition 3.91. *Start with three interlocking spherical Cayley-Menger diamonds*

$$\begin{aligned}\mathbf{x}_1 &= (x_{15}, x_{12}, x_{24}, x_{45}, x_{14}, x_{25})\,,\\ \mathbf{x}_2 &= (x_{16}, x_{12}, x_{25}, x_{56}, x_{15}, x_{26})\,,\\ \mathbf{x}_3 &= (x_{25}, x_{23}, x_{34}, x_{45}, x_{24}, x_{35})\,,\end{aligned}$$

arranged as in Figure 3.17.

If

$$x_{25}\left(x_{25}-\tfrac{4}{K}\right)H^K(x_{24},x_{25},x_{45})H^K(x_{12},x_{15},x_{25})\neq 0\,,$$

then there exists a unique $x_{36}\in\mathbb{C}$ *such that the tuple* $\mathbf{x}_4=(x_{26},x_{23},x_{35},x_{56},x_{25},x_{36})$ *together with* $\mathbf{x}_1,\mathbf{x}_2,\mathbf{x}_3$ *satisfy the coherence condition* (3.5.13)*. As a consequence,* $\mathbf{x}_4$ *turns out to be a spherical Cayley-Menger diamond, i.e.* $M_4^K(\mathbf{x}_4)=0$*.*

Similarly, let $\mathbf{x}_2,\mathbf{x}_3,\mathbf{x}_4$ *be three interlocking spherical Cayley-Menger diamonds. If*

$$x_{25}\left(x_{25}-\tfrac{4}{K}\right)H^K(x_{25},x_{26},x_{56})H^K(x_{23},x_{25},x_{35})\neq 0\,,$$

then there exists a unique $x_{14}\in\mathbb{C}$ *such that the tuples* $\mathbf{x}_1,\mathbf{x}_2,\mathbf{x}_3,\mathbf{x}_4$ *satisfy the coherence condition. The tuple* $\mathbf{x}_1$ *is therefore a spherical Cayley-Menger diamond and satisfies* $M_4^K(\mathbf{x}_1)=0$*.*

Proof. Consider the second case, where we know the values for $\mathbf{x}_2,\mathbf{x}_3,\mathbf{x}_4$ and want to solve for x_{14} to complete $\mathbf{x}_1$. We want the resulting collection of four spherical Cayley-Menger diamonds to satisfy the coherence condition (3.5.13)

$$\begin{aligned}\tfrac{\partial}{\partial x_{14}}M_4^K(x_{15},x_{12},x_{24},x_{45},x_{14},x_{25})\tfrac{\partial}{\partial x_{36}}M_4^K(x_{26},x_{23},x_{35},x_{56},x_{25},x_{36})=\\ \tfrac{\partial}{\partial x_{16}}M_4^K(x_{16},x_{12},x_{25},x_{56},x_{15},x_{26})\tfrac{\partial}{\partial x_{34}}M_4^K(x_{25},x_{23},x_{34},x_{45},x_{24},x_{35})\,.\end{aligned}$$

This equation is linear in the variable x_{14}, its coefficient is $Kx_{25}\left(x_{25}-\frac{4}{K}\right)\partial_{\rightarrow}M_4^K(\mathbf{x}_4)$. By assumption and Lemma 3.83, we have

$$\left(Kx_{25}\left(x_{25}-\tfrac{4}{K}\right)\right)^2\left(\partial_{\rightarrow}M_4^K(\mathbf{x}_4)\right)^2=\left(Kx_{25}\left(x_{25}-\tfrac{4}{K}\right)\right)^2\cdot 4H_{256}^KH_{235}^K\neq 0\,,$$

and so we get a unique solution for x_{14} such that the coherence condition holds for the four diamonds $\mathbf{x}_1,\mathbf{x}_2,\mathbf{x}_3,\mathbf{x}_4$.

In the first case we can similarly solve for x_{36}. In both cases, to see that the resulting tuple is a spherical Cayley-Menger diamond, apply Lemma 3.90. □

Remark 3.92. If all the input data are real and the diamonds arise from a polygon $A_1\cdots A_n$ on a sphere, the condition

$$x_{25}\left(x_{25}-\tfrac{4}{K}\right)H^K(x_{24},x_{25},x_{45})H^K(x_{12},x_{15},x_{25})\neq 0$$

is equivalent to requiring that neither of the triples $\{A_2,A_4,A_5\}$ or $\{A_1,A_2,A_5\}$ lie on a great circle of $\mathbf{S}$.

We will now show how to recover the entries of a spherical Cayley-Menger frieze from a small initial data set.

Definition 3.93. Let $n \geq 4$. Let $\pi = ((i_1, j_1), \ldots, (i_{n-1}, j_{n-1}), l_1, \ldots, l_{n-2})$ be a traversing path in a spherical Cayley-Menger frieze of order n.

Define a thickening of π, denoted $\overline{\pi}$, to be the original path π along with each of the interior nodes in the frieze shifted by $(1, 1)$ (to the right) from π. Formally,

$$\overline{\pi} = ((i_1, j_1), \ldots, (i_{n-1}, j_{n-1}), (i_1 + 1, j_1 + 1), \ldots, (i_{n-1} + 1, j_{n-1} + 1), l_1, \ldots, l_{n-2}).$$

A thickened path $\overline{\pi}$ has $3n - 4$ indices, see Figure 3.18.

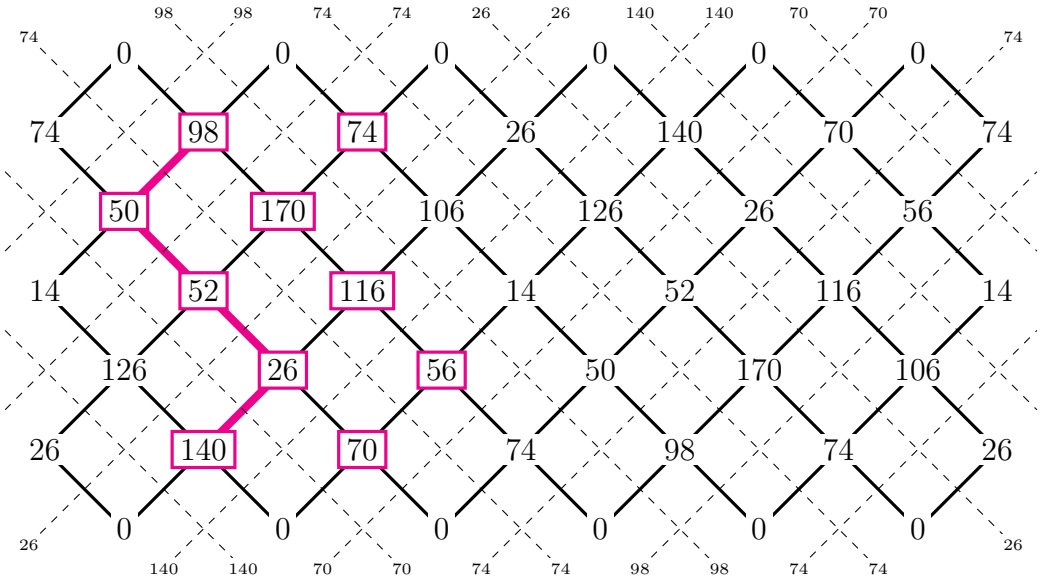


Figure 3.18: The same Cayley-Menger frieze as Figure 3.15. The entries highlighted in magenta are the thickening of the traversing path on the left indicated by magenta lines.

Theorem 3.94. *Let $\widehat{\mathbf{z}} = (z_\alpha)_{\alpha \in I_n^{SCM}}$ be a coherent spherical Cayley-Menger frieze of order n such that*

$$z_{(i,j)} \notin \left\{0, \tfrac{4}{K}\right\} \text{ for any } (i,j) \in \mathbb{Z}^2 \text{ with } 2 \leq j - i \leq n - 2, \text{ and} \tag{3.5.18}$$

$$\begin{cases} H^K(z_{(i,j)}, z_{(i+1,j)}, z_{(i+\frac{1}{2},\diagup)}) \neq 0\,, \\ H^K(z_{(i,j-1)}, z_{(i,j)}, z_{(\diagdown,j-\frac{1}{2})}) \neq 0 \end{cases} \text{for } (i,j) \in \mathbb{Z}^2,\ 2 \leq j - i \leq n - 1\ . \tag{3.5.19}$$

Then $\widehat{\mathbf{z}}$ is uniquely determined by its entries in the thickening $\overline{\pi}$ of any traversing path π.

Proof. Fix a traversing path π and its thickening $\overline{\pi}$. The boundary condition (3.5.4) ensures that all entries indexed by (i, i), $(i, i + n)$ for $i \in \mathbb{Z}$ (the top and bottom rows) are zero.

For the interior nodes, we can propagate outwards from $\overline{\pi}$ by applying Proposition 3.91 to ensure coherence of the resulting frieze. The conditions (3.5.18)-(3.5.19) provide the required non-vanishing conditions. Because Proposition 3.91 guarantees uniqueness of the resulting entries, they must agree with those in $\widehat{\mathbf{z}}$.

The boundary conditions (3.5.5) and (3.5.6) give us the lines intersecting just above and just below the thickened path $\overline{\pi}$. □

Remark 3.95. We can uniquely recover a spherical Heronian frieze from a traversing path (cf. Corollary 3.54), and a spherical Cayley-Menger frieze from a thickening of a traversing path (cf. Theorem 3.94). The conditions for doing so are slightly different. While both propagation algorithms require the non-vanishing of the entries at the interior integer nodes (cf. conditions (3.3.17) and (3.5.18)), recovering a spherical Cayley-Menger frieze additionally requires the non-vanishing of Heron polynomials (cf. condition (3.5.19)).

By Corollary 3.55, any sufficiently generic spherical Heronian frieze arises from a spherical polygon. The following result shows that the same is true for sufficiently generic coherent spherical Cayley-Menger friezes.

Theorem 3.96. *Let $\widehat{\mathbf{z}} = (z_\alpha)_{\alpha \in I_n^{SCM}}$ be a coherent spherical Cayley-Menger frieze of order n satisfying the conditions in Theorem 3.94. Then there exists an n-gon P on $\mathbf{S}$ such that $\widehat{\mathbf{z}} = \widehat{\mathbf{z}}(P)$. Consequently $\widehat{\mathbf{z}}$ has glide symmetry.*

We will prove Theorem 3.96 at the end of Section 3.6.

3.6 Spherical Cayley-Menger friezes vs. spherical Heronian friezes

In this section, we show when and how a spherical Heronian frieze gives rise to a spherical Cayley-Menger frieze and vice versa. This generalizes the results in [FS21, Section 6] to the case of arbitrary K.

We begin by establishing genericity conditions under which a spherical Heronian diamond restricts to a spherical Cayley-Menger diamond.

Lemma 3.97. *Let $\mathbf{xS} = (a, b, c, d, e, f, p, q, r, s) \in \mathbb{C}^{10}$ be a spherical Heronian diamond satisfying either*

$$a = q = r = 0\,, \quad \text{or} \tag{3.6.1}$$

$$c = p = s = 0\,, \quad \text{or} \tag{3.6.2}$$

$$\left(e\left(e - \tfrac{4}{K}\right), f\left(f - \tfrac{4}{K}\right)\right) \neq (0, 0)\,. \tag{3.6.3}$$

Then

$$-2rs = \partial_{\leftarrow} M_4^K(a,b,c,d,e,f)\,, \qquad -2pq = \partial_{\rightarrow} M_4^K(a,b,c,d,e,f)\,, \tag{3.6.4}$$

$$2qs = \partial_{/} M_4^K(a,b,c,d,e,f)\,, \qquad 2pr = \partial_{\backslash} M_4^K(a,b,c,d,e,f)\,, \tag{3.6.5}$$

$$2ps = \partial_{\uparrow} M_4^K(a,b,c,d,e,f)\,, \qquad 2rq = \partial_{\downarrow} M_4^K(a,b,c,d,e,f)\,. \tag{3.6.6}$$

Proof. First assume condition (3.6.1). By Lemma 3.41, we see that

$$d = e\,,$$
$$f = b\,,$$
$$ps = p^2 = H^K(b,c,e)\,.$$

Substituting these values into $\partial_{\uparrow} M_4^K(a,b,c,d,e,f)$, we can now manually verify equation (3.6.6). The other equations and the case of condition (3.6.2) can be similarly checked.

Consider the case where condition (3.6.3) holds. Assume without loss of generality that $e \notin \left\{0, \frac{4}{K}\right\}$. Triangulate a four-cycle G by connecting the first and third vertices, and assign the elements of $\mathbf{xS}$ to the edges in G in accordance with Example 3.15 (you will not use f, r, s). By Proposition 3.32 there is a spherical 4-gon P on $\mathbf{S}$ with $\mathbf{xS} = \mathbf{xS}_G(P)$. By Proposition 3.35 the remaining measurements for P will be f, r, s. Then by Proposition 3.84, we get equations (3.6.4)-(3.6.6) by recalling that $S_{123}^K = p$, $S_{134}^K = q$, etc. □

Proposition 3.98. *Let $(a,b,c,d,e,f,p,q,r,s) \in \mathbb{C}^{10}$ be a spherical Heronian diamond satisfying one of the conditions* (3.6.1)-(3.6.3)*. Then (a,b,c,d,e,f) is a spherical Cayley-Menger diamond.*

Proof. Remark 3.74 addresses the case of condition (3.6.3). In the case of condition (3.6.1), we have $d = e$ and $f = b$ (see Lemma 3.41) and we can manually check that $M_4^K(a,b,c,d,e,f) = 0$. The case of condition (3.6.2) is similar. □

When we restrict a spherical Heronian frieze to form a spherical Cayley-Menger frieze, it automatically satisfies the coherence condition:

Proposition 3.99. *Let $\mathbf{x}_1, \mathbf{x}_2, \mathbf{x}_3, \mathbf{x}_4$ be four interlocking spherical Heronian diamonds arranged as shown in Figure 3.19. Suppose that each $\mathbf{x}_i$ satisfies one of the conditions* (3.6.1)-(3.6.3)*. Then the corresponding interlocking spherical Cayley-Menger diamonds (cf. Proposition 3.98) satisfy the coherence condition* (3.5.13)*.*

Proof. Applying Lemma 3.97 to $\mathbf{x}_1, \mathbf{x}_2, \mathbf{x}_3, \mathbf{x}_4$, we see that each side of the coherence condition is the product of the starred entries in Figure 3.19. □

We next discuss the other direction: constructing a spherical Heronian frieze from a spherical Cayley-Menger frieze.

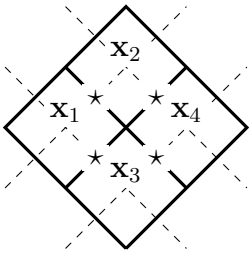


Figure 3.19: Four interlocking spherical Heronian diamonds as in Proposition 3.99. The starred entries appear in the coherence condition on the corresponding spherical Cayley-Menger diamonds.

Proposition 3.100. *Let* $\mathbf{x} = (a, b, c, d, e, f)$ *be a spherical Cayley-Menger diamond such that* $\left(e\left(e - \frac{4}{K}\right), f\left(f - \frac{4}{K}\right)\right) \neq (0, 0)$ *and*

$$H^K(b, c, e)H^K(a, d, e)H^K(a, b, f)H^K(c, d, f) \neq 0\,. \tag{3.6.7}$$

Then there exist exactly two spherical Heronian diamonds restricting to $\mathbf{x}$*. These two diamonds differ from each other by the simultaneous sign change of* p, q, r, s*.*

Proof. Since $\mathbf{x}$ is a spherical Cayley-Menger diamond, by Lemma 3.83 and condition (3.6.7), the partial derivatives in Lemma 3.97 do not vanish. This implies that for the tuple $(a, b, c, d, e, f, p, q, r, s)$ to be a spherical Heronian diamond, we must have $pqrs \neq 0$. The pairwise products of p, q, r, s must be given by (3.6.4)-(3.6.6). This means that these numbers are uniquely determined by $\mathbf{x}$ up to a simultaneous change of sign.

Consider the following candidate values for p, q, r, s. Set $p^2 = H^K(b, c, e)$ and select a sign for p (the other choice will cause all signs to change simultaneously, giving the other possible solution). Then, inspired by equations (3.6.4)-(3.6.6), let

$$q = -\frac{\partial_{\rightarrow} M_4^K(x)}{2p}\,, \quad r = \frac{\partial_{\diagdown} M_4^K(x)}{2p}\,, \quad s = \frac{\partial_{\uparrow} M_4^K(x)}{2p}\,.$$

We need to check that the collection $(a, b, c, d, e, f, p, q, r, s)$ satisfies equations (3.2.17)-(3.2.23) and therefore is a spherical Heronian diamond.

The Heron relations (3.2.17)-(3.2.20) are a consequence of our choice of p together with Lemma 3.83. Since we know that $p \neq 0$ (as we've assumed $H(b, c, e) \neq 0$), one can check manually that equation (3.2.21) is equivalent to

$$\begin{aligned} 2H^K(b, c, e) - \partial_{\rightarrow} M_4^K(\mathbf{x}) = \\ \partial_{\diagdown} M_4^K(\mathbf{x}) + \partial_{\uparrow} M_4^K(\mathbf{x}) + K\left(aH^K(b, c, e) - b\partial_{\rightarrow} M_4^K(\mathbf{x}) - e\partial_{\diagdown} M_4^K(\mathbf{x})\right)\,. \end{aligned}$$

Equation (3.2.22) is equivalent to

$$4ef\left(1-\tfrac{Ke}{4}\right) = H^K(b,c,e) - \partial_{\rightarrow} M_4^K(\mathbf{x}) + H^K(a,d,e) + (a-b+c-d)^2 - Ke(a-b)(c-d)\,,$$

which can be verified by direct computation. Similarly, equation (3.2.23) is equivalent to

$$e\left(\partial_{\diagdown} M_4^K(\mathbf{x}) - \partial_{\uparrow} M_4^K(\mathbf{x})\right) = 2H^K(b,c,e)(a-d) - \partial_{\rightarrow} M_4^K(\mathbf{x})(b-c)\,,$$

which can also be checked manually. (Contrary to the remark in the proof of [FS21, Proposition 6.4], this verification does not rely on the condition $M(\mathbf{x}) = 0$.) □

The following result fully clarifies the relationship between spherical Heronian friezes and spherical Cayley-Menger friezes

Theorem 3.101. *Let $\mathbf{z} = (z_\alpha)_{\alpha \in I_n^{SH}}$ be a spherical Heronian frieze such that*

$$z_{(i,j)} \notin \left\{0, \tfrac{4}{K}\right\} \text{ for any } (i,j) \in \mathbb{Z}^2 \text{ such that } 2 \leq j-i \leq n-2 \tag{3.6.8}$$

(same as (3.3.17) or (3.5.18)). Then the restriction of $\mathbf{z}$ to I_n^{SCM} is a coherent spherical Cayley-Menger frieze.

Conversely, let $\widehat{\mathbf{z}} = (z_\alpha)_{\alpha \in I_n^{SCM}}$ be a coherent spherical Cayley-Menger frieze satisfying (3.6.8). Suppose that for every $(i,j) \in \mathbb{Z}^2$ with $2 \leq j-i \leq n-1$, we have

$$H^K\left(z_{(i,j)}, z_{(i+1,j)}, z_{(i+\frac{1}{2},\diagup)}\right) \neq 0, \quad H^K\left(z_{(i,j-1)}, z_{(i,j)}, z_{(\diagdown,j-\frac{1}{2})}\right) \neq 0 \tag{3.6.9}$$

(same as (3.5.19)). Then there exists a spherical Heronian frieze $\mathbf{z} = (z_\alpha)_{\alpha \in I_n^{SH}}$ that extends $\widehat{\mathbf{z}}$. This extension is unique up to a global change of sign of the entries indexed by $I_n^{SH} \setminus I_n^{SCM}$.

Proof. First assume that $\mathbf{z} = (z_\alpha)_{\alpha \in I_n^{SH}}$ is a spherical Heronian frieze satisfying (3.6.8). By Proposition 3.98, each spherical Heronian diamond in the frieze can be restricted to a spherical Cayley-Menger diamond (disregard the values indexed by $\left(i, j+\frac{1}{2}\right)$) and $\left(i+\frac{1}{2}, j\right)$) to get a collection $\widehat{\mathbf{z}}$. By definition $\widehat{\mathbf{z}}$ is a spherical Cayley-Menger frieze. By Corollary 3.55, the spherical Heronian frieze $\mathbf{z}$, hence the spherical Cayley-Menger frieze $\widehat{\mathbf{z}}$, corresponds to a polygon P. It follows by Theorem 3.89 that the spherical Cayley-Menger frieze $\widehat{\mathbf{z}}$ is coherent.

Now let $\widehat{\mathbf{z}} = (z_\alpha)_{\alpha \in I_n^{SCM}}$ be a coherent spherical Cayley-Menger frieze satisfying (3.6.8)-(3.6.9). Let π be a traversing path in I_n^{SCM}, with $\overline{\pi}$ its thickening, see Definition 3.93. Examining I_n^{SH}, denote by $\widetilde{\pi}$ the two adjacent traversing paths that together restrict to $\overline{\pi}$

in I_n^{SCM}. Note that $\widetilde{\pi}$ as a set is strictly larger than $\overline{\pi}$, as it contains values corresponding to midpoint indices $(i, j+\frac{1}{2}), (i+\frac{1}{2}, j)$ that do not appear in I_n^{SCM}.

Let $\diamondsuit_{i,j}(\widehat{\mathbf{z}})$ be a spherical Cayley-Menger diamond in $\overline{\pi}$. Proposition 3.100 gives two spherical Heronian diamonds that restrict to $\diamondsuit(\widehat{\mathbf{z}})$ and differ by a simultaneous change of sign of the midpoint indices that appear in $\widetilde{\pi} \setminus \overline{\pi}$. Select one to create a first spherical Heronian diamond $\mathbf{x}$. As we travel along $\overline{\pi}$ the diamonds overlap, so our choice of signs for the midpoint values in $\mathbf{x}$ determines all subsequent sign choices. We get exactly two sets of interlocking spherical Heronian diamonds $\widetilde{\mathbf{z}_1}$ and $\widetilde{\mathbf{z}_2}$ that agree with $\widehat{\mathbf{z}}$ on $\overline{\pi}$, and differ by a simultaneous sign change of the midpoint entries in $\widetilde{\pi} \setminus \overline{\pi}$.

We have two sets of entries corresponding to $\widetilde{\pi}$. We want to extend these arrays to spherical Heronian friezes that restrict to $\widehat{\mathbf{z}}$. Let $\mathbf{x}_1, \mathbf{x}_2, \mathbf{x}_3$ be three spherical Heronian diamonds indexed by $\widetilde{\pi}$ that share a single node $z_{(i,j)}$. By Corollary 3.40, we construct $\mathbf{x}_4$, a fourth spherical Heronian diamond containing $z_{(i,j)}$. The conditions (3.6.8)-(3.6.9), together with the boundary conditions on spherical Cayley-Menger friezes (3.5.4)-(3.5.6) mean that all four spherical Heronian diamonds meet conditions (3.6.1)-(3.6.3), so by Proposition 3.99 the four corresponding spherical Cayley-Menger diamonds satisfy the coherence condition (3.5.13). We also satisfy the conditions of Proposition 3.91; the fact that the new entry of $\mathbf{x}_4$ is unique means that it agrees with the corresponding entry in $\widehat{\mathbf{z}}$.

Propagate away from $\widetilde{\pi}$ in this way to construct unique spherical Heronian friezes $\mathbf{z}_1$ and $\mathbf{z}_2$ that extend $\widetilde{\mathbf{z}_1}$ and $\widetilde{\mathbf{z}_2}$ respectively and restrict to $\widehat{\mathbf{z}}$. To find values near the boundary, we propagate using rules (3.3.10) and (3.3.12)-(3.3.14) which agree with the corresponding rules for spherical Cayley-Menger friezes (3.5.4)-(3.5.6).

The final claim is that the two spherical Heronian friezes differ by a simultaneous change of sign of the entries indexed by $I_n^{SH} \setminus I_n^{SCM}$. Above, we selected an initial spherical Cayley-Menger diamond $\diamondsuit_{i,j}(\widehat{\mathbf{z}})$ which generated spherical Heronian friezes $\mathbf{z}_1$ and $\mathbf{z}_2$. Suppose we start with a different spherical Cayley-Menger diamond and generate two spherical Heronian friezes $\mathbf{z}_3$ and $\mathbf{z}_4$. By Proposition 3.100 again, the first spherical Cayley-Menger diamond $\diamondsuit_{i,j}(\widehat{\mathbf{z}})$ only extends to two spherical Heronian diamonds, the frieze $\mathbf{z}_3$ must have one and $\mathbf{z}_4$ the other. Therefore $\mathbf{z}_3$ and $\mathbf{z}_4$ must be the same as $\mathbf{z}_1$ and $\mathbf{z}_2$. □

Proof of Theorem 3.96. By Theorem 3.101, the spherical Cayley-Menger frieze $\widehat{\mathbf{z}}$ can be extended to a spherical Heronian frieze, which by Corollary 3.55 arises from a polygon P on $\mathbf{S}$. Thus $\widehat{\mathbf{z}}$ must also arise from P. □

BIBLIOGRAPHY

[AA18] N. V. Abrosimov and V. V. Aseev, Generalizations of Casey's theorem for higher dimensions, *Lobachevskii J. Math.* **39** (2018), no. 1, 1–12.

[AM15] N. V. Abrosimov and L. A. Mikaiylova, Casey's theorem in hyperbolic geometry, *Sib. Élektron. Mat. Izv.* **12** (2015), 354–360.

[ARS10] I. Assem, C. Reutenauer, and D. Smith, Friezes, *Adv. Math.* **225** (2010), 3134–3165.

[Aud11] D. Audet, Déterminants sphérique et hyperbolique de Cayley-Menger, *Bulletin AMQ* **LI** (2011), no. 2, 45–52.

[Ayo07] A. B. Ayoub, Generalizations of Ptolemy and Brahmagupta theorems, *Math. Comput. Educ.* **41** (2007), no. 1, 30–36.

[BCI74] D. Broline, D. W. Crowe, and I. M. Isaacs, The geometry of frieze patterns, *Geom. Dedicata* **3** (1974), 171–176.

[Ber77] M. Berger, *Geometry*, Springer-Verlag, 1977.

[BG43] L. M. Blumenthal and B. E. Gillam, Distribution of points in n-space, *Amer. Math. Monthly* **50** (1943), no. 3, 181–185.

[BM12] G. A. Bajgonakova and A. Mednykh, On Bretschneider's formula for a spherical quadrilateral, *Mat. Zamet. YAGU* **19** (2012), no. 1, 3–11.

[Böh71] J. Böhm, Ein Zusammenhang zwischen Fries-Zahlenmuster und Orthoschemketten, *Wiss. Beitr. Martin-Luther-Univ. Halle-Wittenberg M* **M3** (1971), 107–119.

[BR10] F. Bergeron and C. Reutenauer, SL_k-tilings of the plane, *Illinois J. Math.* **54** (2010), 263–300.

[Bre42] C. A. Bretschneider, Untersuchung der trigonometrischen Relationen des geradlinigen Viereckes, *Arch. Math. Phys.* **2** (1842), 225–261.

[Cas66] J. Casey, On the equations and properties: (1) of the system of circles touching three circles in a plane; (2) of the system of spheres touching four spheres in space; (3) of the system of circles touching three circles on a

sphere; (4) of the system of conics inscribed to a conic, and touching three inscribed conics in a plane, *Proc. Roy. Irish Acad.* **9** (1866), 396–423.

[CC73] J. H. Conway and H. S. M. Coxeter, Triangulated polygons and frieze patterns, *Math. Gaz.* **57** (1973), no. 400, 87–94, no. 401, 175–183.

[CC06] P. Caldero and F. Chapoton, Cluster algebras as Hall algebras of quiver representations, *Comment. Math. Helv.* **81** (2006), no. 3, 595–616.

[CCS06] P. Caldero, F. Chapoton, and R. Schiffler, Quivers with relations arising from clusters (A_n case), *Trans. Amer. Math. Soc.* **358** (2006), no. 3, 1347–1364.

[CH21] M. Cuntz and T. Holm, Subpolygons in Conway-Coxeter frieze patterns, *Algebr. Comb.* **4** (2021), no. 4, 741–755.

[CHJ20] M. Cuntz, T. Holm, and P. Jørgensen, Frieze patterns with coefficients, *Forum Math. Sigma* **8** (2020), Paper No. e17, 36.

[Coo39] J. L. Coolidge, A historically interesting formula for the area of a quadrilateral, *Amer. Math. Monthly* **46** (1939), no. 6, 345–347.

[Cox69] H. S. M. Coxeter, *Introduction to geometry*, 2nd ed., John Wiley and Sons, 1969.

[Cox71] ———, Frieze patterns, *Acta Arith.* **18** (1971), no. 1, 297–310.

[Cox74] ———, *Regular complex polytopes*, Cambridge University Press, 1974.

[CR72] C. M. Cordes and D. P. Roselle, Generalized frieze patterns, *Duke Math. J.* **39** (1972), 637–648.

[CR94] H. S. M. Coxeter and J. F. Rigby, Frieze patterns, triangulations, and dichromatic symmetry, The lighter side of mathematics, vol. 11, The Mathematical Association of America, 1994.

[Cun17] M. Cuntz, On wild frieze patterns, *Exp. Math.* **26** (2017), no. 3, 342–348.

[Cun23] ———, Grassmannians over rings and subpolygons, *Int. Math. Res. Not. IMRN* (2023), no. 9, 8078–8099.

[Dar72] G. Darboux, Sur les relations entre les groupes de points, de cercles et de sphères dans le plan et dans l'espace., *Ann. Sci. Ec. Norm. Supér.* **1** (1872), 323–292.

[dSG25] A. de St. Germain, Visual cluster algebras, 2025.

[dSGHL23] A. de St. Germain, M. Huang, and J.-H. Lu, Friezes of cluster algebras of geometric type, 2023, `arXiv:2309.00906`.

[Dzi00] O. Dziobek, Ueber einen merkwürdigen Fall des Vielkörperproblems, *Astron. Nachr.* **152** (1900), no. 3, 33–46.

[Dö65] H. Dörrie, *100 great problems of elementary mathematics*, Dover Publications, 1965.

[Fab25] E. Faber, Frieze patterns in representation theory, 2025, `arXiv:2509.16764`.

[Fel23] A. Felikson, Ptolemy relation and friends, 2023.

[Fel25] ———, Friezes, 2025.

[FF20] D. W. Fillmore and J. P. Fillmore, The formulas of Euler and Cagnoli, 2020.

[Fom25] S. Fomin, Cluster algebras portal, 2025.

[FR08] H. Fukagawa and T. Rothman, *Sacred mathematics*, Princeton University Press, 2008.

[Fro75] G. Frobenius, Anwendungen der Determinantentheorie auf die Geometrie des Maasses, *J. Reine Angew. Math.* (1875), 185–247.

[FS21] S. Fomin and L. Setiabrata, Heronian friezes, *Int. Math. Res. Not.* **2021** (2021), no. 1, 648–694.

[FT64] L. Fejes Tóth, *Regular figures*, The Macmillan Company, 1964.

[FT18] S. Fomin and D. Thurston, Cluster algebras and triangulated surfaces. Part II: Lambda lengths, *Mem. Amer. Math. Soc.* **255** (2018), no. 1223, v+97 pp.

[Fuh90] W. Fuhrmann, *Synthetische Beweise Planimetrischer Sätze*, Leonhard Simion, 1890.

[FWZ24] S. Fomin, L. Williams, and A. Zelevinsky, *Introduction to cluster algebras*, n.p., 2024.

[FZ02a] S. Fomin and A. Zelevinsky, Cluster algebras. I. Foundations, *J. Amer. Math. Soc.* **15** (2002), no. 2, 497–529.

[FZ02b] ———, The Laurent phenomenon, *Adv. Appl. Math.* **28** (2002), no. 2, 119–144.

[Gre96] R. J. Gregorac, Feuerbach's relation and Ptolemy's theorem in $\mathbb{R}^n$, *Geom. Dedicata* **60** (1996), 65–88.

[GS11] R. Guo and N. Sönmez, Cyclic polygons in classical geometry, *C. R. Acad. Bulgare Sci.* **64** (2011), no. 2, 185–194.

[Gue02] S. Gueron, Two applications of the generalized Ptolemy theorem, *Amer. Math. Monthly* **109** (2002), no. 4, 362–70.

[Haa51] J. Haantjes, A characteristic local property of geodesics in certain metric spaces, *Indag. Math.* **13** (1951), 66–73.

[Ham02] M. Hampton, Concave central configurations in the four-body problem, Ph.D. thesis, University of Washington, 2002.

[Hea21] T. Heath, *A history of Greek mathematics*, vol. II, Clarendon Press, 1921.

[JG20] E. A. José García, Two identities and their consequences, *Matinf* **3** (2020), no. 6, 5–11.

[Jon86] A. Jones (ed.), *Book 7 of the Collection*, Springer-Verlag, 1986.

[JT19] T. Jordán and S. Tanigawa, Global rigidity of triangulations with braces, *J. Comb. Theory Ser. B* **136** (2019), 249–288.

[KK16] A. V. Kostin and N. N. Kostina, An interpretation of Casey's theorem and of its hyperbolic analogue, *Sib. Élektron. Mat. Izv.* **13** (2016), 242–251.

[Kos24] A. V. Kostin, On analogs of Fuhrmann's theorem on the Lobachevsky plane, *Sib. Math. J.* **65** (2024), no. 3, 695–702.

[KPSZ17] G. Khimshiashvili, G. Panina, D. Siersma, and V. Zolotov, Point charges and polygonal linkages, *J. Dyn. Control Syst.* **23** (2017), no. 1, 1–17.

[Kub12] T. Kubota, On the extended Ptolemy's theorem in hyperbolic geometry, *Sci. Rep. Tohoku Univ.* **2** (1912), 131–156.

[Lan75] C. Landauer, Triangulations and frieze patterns, *J. Geom.* **6** (1975), no. 2, 155–183.

[LL15] L. Liberti and C. Lavor, Six mathematical gems from the history of distance geometry, *Int. Trans. Oper. Res.* **23** (2015), no. 5, 897–920.

[LRM96] B. L. Laptev, B. A. Rozenfel'd, and A. I. Markushevich, *Mathematics of the 19th century*, ed. by A. N. Kolmogorov and A. P. Yushkevich, trans. by R. Cooke ed., Birkhäuser Verlag, Basel, 1996.

[Mal23] J. P. Maldonado, Frieze matrices and friezes with coefficients, *Algebra Discrete Math.* **36** (2023), no. 2, 188–201.

[MG15] S. Morier-Genoud, Coxeter's frieze patterns at the crossroads of algebra, geometry and combinatorics, *Bull. Lond. Math. Soc.* **47** (2015), no. 6, 895–938.

[MGOST14] S. Morier-Genoud, V. Ovsienko, R. E. Schwartz, and S. Tabachnikov, Linear difference equations, frieze patterns, and the combinatorial Gale transform, *Forum Math. Sigma* **2** (2014), Paper No. e22, 45.

[MM19] H. Maehara and H. Martini, Bipartite sets of spheres and Casey-type theorems, *Results Math.* **74** (2019), no. 1, 47.

[Mui82] Thomas Muir, *A treatise on the theory of determinants*, Macmillan, 1882.

[Pen87] C. Penner, The decorated Teichmüller space of punctured surfaces, *Commun. Math. Phys.* **113** (1987), 299–339.

[Pen12] R. C. Penner, *Decorated Teichmüller theory*, European Mathematical Society, 2012.

[Plü65] J. Plücker, On a new geometry of space, *Phil. Trans. Roy. Soc. A* **155** (1865), 725–791.

[Pre23] M. Pressland, From frieze patterns to cluster categories, *London Math. Soc. Lecture Note Ser.* **486** (2023), 109–145.

[Pro20] J. G. Propp, The combinatorics of frieze patterns and Markoff numbers, *Integers* **20** (2020), no. A12, 38 pp.

[Pto14] C. Ptolemy, *The Almagest: introduction to the mathematics of the heavens*, Green Lion Press, 2014.

[PV94] V. Popov and E. B. Vinberg, *Invariant theory, in: Algebraic geometry IV*, Springer-Verlag, 1994.

[She76] G. C. Shephard, Additive frieze patterns and multiplication tables, *Math. Gaz.* **60** (1976), no. 413, 178–184.

[Shi26] N. Shiraishi (ed.), *Shamei sanpu*, Rev. by I. Sadaichi ed., n.p., Edo (Tokyo), 1826.

[SM14] D. E. Smith and Y. Mikami, *A history of Japanese mathematics*, The Open Court Publishing Company, 1914.

[Sta99] R. P. Stanley, *Enumerative combinatorics*, vol. 2, Cambridge University Press, 1999.

[Sto] W. W. Stothers, Ptolemy's theorem in hyperbolic geometry.

[Str42] F. Strehlke, Zwei neue Sätze vom ebenen und sphärischen Viereck und Umkehrung des Ptolemäischen Lehrsatzes, *Arch. Math. Phys.* **2** (1842), 323–326.

[Swa] K. Swartz, Great Circle Mapper.

[Tao19] T. Tao, The spherical Cayley-Menger determinant and the radius of the Earth, 2019.

[Tod86] I. Todhunter, *Spherical trigonometry*, Macmillan, 1886.

[Tur60] H. W. Turnbull, *The theory of determinants, matrices, and invariants*, 3rd ed., Dover Publications, 1960.

[Val70a] J. E. Valentine, An analogue of Ptolemy's theorem and its converse in hyperbolic geometry, *Pacific J. Math.* **34** (1970), 817–825.

[Val70b] ———, An analogue of Ptolemy's theorem in spherical geometry, *Amer. Math. Monthly* **77** (1970), no. 1, 47–51.

[Wad25] K. Waddle, University College at the University of Toronto, 2025.

[Wey46] H. Weyl, *The classical groups: their invariants and representations*, 2nd ed., Princeton University Press, 1946.

[Wil14] L. Williams, Cluster algebras: an introduction, *Bull. Amer. Math. Soc. (N.S.)* (2014), no. no. 1, 1–26.

[Zab25] A. Zabolotskii, Wildest SL_2-tilings, *Ex. Counterex.* **8** (2025), 100206.

[Zac42] M. Zacharias, Der Caseysche Satz, *Jahresber. Dtsch. Math.-Ver.* **52** (1942), 79–89.